Addis Ababa University

Addis Ababa Institute of Technology

School of Post Graduate Studies

Civil and Environmental Engineering Department

A Thesis Submitted to the School of Postgraduate Studies in Partial Fulfillment of the Requirements for the Degree of Master of Science in Structural Engineering

on

Seismic Performance of Reinforced Concrete Buildings With Masonry Infill

---

A Thesis in Structural Engineering

By

Girma Zewdie Tsige

Addis Ababa

Ethiopia

January 2017

CERTIFICATION

The undersigned have examined the thesis entitled '**Seismic Performance of Reinforced Concrete Buildings with Masonry Infill.'** Prepared and submitted by **Girma Zewdie** in fulfilment of the requirements for the degree of Master of Science in Structural Engineering complies with the regulations of the university and meets the accepted standards with respect to originality and quality.

Dr.Ing- Adil zekaria		
Advisor	Signature	Date
Dr.Esayas G.Youhannes		
Internal Examiner	Signature	Date
Dr.Ing-Girma Zerayohannes		
External Examiner	Signature	Date
Dr.Agizew Nigussie		
Chair Person	Signature	Date

UNDERTAKING

I certify that research work titled "**Seismic Performance of Reinforced Concrete Buildings with Masonry Infill**" is my own work. The work has not been presented elsewhere for assessment. Where material has been used from other sources it has been properly acknowledged / referred.

Girma Zewdie

ABSTRACT

Nonductile reinforced concrete frames with masonry infill walls are a popular form of construction in seismic regions worldwide. The typical multi-story construction in Ethiopia comprises reinforced concrete (RC) frames with HCB masonry infills. Unreinforced masonry infill wall panels may not contribute towards resisting gravity loads, but contribute significantly, in terms of enhanced stiffness and strength under earthquake (or wind) induced lateral loading. However, in practice, the infill stiffness is commonly ignored in frame analysis, resulting in an under-estimation of stiffness and natural frequency. Also, the infill has energy dissipation characteristics that contribute to improved seismic resistance. It is instructive to study the implications of the common practice of ignoring the infill stiffness with regard to performance under seismic loading. This research quantifies the effect of the presence and configuration of masonry infill walls on seismic collapse risk. Seismic analysis of such buildings indicates that the fully-infilled frame has the lowest collapse risk and the bare frame is found to be the most vulnerable to earthquake-induced collapse.

A typical existing office building located in severe seismic zones of Ethiopia (as per ESEN1998) is identified. The office medium rise building is analyzed for earthquake force by considering three type of structural system. i.e. Bare Frame system ,partially-infilled and fully- Infilled Frame system. Effectiveness of masonry wall has been studied with the help of five different models. Infills were modeled using the equivalent strut approach. Nonlinear static analyses for lateral loads were performed by using standard package ETABS,2015 software. The comparison of these models for different earthquake response parameters like base shear vs roof displacement, Story displacement, Story shear, member forces and seismic performance assessment are carried out. It is observed that the seismic demand in the bare frame is significantly large when infill stiffness is not considered, with larger displacements. This effect, however, is not found to be significant in the infilled frame systems.The results are described in detail in this paper.

Key words: Bare frame; Infilled frame; Equivalent Diagonal strut; infill; plastic Hinge

ACKNOWLEDGMENTS

This report is completed with prayer of many and love of my family and friends. However, there are few people that I would like to specially acknowledge and extend my heartfelt gratitude who have made the completion of this report possible. With the biggest contribution to this report; I would like to thank my advisor, **Dr.-Ing. Adil Zekaria** who had given me his full support in guiding me with stimulating suggestions and encouragement to go ahead in all the time of the thesis work.

I also extend my gratitude towards my friends who in one way or the other helped me in accomplishing this study. In particular, I am very much thankful of **Mr.Utino Worabo** and **Mr.Tewodros welday** who helped me in providing information and editing the document.

At last but not the least my gratitude towards my parents, I would also like to thank **God** for not letting me down at a time of crisis and showing me the silver lining in the dark clouds.

TABLE OF CONTENTS

ABSTRACT ..... **IV**

ACKNOWLEDGMENTS ..... **V**

TABLE OF CONTENTS ..... **VI**

LIST OF TABLES ..... **IX**

LIST OF FIGURES ..... **X**

CHAPTER 1 INTRODUCTION **1**

1.1 Background 1

1.2 Statement of the Problem 2

1.3 Objective 6

1.4 Materials and Methods 7

1.5 Scope of the Present Study 9

1.6 Organization of the Thesis 10

CHAPTER 2 LITERATURE REVIEW **11**

2.1 General 11

2.2 Components of Masonry Infilled RC Frame 12

2.3 Effect of masonry infill on the seismic behavior of frame structures. 13

2.4 Load Effects on Masonry Walls and Frames 17

2.4.1 Strength of Masonry Units 17

2.5 Masonry Infilled Frames and Seismic Behavior of Structures 21

2.6 Failure Modes of Masonry Infills 24

2.7 Modeling of Masonry infilled walls 28

2.7.1 Equivalent Strut Width 29

2.7.2 Eccentricity of Equivalent Strut 33

2.7.3 Partially Infilled Frames 34

2.7.4 Perforated Panels 35

2.7.5 Existing Infill Damage 37

2.8 In-Plane Strength and Stiffness Evaluation of URM Infills 38

2.8.1 In-plane Stiffness of Masonry Infill 39

2.8.2 Masonry infill shear strength. 40
2.8.3 Masonry infill crushing strength. 41
2.8.4 Load-Deformation Behavior of the Eccentric Equivalent Strut 42
2.9 Frame member stiffness 43
2.10 Load Effects on Seismic Behavior - Frame Elements....44
2.11 Out-of-Plane and In-Plane Loadings – Masonry Walls 48
CHAPTER 3 PERFORMANCE BASED SEISMIC DESIGN 51
3.1 General 51
3.2 Structural Performance Levels (ATC, 40) 54
3.2.1 Immediate Occupancy Performance Level (S-1)....54
3.2.2 Life Safety Performance Level (S-3)....54
3.2.3 Collapse Prevention Performance Level (S-5) 54
3.3 Pushover Analysis Using ETABS....55
3.3.1 Purpose of Doing Pushover Analysis 55
3.3.2 Defining how nonlinearity is considered....57
3.3.3 Determining Analysis Cases....58
3.3.4 Defining Loading....58
3.3.5 Selecting the Type of Load Control....59
3.3.6 Analysis Results....60
3.4 Nonlinear Static Procedures....60
3.4.1 Displacement Coefficient Method....61
CHAPTER 4 STRUCTURAL MODELING....64
4.1 Overview 64
4.2 Building Description 64
4.3 Structural configuration 66
4.3.1 Different arrangement of the Building Models....66
4.4 Structural Modeling and Analysis....72
4.4.1 Material Properties to be used....73
4.4.2 Load cases Used....74

4.4.3 Modeling of masonry infill 75
4.4.4 Modeling of Equivalent Strut 76
4.5 Plastic Hinge Placement 77
4.6 Rigid End Offsets 79
4.7 Nonlinear Pushover Analysis Method 80
CHAPTER 5 RESULTS AND DISCUSSIONS 81
5.1 GENERAL 81
5.2 Analysis Results for Push(Load Pattern Acceleration X-Dir) 81
CHAPTER 6 CONCLUSIONS AND RECOMMENDATIONS 93
6.1 Conclusions 93
6.2 Future Recommendations 94
REFERENCES 96
APPENDIX- A: VERIFICATION OF PUSHOVER ANALYSIS 100
APPENDIX- B: MODELING THE FRAME 101
APPENDIX- C: TABULATED RESULTS 107

LIST OF TABLES

Table 1.1 FEMA building categories.----------2
Table 2.1 Behavior Modes for Solid Infilled Panel Components ----------27
Table 2.2 Formulae for width of equivalent diagonal strut----------31
Table 5.1 Comparison of axial force for different models----------79
Table 5.2 Tabular data for the number of hinges in each state of fully infilled frame----83
Table 5.3 Tabular data for the number of hinges in each state of bare frame model-----83
Table A.0.1 Displacement summary----------95
Table B. 0.1 Physical properties of the frame and infill panel----------101
Table C. 1.1 Comparison of Monitored Displacement vs Base shear ----------98
Table C. 1.2 Comparison of story displacement for different models----------98
Table C. 1.3 comparison of story shear for different model----------99

LIST OF FIGURES

Figure. 1.1 Behaviour of infilled frames (Govindan,1986) 4
Figure 1.2 Plan of office building.....9
Figure 2.2 Stress -strain behavior of masonry prism Paulay and Priestly,1992 18
Figure.2.3 Failure mechanism for masonry prisms(Paulay and Priestly,1992).....18
Figure 2.4 Mohr's failure criterion for a masonry unit(Paulay and Priestly,1992) 19
Figure.2.5 Transverse equilibrium of masonry unit and mortar in prism(Paulay and Priestly,1992).....20
Figure 2.6 Bare frame (left) and the same frame with infill in all stories except ground (right) 22
Figure 2.7 Pushover curve comparison for the bare and infilled frames.....23
Figure 2.8 Displacement profile comparison for the bare and infilled frames 23
Figure 2.9 (a) Predominant frame action (b) Predominant truss action(Catherin Jeselia)24
Figure 2.10 Knee-braced frame model for sliding shear failure of masonry infill(Paulay and Priestly,1992).....25
Figure 2.11 Masonry failure with X-shaped cracks due to the R/C frame inter-storey drift(Penils and Kappos,1997) 26
Figure 2.12 Various modes of failure (El – Dakhakhni 2003) 27
Figure 2.13 Equivalent diagonal strut(.Ghassan Al-Chaar).....31
Figure 2.14 Strut geometry(Ghassan Al-Chaar). 32
Figure 2.15 Placement of strut (Ghassan Al-Chaar). 34
Figure 2.16 Partially infilled frame(Ghassan Al-Chaar).....35
Figure 2.17 Perforated panel(Ghassan Al-Chaar).....36
Figure 2.18 Possible strut placement for perforated panel(Ghassan Al-Chaar).. 36
Figure 2.19 Visual damage classification. 38
Figure 2.20 Specimen deformation shape.....39
Figure 2.21 Shear failure of masonry(Ghassan Al-Chaar). 41
Figure 2.23 Gravity Load Effects on Seismic Behavior of Components(Paulay and Priestley, 1992) 45
Figure 2.24 Effects of lateral forces on a building (Paulay and Priestley, 1992) 46
Figure 2.25 Generalized Load-Deformation Relations for Non-degrading Components.(ATC-40,1996) 47

Figure 2.26 Idealized Flexural Mechanisms in Multi-story Frames(ATC-40,1996).....48
Figure 2.27 Response of a masonry wall to biaxial excitation (Paulay and priestly,1992)49
Figure 2.28 Wall out-of-plane mode shapes and periods of a three-story masonry(Paulay and Priestly,1992).....50
Figure 4.2 Elevation view. a) For Fully infilled frame b) For bare frame.....67
Figure 4.3 Plan View Model 2.....68
Figure 4.5 plan View of Model 3.....70
Figure 4.6 Plan view of Model 4 71
Figure 4.8 Eccentric Compression Strut Connections.....76
Figure 4.9 Distance to beam hinge(Ghassan Al-Chaar). 78
Figure 4.10 Plastic hinge placement(Ghassan Al-Chaar).....79
Figure 4.11 Rigid end offset placement(Ghassan Al-Chaar).....80
Figure 5.1 Schematic illustration of the process of estimating target displacement using the Displacement coefficient method, for a given response spectrum and effective period, T83
Figure 5.2 pushover analysis result for 10-story RC building.....84
Figure 5.5 Typical failure mode observed for bare frame at step 10.....90
Figure 5.6 Typical failure mode observed for fully infilled frame at step 10.....90

CHAPTER 1 INTRODUCTION

1.1 Background

This study builds on a number of experimental and analytical efforts to evaluate the effect of masonry infill panels on the seismic behavior of frame structures. Masonry is one of the oldest construction materials currently in use around the world for reasons that include accessibility, functionality, and cost. Masonry infill typically consists of brick, clay tile or concrete block walls, constructed between columns and beams of a RC frame. This material has been used for hundreds of years in construction projects ranging from simple roadways to complex arch designs. Masonry has also commonly been used in frame building structures as infill, where it was intended to act as an environmental divider rather than a structural element. The primary function of masonry was either to protect the inside of the structure from the environment (rain, snow, wind, etc.) or to divide inside spaces.

Extensive research has been done during the last 50 years to determine how the presence of masonry infill influences the in-plane and the out-of-plane behavior of steel/reinforced concrete frame structures (building types 7 or 10 as classified by the Federal Emergency Management Agency **(FEMA310)[50**] in Table 1.1.Experimental research on specimens ranging from full size to 1:8 scale with varying numbers of bays and stories, in addition to analytical work ranging from simple mechanics to complex nonlinear finite element analyses, have yielded great insight into infill-frame interaction and behavior.

Table 1.1 FEMA building categories.

Type	Building Description
1	Wood Light Frames
2	Wood Frames, Commercial and Industrial
3	Steel Moment Frames
4	Steel Braced Frames
5	Steel Light Frames
6	Steel Frames with Concrete Shear Walls
7	Steel Frames with Infill Masonry Shear Walls
8	Concrete Moment Frames
9	Concrete Shear Wall Buildings
10	Concrete Frames with Infill Masonry Shear Walls
11	Precast/Tile-up Concrete Shear Wall Buildings
12	Precast Concrete Frames
13	Reinforced Masonry Bearing Wall Buildings with
14	Reinforced Masonry Bearing Wall Buildings with Stiff
15	Unreinforced Masonry Bearing Wall Buildings

1.2 Statement of the Problem

Infill have been generally considered as non-structural elements, although there are codes such as the Eurocode-8 that include rather detailed procedures for designing infilled R/C frames, presence of infill has been ignored in most of the current seismic codes except their weight. However, even though they are considered non-structural elements the presence of infill in the reinforced concrete frames can substantially change the seismic response of buildings in certain cases producing undesirable effects (tensional effects, dangerous collapse mechanisms, soft story, variations in the vibration period, etc.) or favorable effects of increasing the seismic resistance capacity of the building.

The present practice of structural analysis is also to treat the masonry infill as non- structural element and the analysis as well as design is carried out by only using the mass but neglecting the strength and stiffness contribution of infill. Therefore, the entire lateral load is assumed to be resisted by the frame only.

Contrary to common practice, the presence of masonry infill influence the over- all behavior of structures when subjected to lateral forces.When masonry infill are considered to interact with their surrounding frames, the lateral stiffness and the lateral load capacity of the structure largely increase.

Previous experimental and analytical studies also carried out on the behavior of RC frames with in-fills and the modeling, analysis of the RC frame with and without in-fills. **Stafford- Smith B[2]** used an elastic theory to propose the effective width of the equivalent strut and concluded that this width should be a function of the stiffness of the in-fill with respect to that of bounding frame. By analogy to a beam on elastic foundation, He defined the dimensionless relative parameters to determine the degree of frame in-fill interaction and thereby, the effective width of the strut. Also defined the formulation of empirical equations for the calculation of infill wall parameter as strut model like contact length of strut, effective width of the strut. **Holmes[7]** was the first in replacing the infill by an equivalent pin- jointed diagonal strut. He proposed the modeling of infill wall as the diagonal strut and finding the effective width and contact length of the diagonal strut. A **Das and C.V.R. Murty[28]** carried out non-linear pushover analysis on five RC frame buildings with brick masonry in-fills found to increase the strength and stiffness of the structure, and reduce the drift capacity and structural damage. In-fills reduce the overall structure ductility, but increase the overall strength. Building designed by the equivalent braced frame method showed better overall performance.

The infill may be integral or non-integral depending on the connectivity of the infill to the frame. In the case of buildings under consideration, integral connection is assumed. The composite behavior of an infilled frame imparts lateral stiffness and strength to the building. The typical behavior of an infilled frame subjected to lateral load is illustrated in Figures 1.1 (a) and (b).

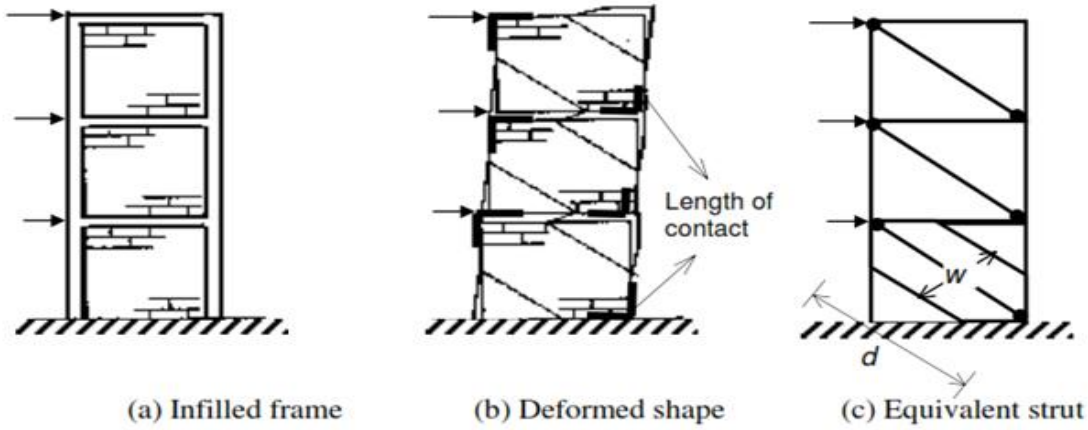

Figure. 1.1 Behaviour of infilled frames (Govindan,1986)

Nowadays the structural engineers and researchers are accepted that infill wall or masonry wall is effective in enhancing the strength and rigidity of the structure. But there is no any provisions for infill wall in EBCS code and also properties, advantages, disadvantages and limitation are not clearly define. So in this study a lot of research work and developments regarding with infill wall considering all point of view of structural design is undertaken for evaluating the seismic performance of bare and infilled frames for in-plane loading. This can be done by making some models in the commercial software **ETABS2015 [23]**.

The recent advent of structural design for a particular level of earthquake performance, such as immediate post-earthquake occupancy, (termed performance based earthquake engineering), has resulted in guidelines such as **ATC-40 (1996)[26], FEMA-273** (1996)**[44]** and **FEMA-356 (2000)** [**25]** and standards such as **ASCE-41 (2006)**, among others. The different types of analyses described in these documents, pushover analysis comes forward because of its optimal accuracy, efficiency and ease of use.

Pushover analysis gives necessary insight into nonlinear behavior without the additional complexities of nonlinear dynamic analysis. Pushover analysis is a static, nonlinear procedure in which the magnitude of the structural loading is incrementally increased in accordance with a certain predefined pattern. As the load increases, the structure begins to yield and become damaged, and the structural deficiencies and failure modes of the building become apparent. The loading is monotonic (i.e., in a single direction) with the effects of the load reversals that occur during a real earthquake being estimated by using

modified monotonic force-deformation criteria and with damping approximations. The goal of static pushover analysis is to evaluate the real strength of the existing structure, rather than to give the lower bound strength for design.

The pushover analysis can be considered as a series of incremental static analyses carried out to examine the non-linear behavior of structure, including the deformation and damage pattern. The procedure consists of two parts. First, a target displacement for the structure is established. The target displacement is an estimate of the seismic top displacement of the building, when it is exposed to the design earthquake excitation. Then, a pushover analysis is carried out on the structure until the displacement at the top of the building reaches the target displacement. The extent of damage experienced by the building at the target displacement is considered to be representative of the damage experienced by the building when subjected to design level ground shaking. A judgment is formed as to the acceptability of the structural behavior for the design of the new building, or the level of damage of an existing building for evaluation purposes.

In the conclusion the effect of infill walls on seismic behavior of a two sample frames with different infill arrangements was investigated.The results yield the following conclusions.

- It is essential to consider the effect of masonry infills for the seismic evaluation of moment resisting RC frames, especially for the prediction of its ultimate state.

- Infills having no irregularity in elevation have beneficial effect on buildings. In infilled frames with irregularities, such as soft story, damage was found to concentrate in the levels where the discontinuity occurs.

- Since infills increases lateral resistance and initial stiffness of the frames they appear to have a significant effect on the reduction of the global lateral displacement.

- Arrangement of infills may effect the post yield behavior and has an influence on distribution and sequence of damage formation. To generalize this, more infill arrangements should be investigated.

- A carefully performed pushover analysis can provide insight into structural aspects that control performance of the structure during a severe earthquake.
- The choice of the static load distribution used in pushover analysis can affect the accuracy of the response estimates

Due to the reasons mentioned above, this research focuses on nonlinear static analysis with an emphasis on RC frame buildings with masonry infill walls. Pushover analysis is demonstrated using the computer software ETABS, which was developed by Berkeley, California-based Computers and Structures Inc. and is one of several available software programs with the capability to conduct pushover analysis.

In this present paper five models of office building with different configuration of masonry infill are generated with the help of ETABS 2015 and effectiveness has been checked. Pushover analysis is adopted for the evaluation of the seismic response of the frames. Each frame is subjected to pushover loading case along negative X-direction. The results are briefly presented and compared. The results yield that it is essential to consider the effect of masonry infills for the seismic evaluation of lateral load resisting RC frames, especially for the prediction of its ultimate state, infill having no irregularity in elevation have beneficial effect on buildings and infills appear to have a significant effect on the reduction of global lateral displacements.

1.3 Objective

The present study focuses on the Seismic Performance of bare frame and infilled frame with different arrangement of masonry infill for multi-story reinforced concrete building, utilizing pushover analysis of nonlinear simulation models.

The specific objectives of the study are:

- To investigate the effects of different arrangement of the masonry wall on the overall seismic response of the reinforced concrete building.
- To identify the effect of masonry walls on reinforced concrete building by generating earthquake response parameters; base shear vs roof displacement, Story displacement, Story shear, member forces.

- To examine how the presence of masonry infill affects seismic collapse risk and seeks to identify design characteristics of vulnerable infilled reinforced concrete frame.

1.4 Materials and Methods

The objective of the research was achieved in accordance with the method outlined below.

I .Literature review: The resource for this thesis work is completely dependent on literatures. Therefore the first three chapters are adopted from literatures to clarify the analysis carried out. Chapter 2 mainly deals with the history of development of masonry infill model and their failure modes and also the effect of seismic load on the masonry infilled reinforced concrete structure. Lateral load resistance evaluated by the stiffness of the frame elements also has been explained. Chapter 3 is concerned with the explanation of performance based seismic analysis method.

II. Data analysis*:* For the hollow concrete block masonry infill walls the frame and the wall connection is assumed to be tight in order to include masonry elements in the model of the physical structure. The study was done with the prevalent construction materials being used in Ethiopia.

Thus, the required material data necessary to make the analytical model of the hollow concrete (HCB) masonry infill were collected from the building code of Ethiopia (**ESEN1996**)[40]

III. Methodology Adopted

Seismic performance is predicted from nonlinear simulation models of non-ductile RC frame buildings with different configuration of masonry walls. Design and detailing characteristics of case study buildings are based on **Eurocode-2005** of 10-story frame buildings with different infill configurations. Models for masonry walls and RC beams, columns and joints have material and geometric nonlinear properties for simulation of sideway collapse. Collapse is predicted through incremental static analysis of nonlinear

simulation models. This analysis provides metrics of seismic safety for this type of building.

For the present study, the frame and the masonry wall connection is assumed to be tight in order to include masonry elements in the model of the physical structure. The frame structure has moment resisting joints. The columns are modeled as a frame element which has the capability to deform axially, in shear, in bending and in torsion. A rigid joint diaphragm action to resist lateral force is taken into account. The beam plus the slab system are assumed to form rigid horizontal elements so that it can be modeled as shear frame for simplified analysis.

Eccentric equivalent struts type of modeling of masonry infill were chosen for this study because, when an infilled frame is loaded laterally, the columns take the majority of the forces exerted on the frame by the infill. Furthermore, the loss of a column is much more detrimental to a structure than the loss of a beam. Therefore, for ultimate capacity purposes, failure was assumed to occur when the columns failed from the infill forces. These forces act as a result of separation of the frame from the infill due to lateral loading. The equivalent struts were estimated using equations derived by **Mainstone (1971)**[4] and **Stafford-Smith and Carter (1969)[2].**

This research focuses on nonlinear static analysis with an emphasis on RC frame buildings with masonry infill walls. Pushover analysis is demonstrated using the computer software ETABS 2015, which was developed by Berkeley, California-based Computers and Structures Inc. and is one of several available commercial software programs with the capability to conduct pushover analysis to study performance based seismic analysis.

The mathematical model should be subjected to monotonically increasing lateral loads until the maximum displacement of the design earthquake is reached or a failure mechanism forms. The target displacement should be calculated following the procedure of **FEMA 273[44]**.Gravity loads should be applied as initial conditions prior to the earthquake loadings.

A building considered for the present study is the office building having (G+9) stories reinforced concrete frame having typical floor height and similar properties of the structures shown in **figure 1.2**

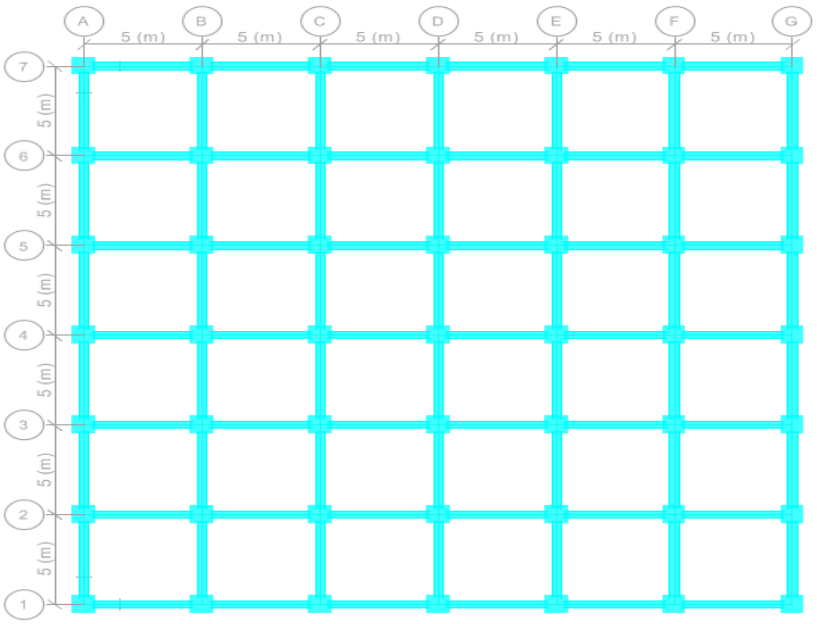

Figure 1.2 Plan of office building

The frame should be modeled according to standard modeling procedures for RC frames in different condition such as **bare reinforced concrete frame**, **reinforced concrete frame with 75% masonry wall reduced from fully infilled**, **reinforced concrete frame with 50% of masonry wall reduced fully infilled frame**, **reinforced concrete frame with 25% of masonry wall reduced from fully infilled frame** and **fully infilled reinforced concrete frame.** Which have been analyzed and designed by ETABS 2015 in accordance with Eurocode-2005 which have similar design provisions with current Ethiopian building code. These analytical models are for frames with infills that have openings and are in full contact with the surrounding frame elements.

1.5 Scope of the Present Study

The procedures presented in this document are applicable to all building structures that have been constructed using reinforced concrete frame structures with unreinforced hollow concrete block (HCB) masonry infill wall. These types of structures correspond to Building Type 10 in accordance with **FEMA 310**[50].

A building considered for the present study is the office building having (G+9) stories reinforced concrete frame having typical floor height and similar properties of the structures without significant setback and infill thickness of 20cm and 15cm in cement sand mortar ratio 1:3.

This research focuses on nonlinear static analysis and the work is based on the **Eurocode-2005**. Hence, the new Ethiopian Building Code Standard is similar with it.

This study only deals with the in-plane stiffness and strength of masonry infill Macro models of infill panels are considered for the simplified analysis.

The Masonry in filled frame is analyzed using ETABS 2015 software up to the failure and the load deformation curves. In this study default hinges are used for frames and user defined hinges for masonry wall.

The present study is concerned only with the macro models of infill panels and the equivalent struts were estimated using equations derived by **Stafford- Smith** and **Carter (1969)[2]** for their consistently accurate predictions of infilled frame in-plane behavior when compared with experimental results **(Ghassan Al-Chaar)[29]**

1.6 Organization of the Thesis

The thesis is organized as per detail given below:

Chapter 1: Introduces to the topic of thesis in brief.

Chapter 2: Discusses the literature review i.e. the work done by various researchers in the field of effect of infill on seismic performance of masonry in filled frames and modeling of structural members by pushover analysis.

Chapter 3: In this chapter Performance based earthquake engineering philosophy is introduced

Chapter 4: Deals with the details of the structure modeled in ETABS 2015.

Chapter 5: The results from the analysis, comparison between the RC frames with and without the masonry walls all are discussed in this chapter.

Chapter 6: Finally, salient conclusions and recommendations of the present study are given in this chapter followed by the references and appendix.

CHAPTER 2 LITERATURE REVIEW

2.1 General

A large number of buildings now days are constructed with masonry infills for commercial, industrial and multi-family residential uses in seismic-prone regions for functional and architectural reasons. Masonry infill typically consists of brick, clay tile or concrete block walls, constructed between columns and beams of a RC frame. Usually the RC frame is filled with hollow concrete block (HCB) as non- structural wall for partition of rooms, Social and functional needs for vehicle parking, shops, reception etc. are compelling to provide an open first story in high rise building. These buildings are generally designed as framed structures without regard to structural action of masonry infill walls. They are considered as non-structural elements. Due to this in seismic action, RC frames purely acts as moment resisting frames leading to variation in expected structural response. In reality the presence of infill wall changes the behavior of frame action into truss action thus changing the lateral load transfer mechanism **Patnala V [27]** .Infill walls tend to interact with the frame when the structure is subjected to lateral loads, and also exhibit energy-dissipation characteristics under seismic loading. Masonry walls contribute to the stiffness of the frame under the action of lateral load. The term 'infilled frame' is used to denote a composite structure formed by the combination of a moment resisting frame and infill walls.

To provide a detailed review of the literature related to modeling of structures in its entirety would be difficult to address in this chapter. A brief review of previous studies on the seismic performance of RC frames with masonry walls and application of pushover analysis of structures is presented is this section.

This literature review focuses on recent contributions related to seismic performance of RC frames with masonry walls and application of pushover analysis of structures and past efforts most closely related to the needs of the present work.

2.2 Components of Masonry Infilled RC Frame

Infilled frame elements are made up of infilled-panel and frame components. Infilled panels are categorized according to the material and geometric configuration. Hollow concrete block (HCB) is the most common and traditional type of infill. Most often it is unreinforced except in modern buildings where it may be reinforced, grouted-cavity wall construction (**FEMA 356, 1998**)[25]. At still a relatively modern form of unreinforced masonry infill construction hollow clay tile (HCT) is used. Concrete masonry unit (CMU) is also the commonest form using hollow concrete blocks laid up with mortar. CMU may be left hollow or filled with grout. Concrete with usual minimal reinforcement is also used as infill.

Infills have a wide variety of geometric configurations. Aspect ratios (length/height) for infilled panels usually vary from approximately 1:1 to 3:1 with most ranging from 1.5:1 to 2.5:1. For the sake of partition and/or facade suiting, infills can be configured in varied forms. There may be eccentricity between the frame components and infill axes. Based on geometric configuration there are two categories for infilled panel components - solid panels and panels with openings. Doors and windows are the two most prevalent opening types.

The frame components are categorized primarily by material. Steel frames are popular for modern high rise buildings and low-rise, light-weight, commercial building constructions. Most often I-sections or wide flange sections are used. Many of the steel frame elements are enclosed by concrete. Because of the relatively high shear capacity of steel columns, the fully restrained mode of behavior may be dominant.

Concrete frames are also common forms of construction: they may be classified as either ductile or non-ductile. Ductile detailing requires closely spaced transverse hoops in the beams, columns and connections. When infills are present, shear force demands are considerably higher leaving the beam or column vulnerable to shear failure. Precast, prestressed,concrete frames are also commonly encountered with infilled panels.

2.3 Effect of masonry infill on the seismic behavior of frame structures.

Reinforced concrete (RC) frame buildings with unreinforced masonry (URM) infill walls are commonly built throughout the world, including in seismically active regions. URM infill walls are widely used as partitions throughout Ethiopia, and despite often being considered as non-structural elements, they affect both the structural and non-structural performance of RC buildings. Structural engineers recognize that many buildings of this type have performed poorly and have even collapsed during recent earthquakes in Turkey, Taiwan, India, Algeria, Pakistan, China, Italy and Haiti, as Figure 2.1 shows. **(M. Selim Gunay) [30].**

Figure 2.1 Masonry infill-related damage in recent earthquake

(Ghassan Al-Chaar)[29]. Masonry infill panels should be evaluated in both the in-plane and out-of-plane direction while accounting for the effects of out-of-plane loading on in-plane capacity. In general, infills can be grouped into two different categories: isolated infills and "regular" infills (sometimes referred to as shear infills). Isolated infills are

panels totally isolated from the confining frame at the top and on both sides. The isolation (gaps) between the infill and the frame must be greater than any possible deformation expected by the frame, thus prohibiting any infill/frame interaction. These infills are not considered as structural elements.

This report focuses on the second category, "regular" infills, where the panels act as part of the lateral force-resisting system of the structure. An infill in this category must be fully in tight contact with its confining frame on all four of its sides. Any gaps must be completely filled to guarantee full mortar bonding contact.

However, contrary to the experience gathered from these earthquakes, these buildings continue to be built in many seismic regions around the world.

Particularly in countries with emerging economies, vulnerable infilled frame buildings continue to be built at a rapid rate in order to keep up with urban population growth and contribute greatly to increased global earthquake risk. When the seismic vulnerabilities present in the RC system (such as lack of confinement at the beam and column ends and the beam column joints, strong beam-weak column proportions, and presence of shear-critical columns) are combined with the complexity due to the interaction of the infill walls and the surrounding frame and the brittleness of the URM materials, non- ductile RC frames with URM infill walls may be considered as one of the world's most common types of seismically vulnerable buildings. Therefore, it is essential to apply existing knowledge on the behavior of this complex structural system to develop proper modeling techniques and adequate retrofit methods.

URM infill walls are generally treated as non- structural elements which are used mainly for architectural purposes. However, many researchers (**e.g., Humar et al., 2001[33]**; **Korkmaz et al., 2007[19]**) and the experiences in past earthquakes have shown that the presence of URM walls changes the seismic response of framed building.

The URM walls function as structural elements, and they may have beneficial or detrimental effects. Infill walls contribute to the lateral force resisting capacity and damping of the structure up to a certain level of structural response. They increase the initial stiffness and decrease the initial period of the structure, which might be beneficial or detrimental depending on the frequency content of the experienced ground motion.

URM infill walls are prone to early brittle failure. Infill walls interacting with frames tend to alter the building's overall strength and stiffness distribution. This may be despite the design intent of the engineer, because infill walls are typically considered as "non-structural" and therefore neglected in the frame design. Many buildings have a soft story created by commercial space (shops) or parking at the ground floor (**Figure 2.1a and b**). Even in buildings without open spaces at the ground floor, brittle infill wall failure may lead to the formation of a weak and soft story during ground shaking in buildings that would have otherwise not had one (**Figure 2.1c and d**). In addition, infill walls interact with the surrounding frame in such a way that column shear failure is made more likely (**Figure 2.1e).** Infill walls can also induce torsion when some sides of the building have solid infill walls and the other sides have either infill walls with openings or no infill walls for architectural or usage purposes (**Figure 2.1f**).

Considering the severity of the detrimental effects of infill – they can cause collapse – proper modeling of URM infill walls within RC frames is essential for seismic evaluation and consequently for the selection of adequate retrofit solutions to reduce damage and its consequences.

Polyakov (1960)[1] conducted experimental tests on masonry-infilled frames, first proposing that the infill system works as a braced frame, with the wall forming compression "struts"

Holmes (1961)[7] proposed a linear equivalent strut model for computing maximum strength and stiffness of masonry walls.

Stafford-Smith (1962)[2] and Mainstone (1971)[4], among others, proposed methods for calculating the effective width of the diagonal strut, supported by test results from mortar panels and infilled frames, respectively.

Klingner and Bertero (1978) [5] tested a one-third scale 3.5 story representation of an 11-story 1970s-era RC apartment building. Their study concluded that reinforced infill panels reduce the risk of incremental collapse, compared to a bare RC frame.

Dhanaskar and Page (1986)[9] modeled an infilled frame using nonlinear finite brick elements, comparing the results with several half-scale experiments.

Mehrabi et al. (1996)[10] tested twelve ½-scale single-story single-bay frame specimens and observed that the frames with infill showed better seismic performance than the bare frames.

Flanagan and Bennett (1999)[8] used a piecewise-linear equivalent strut to model infill and proposed an analytical procedure to calculate the strength of the infill, based on experimental results of 21 steel frames with clay tile infill walls.

Mehrabi and Shing (1997)[6] used a smeared-crack finite element model to represent masonry units and RC frames, developing a constitutive model for mortar joints.

Ghassan Al-Chaar (2002)[29] provide guidelines for evaluating strength and stiffness of unreinforced masonry (URM) infill panels in military structures subjected to lateral forces.

Stavridis and Shing (2009)[11] have developed a complex nonlinear finite element model for RC frames with masonry infill, combining the smeared and discrete crack approaches to capture different failure modes observed in experiments.

Siamak Sattar and Abbie B. liel(2010)[32], Predicted Seismic performance utilizing Nonlinear analysis models for the RC frame structures consist of the two-dimensional three-bay frame. Concluded the fully-infilled frame has approximately 15 times larger stiffness and 1.5 times greater peak strength than the bare frame.

More recent research has combined analytical and experimental methods to evaluate the seismic performance of RC frames with masonry infill more generally. **Dolsek and Fajfar (2008)[12]** used concentrated plasticity beam-column model elements with equivalent strut wall elements to evaluate the seismic performance of masonry-infilled RC frames, looking at “damage limitation”, “significant damage” and “near collapse” limit states. **Dymiotis et al. (2001)[13]** assessed the seismic vulnerability of a 10-story infilled RC frame at “serviceability” and “ultimate” limit states. **Madan and Hashmi (2008)[14]** evaluated the performance of 7 and 14-story RC frames with masonry infill subjected to near-fault ground motions. **D.V.Mallick and R.T Severn[22],** Investigate the behaviour of five reinforced RC frames with various arrangement of infill when subjected to dynamic earthquake loading. Concluded providing infill wall in RC building controlled the displacement, storey drift and lateral stiffness. **Mohammad H.**

Jinya V. R,[31] Analysis of Bare Frame and Infilled Frame with Different Position of Shear wall by making some models in the software STADDProV8i and the Comparative study made for different models in terms of story drift and column axial force. Concluded the axial force of the bare frame is maximum than the infilled frame. But when shear wall provided in bare frame and infilled frame it will help to reduce axial force significantly in bare frame and infilled frame.Infilled frame type structural system become economical as compared to the Bare Frame structural system. **D. B. Karwar and Dr. R. S. Londhe(2014)[15],** Investigate the behaviour of Reinforced Concrete framed structures by using nonlinear static procedure (NSP) or pushover analysis in finite element software "SAP2000".and the Comparative study made for different models in terms of base shear, displacement, performance point. Concluded base shear is minimum for bare frame and maximum for frame with infill for G+8 building.

The assessment of RC frames with masonry infill panels here simulates structural collapse, evaluating life safety with nonlinear models and limit-state checks. Performance-based earthquake engineering techniques account for uncertainties in ground motions and modeling.

2.4 Load Effects on Masonry Walls and Frames

2.4.1 Strength of Masonry Units

It is less easy to predict the compressive strength of masonry as it depends on the properties of the masonry units, the mortar and the grout. As a consequence, most masonry design codes specify low design values for compressive strength f'_m unless prism tests are conducted to confirm higher values.

The compressive strength of the hollow concrete block may vary from as low as 1MPa for low quality hollow concrete blocks to over 100 MPa for high-fired ceramic clay units. A minimum strength of about 1MPa is typically required by design codes**(ESEN1996,2015)[40].**The strength of mortar test specimens bears little relationship to mortar strength in the wall, because of absorption of moisture from the mortar by the masonry units.

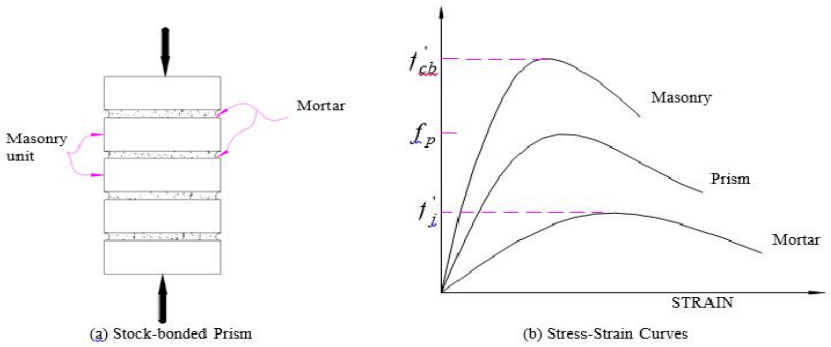

Figure 2.2 Stress -strain behavior of masonry prism Paulay and Priestly,1992

The combined effects of lower modulus of elasticity and higher Poisson's ratio result in a tendency for lateral mortar tensile strains to greatly exceed the lateral masonry unit strains. Friction and adhesion at the mortar masonry interface constrains the lateral strains of mortar and masonry unit to be equal. Hence, there will be set up of self-equilibrating lateral forces between compression in the mortar and tension in the masonry unit (Fig. 2.3).

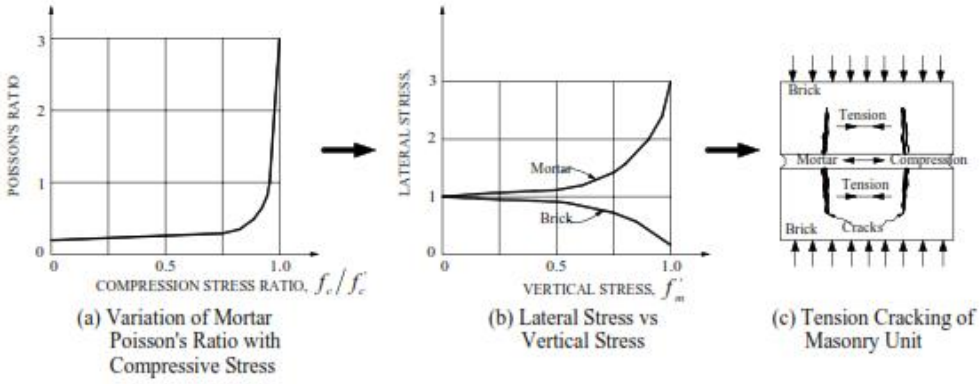

Figure.2.3 Failure mechanism for masonry prisms(Paulay and Priestly,1992)

The resulting tri-axial compressive stress state in the mortar enhances its crushing strength, while the combination of longitudinal compression and lateral biaxial tension in the masonry unit reduces its crushing strength and induces tendency for vertical splitting.

Strength of the confined mortar may be approximated by (Paulay and Priestley, 1992),

$$f'_{cj} = f'_{cb} + 4.1f_1 \quad (2.1)$$

Where;

f'_{cj} - Compressive strength of confined mortar

f'_{cb} - Uniaxial compressive strength of masonry unit.

f_1- Lateral compressive stress developed in the mortar.

Linear failure criterion (after Hilsdorf,1969)

For the masonry unit:

$$\frac{f_x}{f'_{tb}} + \frac{f_y}{f'_{cb}} = 1 \quad \text{---------- (2.2)}$$

Where;

f'_{tb} - Biaxial tensile strength of masonry unit.

f_x- Lateral tensile stress at failure.

f_y- Axial compressive stress at failure.

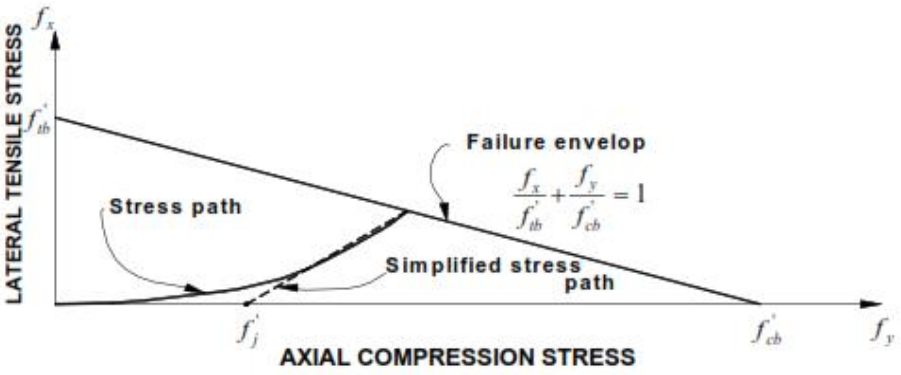

Figure 2.4 Mohr's failure criterion for a masonry unit(Paulay and Priestly,1992)

By considering the transverse equilibrium requirements of a mortar joint of thickness j_t, and a tributary height of masonry unit equal to one-half a masonry unit above and

below the joint in Conjunction with equations (2.1) and (2.2),the longitudinal stress f_p' that causes failure is found to be

$$f_p' = f_y = \frac{f_{cb}'\left(f_{tb}' + \alpha f_j'\right)}{U_u\left(f_{tb}' + \alpha f_{cb}'\right)} \qquad \text{----------} \quad (2.3)$$

$$\alpha = \frac{j_t}{4.1 h_u}$$

Where:

f_j' - compression strength of mortar bed

h_u - height of the masonry unit

U_u - Stress non-uniformity coefficient (U_u = 1.5 ; Hilsdorf ,1969)

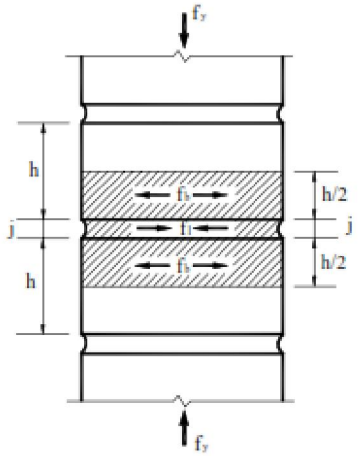

Figure.2.5 Transverse equilibrium of masonry unit and mortar in prism(Paulay and Priestly,1992)

It is advisable to adopt conservatively high value for the modulus of elasticity, E_m, to ensure seismic lateral design forces are not underestimated**,(Paulay and Priestley, 1992):**

2.5 Masonry Infilled Frames and Seismic Behavior of Structures

It is a common misconception that masonry infill in structural steel or reinforced concrete frames can only increase the overall lateral load capacity, and therefore must always be beneficial to seismic performance. In fact there are numerous examples of earthquake damage, some of which are can be traced to structural modification of the basic frame by so called non-structural masonry partitions and infill panels. Even if they are relatively weak, masonry infill can drastically alter the intended structural response, attracting forces to parts of the structure that have not been designed to resist them**(Paulay and Priestley, 1992)[42].**

The presence of masonry infill affects the seismic behavior of buildings in the following ways **(Penelis and Kappos, 1997) [39].**

1. As a consequence of increase in stiffness of buildings, the fundamental period is decreased and the base shear is increased.

2. The lateral stiffness in plan and elevation is modified.

3. The structural system is relieved of seismic action as part of the load is carried by the infills.

4. Energy dissipation capacity of the building is substantially increased.

5. The more flexible the structural system, the greater the above effects of the infills.

The high degree of uncertainties on the analysis of buildings due to effects of infill includes:

1. The variability of their mechanical properties, and hence the low reliability in their strength and stiffness.

2. Tightness when connected to the surrounding frame (wedging condition)

3. The potential modification of their integrity during the use of the building.

4. The non-uniform degree of their damage during the earthquake.

Thus the safety of the structure cannot rely, not even partly, upon the infills and only their probable negative influence is taken into account **(Penelis and Kappos, 1997)[39]**

Consider the following example of the effect of unreinforced masonry infill(**M.SelimGunay)[30]**.He used pushover analysis and compare here the differences in behavior between a bare frame and the same frame with infill walls in all the stories except the first, shown in Figure 2.6 below. The effect of the infill is simulated by a single diagonal compression strut in each bay.

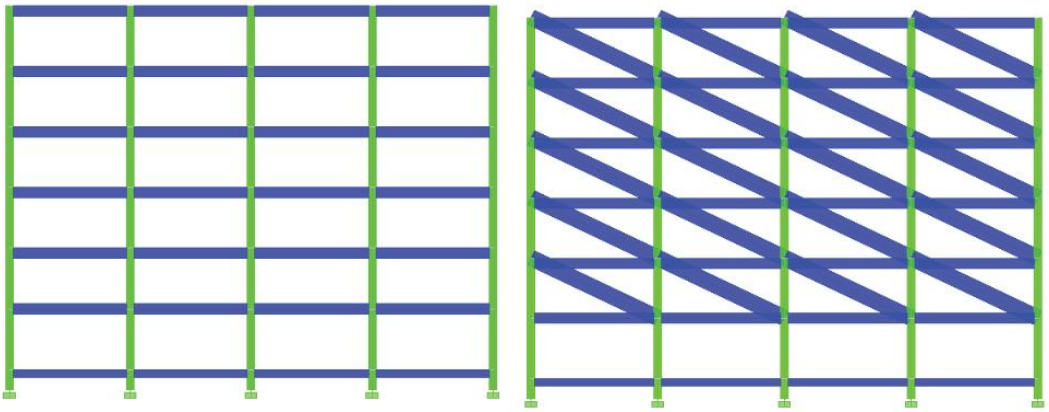

Figure 2.6 Bare frame (left) and the same frame with infill in all stories except ground (right)

The pushover curves are compared in Figure 2.7. The strength and stiffness of the infilled frame is significantly increased due to the presence of infill, but the displacement capacity decreases and a soft story develops, which is evident from the displacement profiles in Figure 2.8. The deformation accumulates in the bottom story – the true behavior during an earthquake – when infill is considered in the analysis, rather than being distributed evenly over all stories when the designer ignores the infill and incorrectly models the building as a bare frame.

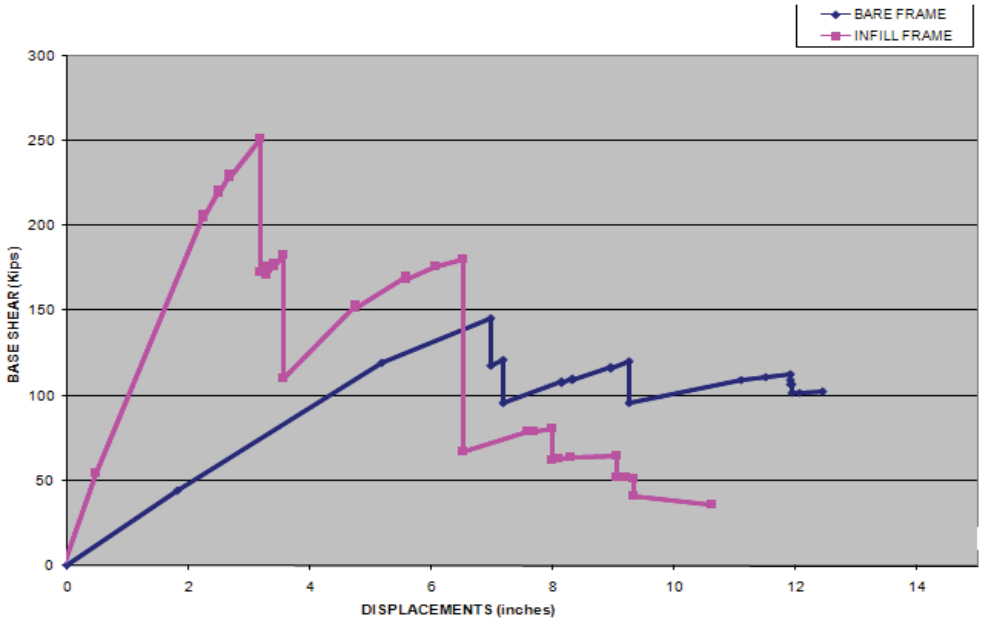

Figure 2.7 Pushover curve comparison for the bare and infilled frames

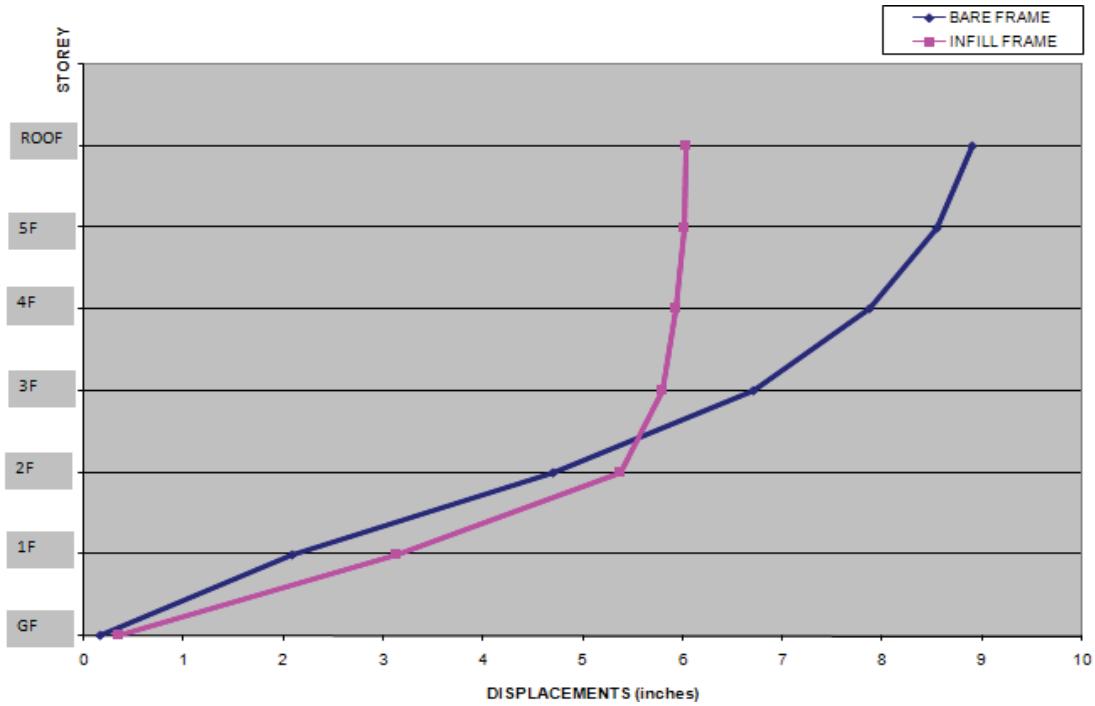

Figure 2.8 Displacement profile comparison for the bare and infilled frames

So, based on these results, infill walls can be beneficial as long as they are properly taken into consideration in the design process and the failure mechanism is controlled (i.e., no weak story is allowed to occur). However, this example also shows that failing to consider infill walls during structural design can lead to deadly weak-story collapses.

Masonry infill have a very high initial in-plane lateral stiffness and low deformability. It contributes to significant lateral stiffness, strength, overall ductility and high energy dissipation capacity; however under seismic loading it can also cause some undesirable effects like torsion, short-column effect, soft-storey effect and out-of-plane collapse. Therefore, under seismic loads, the whole lateral force transfer mechanism of the structure changes from a predominant frame action to predominant truss action which is shown in fig 2.9 a & b**. Catherin Jeselia[18]**

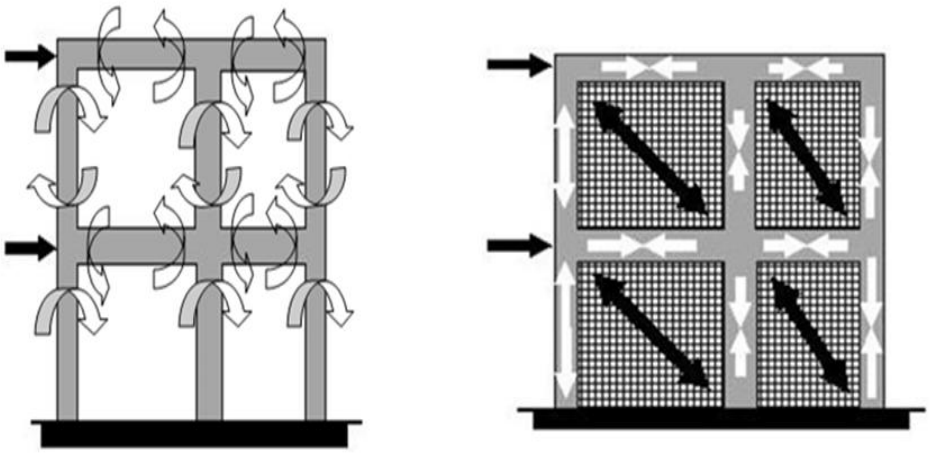

Figure 2.9 (a) Predominant frame action (b) Predominant truss action(Catherin Jeselia)

2.6 Failure Modes of Masonry Infill

Behavior of infilled frame systems subjected to in-plane lateral forces is influenced by mechanical properties of the frame and infill materials, stress or lateral deformation levels, existence of openings in the infill, and the geometrical proportions of the system. Existence of an initial gap between the frame members and the infill also influences the behavior of the system.

Under small deformations the stiffness behavior is dominated by the panel stiffness characteristics **(FEMA 356, 1998)[30].** Hence, the events that define the shape of the force deformation curve are bed-joint sliding, diagonal tension, corner crushing, general shear failure, and out-of-plane failure. As the deformation increases the panel characteristics will be a function of its element properties. Stair-stepped pattern of cracks through head and bed joints will result when the masonry units are strong relative to the mortar. When the mortar is stronger than the units, rather a rare case, cracks will develop through the units as well as the mortar.

i). Bed-Joint Sliding: Bed-joint sliding is likely to occur when the bounding frame is strong and flexible (such as steel frames). If the mortar beds are relatively weak compared to the adjacent masonry units (especially bricks), a plane of weakness forms, usually near the mid- height level of the infill panel. There is really no limit to the displacement capacity of this behavior mode.

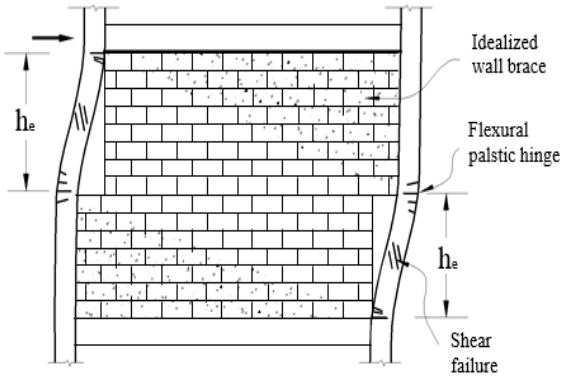

Figure 2.10 Knee-braced frame model for sliding shear failure of masonry infill(Paulay and Priestly,1992)

(ii). Diagonal Cracking: Transverse to the principal compression formed across the diagonal of an infill strains are tension strains. Diagonal cracks are formed as a result of the tensile strain exceeding the cracking strain of the infill panel material. These cracks commence in the center of the infill and run parallel to the compression diagonal. The cracks tend to propagate until they extend from one corner to the diagonally opposite corner. Diagonal cracking behavior usually signals the formation of a new diagonal strut behavior mode.

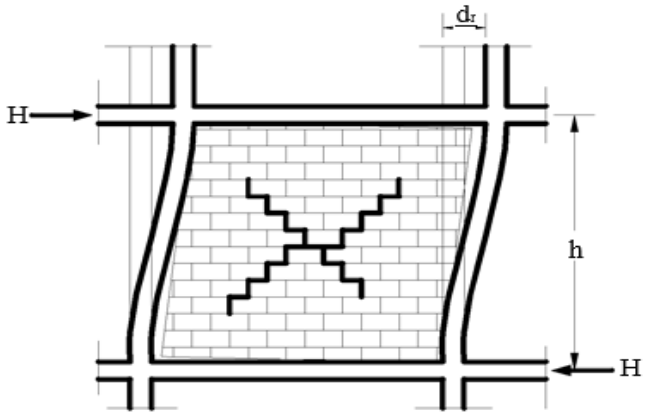

Figure 2.11 Masonry failure with X-shaped cracks due to the R/C frame inter-storey drift(Penils and Kappos,1997)

(iii). Corner Compression: This is because of the high stress concentrations at each corner of the compression diagonal. Corner crushing is located over a relatively small region for strong/stiff columns and beams; whereas for weaker frames, especially concrete frames, corner crushing is more extensive and the damage extends into the concrete frame itself.

(iv). Out-of-Plane Failure: The failure is due to ground shaking transverse to the plane of a wall. Out-of-plane failure may occur in the upper stories of high-rise buildings, where the floor accelerations are basically resonance amplifications of prominent sinusoidal ground motion input. In lower stories, when out-of-plane shear is combined with high in-plane story shears, infill panels tend to progressively "walkout" of the frame enclosure.

(v). Premature Failure of Frame Elements or Connections: Failures of columns, beams, and connections due to compressive "strut" reactions imparted to them by the masonry infill. Another mode of failure of frame elements is the failure of the tension or compression chords of the infill frame acting as a monolithic flexural element. The latter is predominant in cases of slender infilled frame and a single bay infilled in a multi-bayed multistory building.

(vi). Failure of the Frame: The response of the frame with the infill missing should be assessed, keeping in mind the likelihood that a soft story configuration or stiffness eccentricity may have resulted.

Table 2.1 Behavior Modes for Solid Infilled Panel Components (FEMA 306, 1998)

Behavior Mode	Description/Likelihood of Occurrence	Ductility
Bed-joint sliding	Occurs in brick masonry, particularly when length of panel is large relative to height. Aspect ratio is large and mortar strength is low	High
Diagonal cracking	Likely to occur in some form	Moderate
Corner compression	Crushing generally occurs with stiff columns	Moderate
Out-of-plane failure	More likely to occur in upper stories of buildings. However, out-of-plane is likely to occur in the bottom stories, due to concurrent in-plane loading.	Low

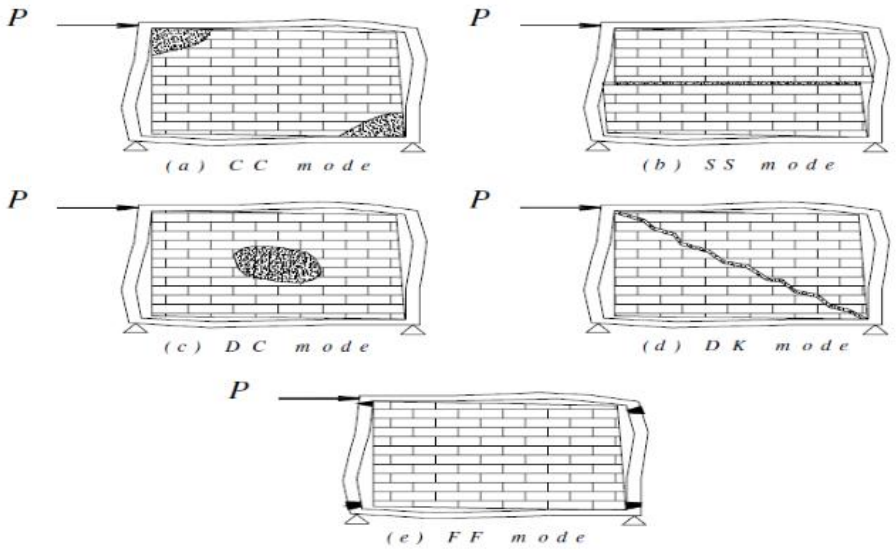

Figure 2.12 Various modes of failure (El – Dakhakhni 2003)

Corner crushing mode (CC), represents crushing of the infill in at least one of its loaded corners. Sliding shear (SS) mode represents the horizontal sliding shear failure through bed joints of a masonry infill. Diagonal compression mode (DC), represents crushing of the infill within its central region. A crack is formed across the compressed diagonal of

the infill panel in Diagonal cracking (DK) mode. Plastic hinges are developed in the columns or in beam-column junctions, which results in the Frame failure (FF) mode.

2.7 Modeling of Masonry infilled walls

Unless masonry infill walls are adequately isolated from the concrete frame members and the floor above, masonry elements shall be included in the model of the physical structure. The mathematical model of the physical structure shall represent the spatial distribution of mass and stiffness of the structure to an extent which is adequate for the calculation of the significant features of its dynamic response.

Masonry exhibits distinct directional properties, due to the influence of mortar joints acting as planes of weakness. Depending upon the orientation of the joints to the stress directions, failure can occur in the joints alone or simultaneously in the joints and blocks. The great number of the influencing factors, such as dimension and anisotropy of the HCB, joint width and arrangement of bed and head joints, material properties of both HCB and mortar, and quality of workmanship, make the simulation of plain HCB masonry extremely difficult.

The following two levels of refinement for masonry models can summarize the analytical procedures (**Asteris et al, 2003**)[36]:

- **Micro models**

Micro-modeling is a complex method of analysis and it is always done by using finite element method. The benefits of using finite element approach is that, all possible modes of failure i.e., all the local effects are discussed in detail but its use is limited due to the greater computational effort and time-requirement. **Mallick** and **Severn[22]** were the first one to use this FEM approach. The interface between frame and infill was modeled by considering frictional shear forces in the contact region using link element. This element was able to transfer compressive forces, but incapable of resisting tensile forces. They identified that the element was able to transfer compressive and bond forces, but incapable of resisting tensile forces. Later two schemes i.e., exact and constrained schemes were suggested by **Axely and Barter[34]** to find the stiffness of frame infill system. These models captured corner crushing with failure in columns, beams and

diagonal crushing of the infill. **Dhanasekar [9]** considered non-linear isotropic six-node elements for both the mortar and the bricks and have developed a model of brick masonry wall considering bricks and mortar joints separately. **Dymiotis C[27], Kappos[13].**proposed a model similar to **Dhanasekar[9]** but with four-node quadrilateral elements with a fine mesh near the loading point was used.

Asteris et al[36]. Used the frame-infill separation criteria to find the geometrical equilibrium condition for the composite structure of the in-filled frame under certain loading conditions. The infill/frame contact lengths and the contact stresses were estimated as an integral part of the solution**. V.K.R.Kodur** [37] verified the analytical procedures of the previous authors with the experimental results of a new model which included interface elements at the frame-infill interface. The results obtained showed that the numerical model was not only capable of predicting the load carrying capacities of infilled frames, but could also provide detailed information on the failure mode, ductility, and cracking. **Das & Murthy[28]** performed a non-linear pushover analysis on five RC frame buildings with brick masonry infill, designed as per Euro code, Nepal Building Code, Indian Codes (IS 456, IS 13920) and by Equivalent Braced Frame (EBF) methods. From the different design procedures as per various codes, the EBF method was found to be very beneficial

- **Macro models**

Macro-models are the ones in which the masonry infill is replaced by an equivalent pin-jointed diagonal strut system. The basic parameter which affects the stiffness and strength of these struts is their equivalent width which depends on the relative infill-frame stiffness. In the literature since then, a number of macro-models have been proposed by other researchers.

2.7.1 Equivalent Strut Width

The evaluation of the equivalent width, *a*, varies from one reference to the other. The most simplistic approaches presented by **Paulay and Priestley (1992**)[42] has assumed constant values for the strut width, *a*, between 12.5 to 25 percent of the diagonal dimension of the infill, with no regard for any infill or frame properties. **Stafford-Smith and Carter (1969)[2], Mainstone (1971)[4],** and others, derived complex expressions to estimate the equivalent strut width, a, that consider parameters like the length of

contact between the column/beam and the infill, as well as the relative stiffness of the infill to the frame.

Polyakov[1] was the first in replacing the masonry infills by an equivalent pin-jointed diagonal strut by experimenting it on steel frames. **Holmes[7]** proposed that the effective width of equivalent strut found to be 1/3rd of the diagonal length of infill panel. **Stafford Smith Smith[3]** studied that the effective width varies from d/4 for a square infill to d/11 for an infill having a side's ratio of 5 to 1, where'd' is the length of the masonry infill. **Stafford Smith[3]** discussed about the interaction between frame and infill, and developed a set of empirical curves that relate the stiffness parameter to the effective width of an equivalent strut.

Liauw and Kwan[45] extended the study of diagonal strut for the masonry infilled frames with and without openings, and concluded that the position of opening greatly affected the strength and stiffness of the infills. **Hendry[46]** also presented the equivalent strut width as half the width proposed by Smith. **Liauw** and **Kwan[45]** studied both experimentally and analytically the behavior of non-integral infilled frames considering the nonlinearities of the material and the structural interface.

Table 2.2 Formulae for width of equivalent diagonal strut

Author	Year	Formulae for width of equivalent diagonal strut		
Holmes	1961	$W = \frac{d_m}{3}$		Where, t = Thickness of Masonry Infill L = Length of Masonry Infill H_m = Height of Masonry Infill E_c = Elastic modulus of concrete E_m = Elastic modulus of masonry I_c = Moment of
Smith	1962	$W = 0.25\,d_m$		
Smith & Carter	1969	$W = 0.58\left(\frac{1}{H}\right)^{-0.445}(\lambda_h H')^{0.335 d_z}\left(\frac{1}{H}\right)^{0.064}$ $\lambda_h = \sqrt[4]{\frac{E_m t \sin 2\theta}{4 E_c I_c H_m}}$		
Mainstone	1971	$W = 0.16 d_m (\lambda_h)^{-0.3}$		
Hendry	1981	W = half the width proposed by Smith (1962)		
Liaw& Kwan	1984	$W = \frac{0.95 H \cos\theta}{\sqrt{\lambda_h H'}}$		
Deccanini&Fantin	1986	Uncracked Masonry	$W = \left(\frac{0.748}{\lambda_h} + 0.085\right) d_m$	

The expressions used in this report for determination of equivalent strut width have been adopted from **Mainstone (1971)[4]** and **Stafford-Smith and Carter (1969)[2]** for their consistently accurate predictions of infilled frame in-plane behavior when compared with experimental results **Mainstone (1971)[4]; Stafford-Smith and Carter 1969[2]; Klingner and Bertero 1978[5]** as stated by the study of **Ghassan Al-Chaar[29].**

The masonry infill panel will be represented by an equivalent diagonal strut of width, *a*, and net thickness t_{eff} as shown in Figure 2.13

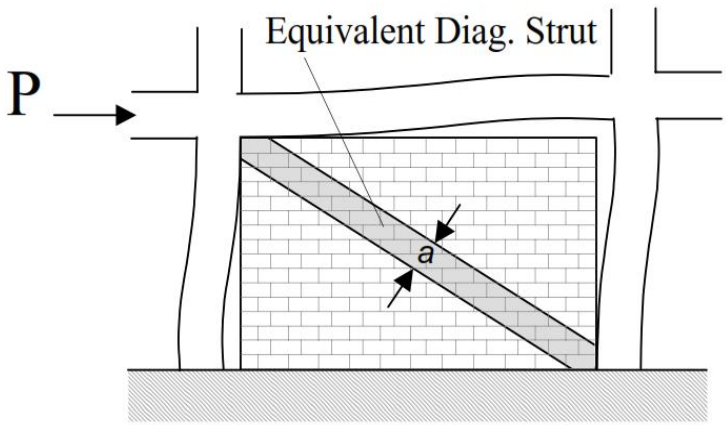

Figure 2.13 Equivalent diagonal strut(. Ghassan Al-Chaar)

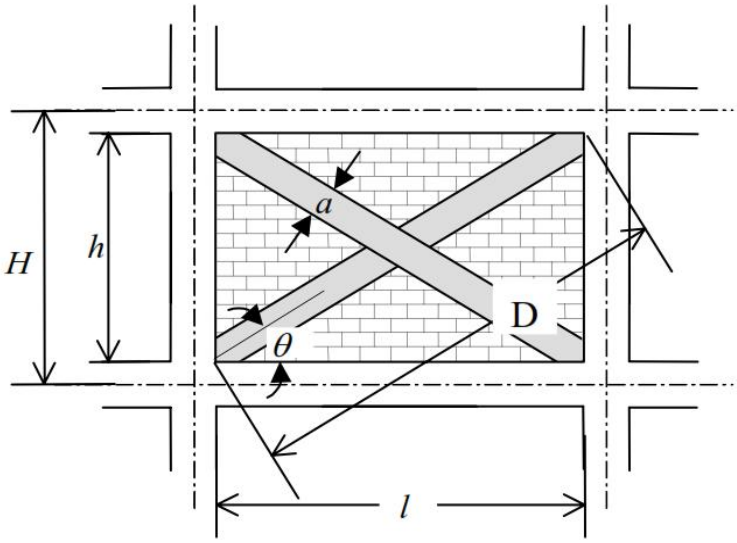

Figure 2.14 Strut geometry(Ghassan Al-Chaar**).**

The equivalent strut width, *a*, depends on the relative flexural stiffness of the infill to that of the columns of the confining frame.The relative infill to frame stiffness shall be evaluated using equation 2.4 **(Stafford-Smith and Carter 1969)[2]:**

$$\lambda_1 = \sqrt[4]{\frac{E_m t \sin 2\theta}{4 E_c I_{col} h}} \quad \text{---------- (2.4)}$$

Using this expression, **Mainstone (1971)[4]** considers the relative infill to frame flexibility in the evaluation of the equivalent strut width of the panel as shown in equation 2.5

$$a = 0.175 D (\lambda_1 H)^{-0.4} \quad \text{---------- (2.5)}$$

Where:

$\lambda_1 = Relative\ infill\ to\ frame\ stiffness\ parameter$

$a =$ Equivalent width of infill strut in the elastic range , cm

$E_m = modulus\ of\ elasticity\ of\ masonry\ material\ in\ compression, MPa$

$E_c = modulus\ of\ elasticity\ of\ confining\ frame, MPa$

I_{column} = modulus of elasticity of masonry material in compression, cm^4

t − Gross thickness of the infill, cm

h = height of the infill panel, cm

θ = Angle of the concentric equivalent strut, radians

D = Diagonal length of infill, cm

H = Height of the confining frame, cm

However, if there are openings present and/or existing infill damage, the equiavalent strut width must be reduced using Equation 2.6

$$a_{red} = a(R_1)_i(R_2)_i \text{------------------} (2.6)$$

Where:

$(R_1)_i$ = reduction factor for in-plane evaluation due to presence of opening defined in the section on perforated panels (equation 2.9).

$(R_2)_i$ = reduction factor for in-plane evaluation due to existing infill damage defined in the corresponding section on (Table 2.3).

2.7.2 Eccentricity of Equivalent Strut

The equivalent masonry strut is to be connected to the frame members as depicted in Figure 2.15. The infill forces are assumed to be mainly resisted by the columns, and the struts are placed accordingly. The strut should be pin-connected to the column at a distance l_{column} from the face of the beam. This distance is defined in Equations 2.7 and 2.8 and is calculated using the strut width, a, without any reduction factors.

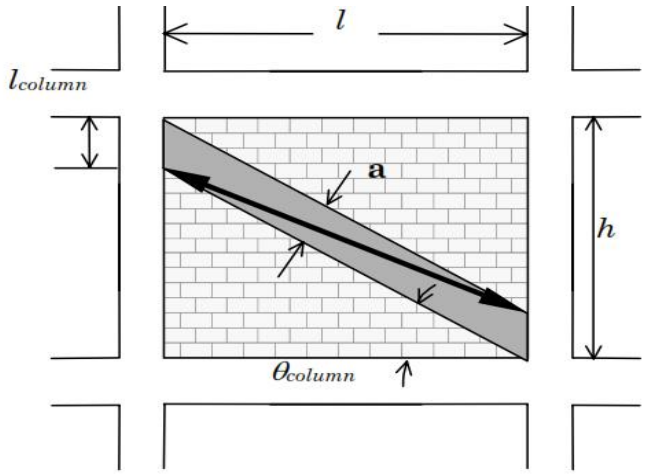

Figure 2.15 Placement of strut (Ghassan Al-Chaar).

$$l_{column} = \frac{a}{cos\theta_{colun}} \quad (2.7)$$

$$tan\theta_{column} = \frac{h - \frac{a}{cos\theta_{colun}}}{l} \quad (2.8)$$

Where:

l_{column} = Distance from the face of the beam to the first beam plastic, cm

l = Length of the infill panel ,cm

θ_{column} = Angle between face of the eccentric equivalent strut and the horizontal if the strut were to be modeled eccentrically along the column ,$radians$

$h = height\ of\ the\ infill\ panel, cm$

a = Equivalent width of infill strut in the elastic range ,cm

Using this convention, the strut force is applied directly to the column at the edge of its equivalent strut width, *a*.

2.7.3 Partially Infilled Frames

In the case of a partially infilled frame, the reduced column length, l_{column}, shall be equal to the unbraced opening length for the windward column, while l_{column} for the

leeward column is defined as usual (Figure 2.16).The strut width should be calculated from Equation 2.9, using the reduced infill height for *h* in Equation 2.1. Furthermore, the only reduction factor that should be taken into account is $(R_2)_i$, which accounts for existing infill damage. **Ghassan Al-Chaar(2002)[29]**

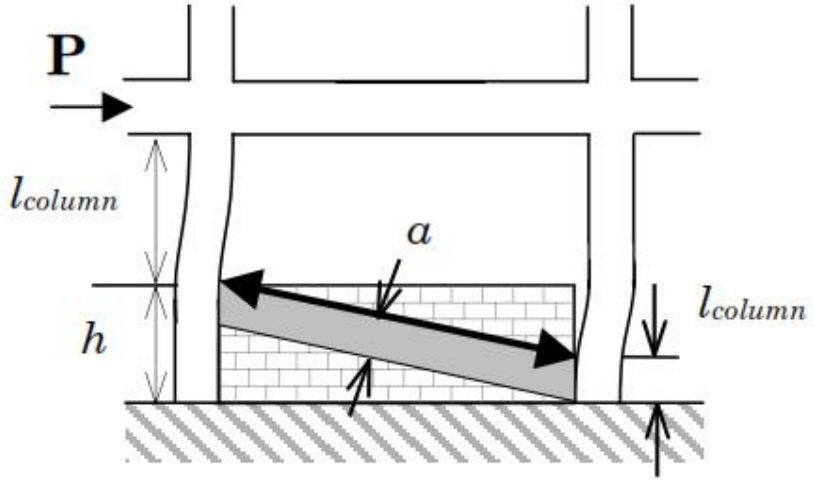

Figure 2.16 Partially infilled frame(Ghassan Al-Chaar)**..**

2.7.4 Perforated Panels

In the case of a perforated masonry panel, the equivalent strut is assumed to act in the same manner as for the fully infilled frame. Therefore, the eccentric strut should be placed at a distance l_{column} from the face of the beam as shown in Figure 2.17.The equivalent strut width, a, shall be multiplied, however, by a reduction factor to account for the loss in strength due to the opening. The reduction factor, (R1)i, is calculated using Equation 2.9. **Ghassan Al-Chaar(2002)[29]**

$$(R_1)_i = 0.6\left(\frac{A_{open}}{A_{Panel}}\right)^2 - 1.6\left(\frac{A_{open}}{A_{Panel}}\right) + 1 \quad (2.9)$$

Where:

A_{open} $-$ *area of the openings* (cm^2)

A_{Panel} = area of the infill panel (cm^2)

Note: If the area of the openings (A_{open}) is greater than or equal to 60 percent of the area of the infill panel (A_{panel}), then the effect of the infill should be neglected, i.e., $(R_I)_i = 0$.

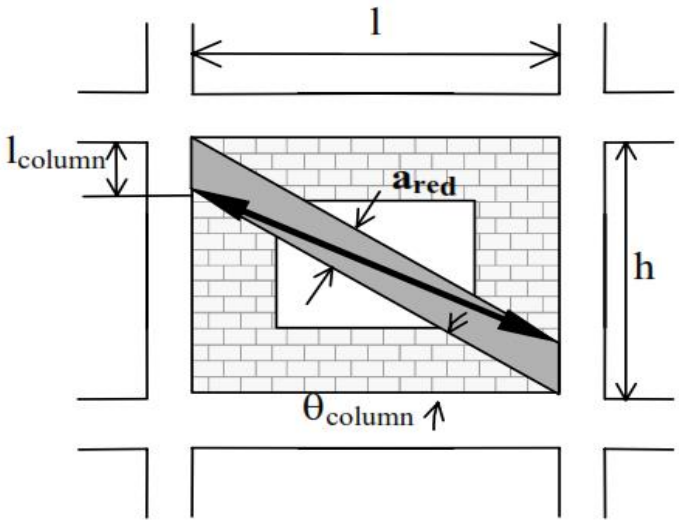

Figure 2.17 Perforated panel(Ghassan Al-Chaar)**..**

Note that reducing the strut width to account for an opening does not necessarily represent the stress distributions likely to occur. This method is a simplification in order to compute the global structural capacity. Local effects due to an opening should be considered by either modeling the perforated panel with finite elements or using struts to accurately represent possible stress fields as shown in figure 2.18

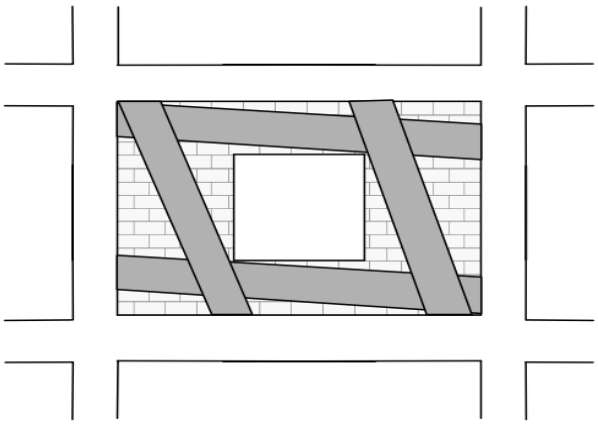

Figure 2.18 Possible strut placement for perforated panel(Ghassan Al-Chaar)**..**

2.7.5 Existing Infill Damage

Masonry infill panel behavior deteriorates as the elastic limit is exceeded. For this reason, it is important to determine whether the masonry in the panel has exceeded the elastic limit and, if so, by how much. The extent of existing infill damage can be determined by visual inspection of the infill. Existing panel damage (or cracking) must be classified as either: no damage, moderate damage, or severe damage as presented in Figure 2.19. If in doubt as to the magnitude of existing panel damage, assume severe damage for a safer (conservative) estimate. A reduction factor for existing panel damage $(R_2)_i$ must be obtained from Table 2.3**(Ghassan Al-Chaar)**..Notice that, if the slenderness ratio (h/t) of the panel is greater than 21, (R2)i is not defined and repair is required. For panels with no existing panel damage, the reduction factor $(R_2)_i$ must be taken as 1.0.

Table 2.3 In-plane damage reduction factor

	$(R_2)_i$ for Type of Damage	
h/t	*Moderate*	*Severe*
≤ 21	0.7	0.4
> 21	Requires Repair	

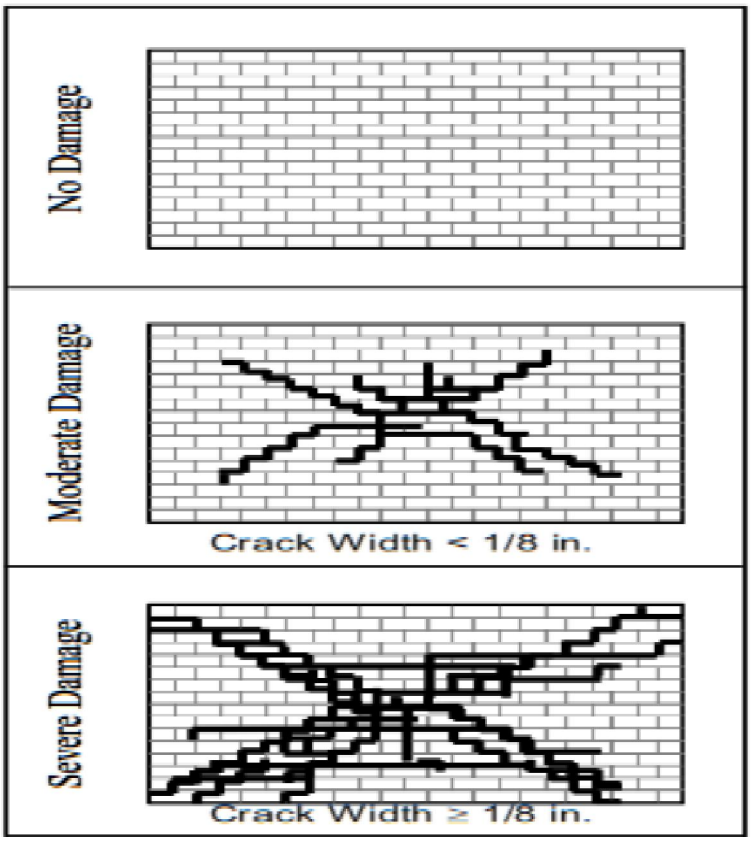

Figure 2.19 Visual damage classification.

2.8 In-Plane Strength and Stiffness Evaluation of URM Infills

The transfer of lateral forces across infilled frames causes non uniform stress distribution within the infill and frame elements. As the lateral forces are increased, the stress distribution varies until failure of the infill occurs. Failure of the infill occurs when either its shear or compressive strength is reached.

The expected flexural and shear strength of the frame elements confining the infill panel must also be evaluated. Column and beam shear and flexural strengths must exceed the horizontal/vertical components of the force required for failure of the infill. This procedure assures failure of the infill before failure in the confining frame occurs.

The lateral load capacity of frame-infill systems should be found using a nonlinear finite element program which captures the nonlinear behavior of all material components: masonry, mortar and concrete. Because this option is not available or is impractical in

most situations, however, a simpler analytical method is proposed. The proposed method is a pushover analysis of a frame containing eccentric equivalent struts that represent the masonry. The method can be used for fully infilled frames as well as partially infilled and perforated masonry panels. Using eccentric struts in this global analysis will yield infill effects on the column directly, which will negate the need to evaluate these members locally. This method relies on the development of plastic hinges to capture the nonlinearities of the structural system.

In-plane strength predictions of infilled frames are a complex, statically indeterminate problem. The strength of a composite-infilled frame system is not simply the summation of the infill properties plus those of the frame. Great efforts have been invested, both analytically and experimentally, to better understand and estimate the composite behavior of masonry-infilled frames. **Polyakov (1960)** [1](work dating back to the early 1950s), **Stafford-Smith (1962, 1966, 1969)[3], Main- stone (1971)[4], Klingner and Bertero (1976, 1978)[5],** to mention just a few, formed the basis for understanding and predicting infilled frame in-plane behavior. Their experimental testing of infilled frames under lateral loads resulted in specimen deformation shapes similar to the one illustrated in Figure 2.20

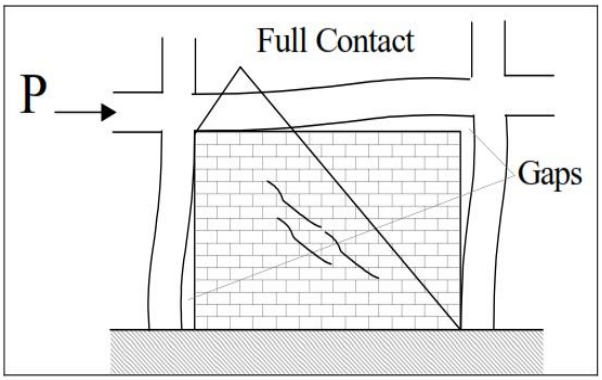

Figure 2.20 Specimen deformation shape.

2.8.1 In-plane Stiffness of Masonry Infill

Prior to cracking the relative elastic in-plane stiffness of a solid unreinforced masonry infill panel to frame stiffness shall be evaluated using equation 2.10 **(Stafford-Smith and Carter 1969)[2]:** The thickness and modulus of elasticity of the equivalent strut shall be the same as the infill panel **(FEMA 306, 1998)[47].**

$$\lambda_1 = \sqrt[4]{\frac{E_m t \sin 2\theta}{4 E_c I_{col} h}} \quad (2.10)$$

Where:

$\lambda_1 = Relative\ infill\ to\ frame\ stiffness\ parameter$

a = Equivalent width of infill strut in the elastic range , cm

$E_m = modulus\ of\ elasticity\ of\ masonry\ material\ in\ compression, MPa$

$E_c = modulus\ of\ elasticity\ of\ confining\ frame, MPa$

$I_{column} = modulus\ of\ elasticity\ of\ masonry\ material\ in\ compression, cm^4$

$t = Gross\ thickness\ of\ the\ infill, cm$

$h = height\ of\ the\ infill\ panel, cm$

θ = Angle of the concentric equivalent strut , degrees

D = Diagonal length of infill , cm

H = Height of the confining frame , cm

2.8.2 Masonry infill shear strength.

The capacity of masonry to shear forces is provided by the combination of two different mechanisms: the bond shear strength and the friction between the masonry and the mortar. The concept of the bond shear strength is illustrated in Figure 2.21, where a typical stair-stepped shear crack is approximated by a single shear crack through a bed joint. This simplification is valid because the vertical component of the stair-stepped crack will be in tension, and its contribution to the shear strength should be neglected. Therefore, the horizontal lateral load required to reach the infill shear strength is calculated by Equation 2.11

$$R_{shear} = A_n f'_v (R_1)_i (R_2)_i \quad \text{---------- (2.11)}$$

Where:

A_n = net cross sectional mortar/grouted area of infill panel along its length (cm^2)

f'_v = masonry shear strength (MPa)

Note: Although vertical loads on infills may not be accurately estimated, 20 per- cent of the normal stress may be assumed to be resisted by the infill and included in the friction component of the resisting mechanism.

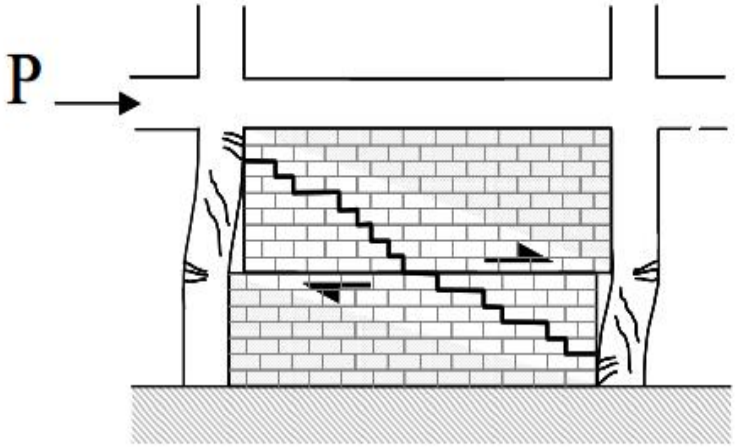

Figure 2.21 Shear failure of masonry(Ghassan Al-Chaar)**.**

2.8.3 Masonry infill crushing strength.

The masonry infill crushing strength corresponds to the compressive load that the equivalent masonry strut can carry before the masonry is crushed (R_{cr}).The applied load that corresponds to the crushing strength of the infill is evaluated using Equation 2.12

$$R_{cr} = a_{red} t_{eff} f'_m \quad \text{---------- (2.12)}$$

Where:

f'_m = Compressive strength of the masonry, MPa

t_{eff} = net thickness of masonry panel, mm

2.8.4 Load-Deformation Behavior of the Eccentric Equivalent Strut

The eccentric equivalent strut used to model the masonry infill is pin-connected to the frame elements so that no moment transfer occurs. The stiffness of the strut will be governed by the modulus of elasticity of the masonry material *(E_m)* and the cross-sectional area (a x t_{eff}). The strength of the strut is determined by calculating the load required to reach masonry infill crushing strength (R_{cr}) (Equation 2.12) and the load required to reach the masonry infill shear strength (R_{shear}) (Equation 2.11).The component of these forces in the direction of the equivalent strut will be used to assign the strut a "compressive" strength. This strength is defined as $\boldsymbol{R_{strut}}$ (Equation 2.13) and governs the strength of the plastic hinge in the strut.

$$R_{strut} = min\left\{ R_{shear} \Big/ cos\theta_{strut} \right. \quad \text{(2.13)}$$

$$tan\theta_{strut} = \frac{h - 2l_{column}}{l} \quad \text{(2.14)}$$

Where:

θ_{strut} =The angle of the eccentric strut with respect to the horizontal, as illustrated in Figure 2.22

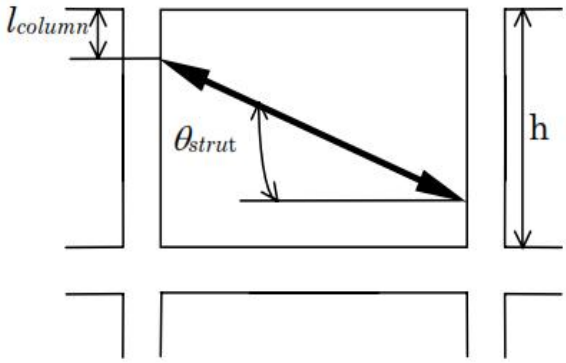

Figure 2.22 Geometry of Strut(Ghassan Al-Chaar)**.**

The equivalent strut is assumed to deflect to nonlinear drifts as Figure 2.23 shows.

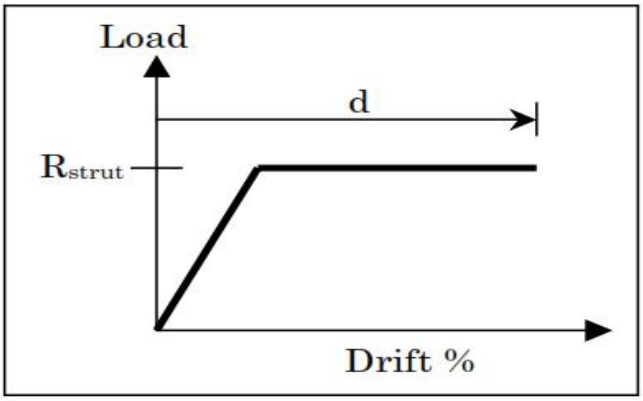

Figure 2.23 Load-deformation behavior(FEMA 273).

The parameter *d*, which represents the nonlinear lateral drift associated with the infilled panel, is defined in **FEMA 273**[44].

2.9 Frame member stiffness

Frame member stiffness should reflect the degree of cracking and inelastic action which has occurred along each member before yielding. Non-linearity arises from the stress strain relation of the materials. The development of cracks in the concrete and secondary load-deflection (slenderness) effects lead to a situation in which the maximum load and bending moment induced in a column cannot readily be related to the loads acting on the structure. The column rigidity depends on the axial load of the moment variation along the length, the percentage reinforcement, the steel placement, the strength of steel and concrete, and their critical strain values. However, in braced frames the relative values of stiffness are important. Two usual assumptions are to use gross EI values for all members or, to use half the gross EI of the beam stem for beams and the gross EI for columns. For frames that are free to sway, a realistic estimate of EI is desirable and should be used if 2^{nd} order effect is carried out.

The stiffness's appropriate for strength calculations must estimate the lateral deflections accurately at the factored load level. They must be simple to apply, because a frame consists of many cross sections, with differing reinforcement ratios and differing degrees of cracking. Furthermore, the reinforcement amounts and distributions are not known at

the time the analysis is carried out. Using studies of the flexural stiffness of beams with cracked and uncracked regions, MacGregor and Hage recommended that the beam stiffness's be taken as 0.4EcIg when carrying out a second-order analysis.

In **ACI Code**, this value has been multiplied by a stiffness-reduction factor of 0.875, giving I = 0.35Ig. Two levels of behavior must be distinguished in selecting the *EI* of columns. The lateral deflections of the frame are influenced by the stiffness of all the members in the frame and by the variable degree of cracking of these members. Thus, the *EI* used in the frame analysis should be an average value. On the other hand, in designing an individual column in a frame, the *EI* used in calculating must be for that column. This EI must reflect the greater chance that a particular column will be more cracked, or weaker, than the overall average; hence, this EI will tend to be smaller than the average *EI* for all the columns acting together. **ACI Code** gives this value multiplied by 0.875, $EI=0.70EcI_g$ or for this purpose. The value of *EI* for shear walls may be taken equal to the value for beams in those parts of the structure where the wall is cracked by flexure or shear and equal to the value for columns where the wall is uncracked. If the factored moments and shears from an analysis based on for the walls indicate that a portion of the wall will crack due to stresses reaching the modulus of rupture of the wall concrete, the analysis should be repeated with for the cracked parts of the wall.

Euro code 8-2005[41] states unless a more accurate analysis of the cracked elements is performed, the elastic flexural and shear stiffness properties of concrete and masonry elements may be taken to be equal to one half of the corresponding stiffness of the un-cracked elements.

This study is based on **Mac-Grigor[48]** who recommends these two equations when carrying out second order analysis. EIbeam= 0.35EcIg; EIcolumn= 0.7EcIg

2.10 Load Effects on Seismic Behavior - Frame Elements

The analysis of a structure should include the simultaneous effects of gravity and lateral loads. Gravity loads should include dead loads and likely live loads. The nonlinear response of a structure to lateral loads depends (in a nonlinear way) on the gravity loads present at the time of lateral loading. Considering a beam (Figure 2.24a), the effect of light gravity load is to reduce the reserve moment and shear strengths at the right end

and increase the reserve strengths at the left end (reserve strength is defined as the difference between the total strength and the resistance used up by gravity load). Therefore, for a given lateral drift, the gravity load will increase the inelastic rotation demands at the right end of the beam and decrease them at the left end. For larger gravity loads, the effects are increased, and the inelastic mechanism may shift from beam hinging at the ends to hinging along the beam span. In the case of column (Figure 2.24b), variations in gravity load produce variations in column axial force, with consequent changes in both column strength and deformability. Increases in axial load invariably decrease flexural deformability. Increases in moment strength result in increased shear demands and may result in shear failure that would not be expected at lower axial loads.

In general, because of the nonlinear nature of the interactions, it is not appropriate to carry out the gravity load analysis and lateral load analysis separately and then superimpose their results. Instead, the gravity loads should be applied to the numerical model and should be maintained as the lateral deformations are imposed.

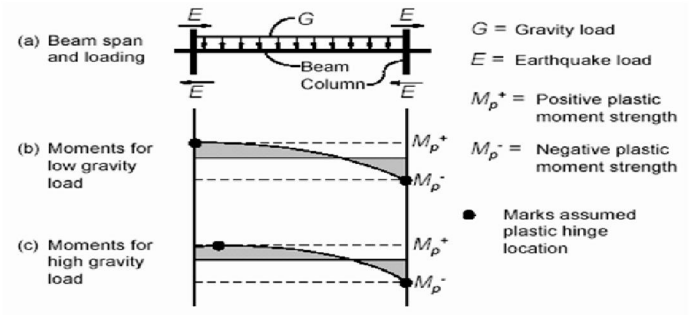

(a)

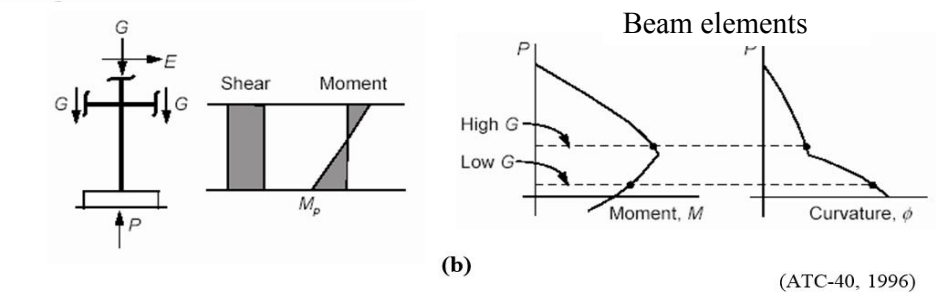

(b)

(ATC-40, 1996)

Figure 2.22 Gravity Load Effects on Seismic Behavior of Components(Paulay and Priestley, 1992)

During an earthquake, acceleration-induced inertia forces will be generated at each floor level, where the mass of an entire story may be assumed to be concentrated. Hence the location of a force at a particular level will be determined by the center of the accelerated mass at that level. The summation of all the floor forces, F_i (Figure 2.25), above a given story will then locate the position of the resultant force V_i within that story.

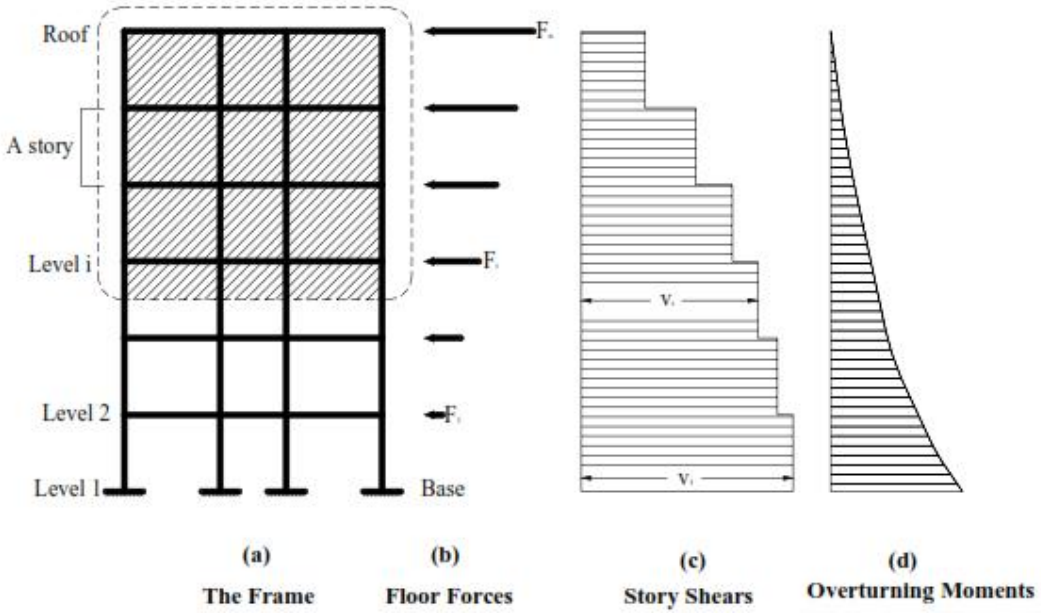

Figure 2.23 Effects of lateral forces on a building (Paulay and Priestley, 1992)

Figure 2.26 illustrates a generalized load-deformation relation appropriate for most concrete components. The relation is described by linear response from A (unloaded component) to an effective yield point B, linear response at reduced stiffness from B to C, sudden reduction in lateral load resistance to D, response at reduced resistance to E, and final loss of resistance thereafter (Fig 2.26a). Deformations beyond point E are not permitted because gravity load can no longer be sustained (Fig 2.26b). In some cases, initial failure at C will result in loss of gravity load resistance, in which case E is a point having deformation equal to that at C and zero resistance (ATC-40, 1996). The above main points are shown on the load-deformation relation of Figure 2.26.

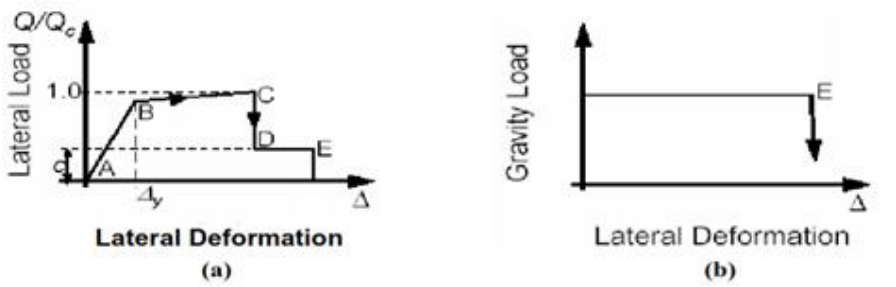

Figure 2.24 Generalized Load-Deformation Relations for Non-degrading Components.(ATC-40,1996)

Where, Q_c - refers to the strength of the component.

Q - refers to the demand imposed by the earthquake

Lateral loads should be applied in predetermined patterns that represent predominant distributions of lateral inertial loads during critical earthquake response. Lateral loads commonly may be lumped at floor levels if the floor diaphragms are sufficiently rigid in their plane. The taller a building, the more significant the effect of lateral forces will be. As a structure is displaced laterally, its lateral load stiffness usually decreases with increasing lateral displacement.

For the same maximum displacement at roof level, the overall ductility demand in terms of the large deflection is much more readily achieved when plastic hinges develop in all the beams (Fig 2.27b) instead of only in the soft-story column (Fig 2.27c). The column sway mechanism, also referred to as a soft-story, may impose plastic hinge rotations, which even with good detailing of affected regions, would be difficult to accommodate **(Paulay and Priestley, 1992)[42].**

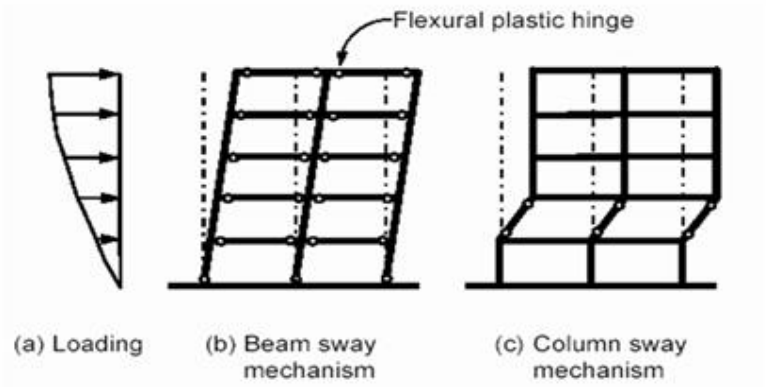

Figure 2.25 Idealized Flexural Mechanisms in Multi-story Frames(ATC-40,1996)

It is important to recall the reader at last that the above detail of the effect of loads on the frames is to show the actual behaviors during devastating earthquake but this thesis work has already simplified such complex situations by considering moderate seismic forces and hence omitting the possibility of formation of hinges neither in the beams nor in the columns.

2.11 Out-of-Plane and In-Plane Loadings – Masonry Walls

Walls will be subjected to simultaneous vertical, in plane, and out of plane load, because of the multi-axial nature of ground shaking under seismic forces.

The in-plane response will primarily be a result of the resistance of the wall to inertia forces from other parts of the structure, such as floor masses. The-out-of-plane response will be due to the inertia mass of the walls themselves responding to the floor-level excitation.

The design envelope of in-plane moments exceeds those resulting from the code distribution of forces at levels above the base due to higher-mode effects (**Paulay and Priestley, 1992**)[42].

Magnitude of out-of-plane moments will be larger in the upper than in the lower stories.

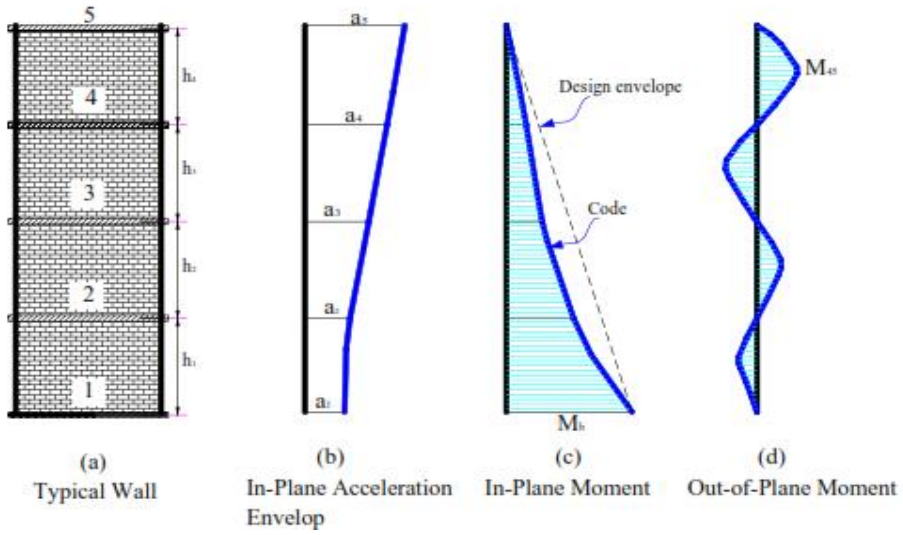

Figure 2.26 Response of a masonry wall to biaxial excitation (Paulay and priestly,1992)

The first out-of-plane mode of the wall with contra-flexure points at the floor level is more conservative than assuming excitation of any higher mode, which would result in lower maximum bending moments. Due to in-plane action, tension cracking will reduce the ability of the walls to provide restraining moments at floor levels. It should be noted that maximum in-plane moments occur at the base of wall, while maximum out-of-plane moments occur in the top story, where in plane moments are low.For the wall of Figure 2.29, the maximum out-of-plane moment M45 will be approximately:

$m_{45} = 0.1ma_{45}h_4^2$ - for unit horizontal length of wall(**Paulay and Priestley, 1992**)[42]

m - Wall mass per unit area.

a_{45}- Maximum response acceleration at mid height of the fourth story.

At mid-height of the story there is possibility of resonant response as a result of near coincidence of natural periods of out-of-plane response of the wall, T_w, and transverse in- plane response of the structure as a whole, T_s.

Fig.2.29 shows the first four out-of-plane mode shapes and periods for a three story masonry wall. The modes include the effect of the transverse structural stiffness, and hence are not Symmetrical.

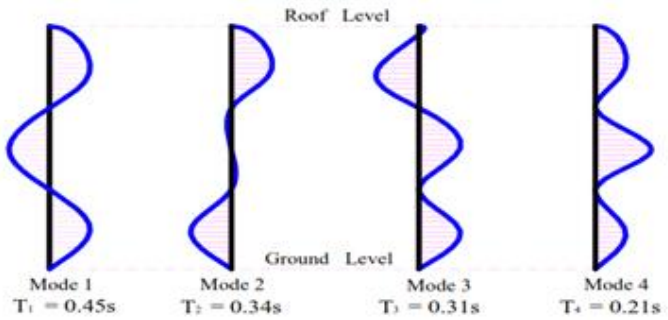

Figure 2.27 Wall out-of-plane mode shapes and periods of a three-story masonry(Paulay and Priestly,1992)

It is extremely likely that some degree of resonance will occur between out-of-plane and transverse structure response.

CHAPTER 3 PERFORMANCE BASED SEISMIC DESIGN

3.1 General

Seismic hazard in the context of engineering design is generally defined as the predicted level of ground acceleration which would be exceeded with 10% probability at the site under consideration due to the occurrence of an earthquake anywhere in the region, in the next 50 years. A lot of complex scientific perception and analytical modelling is involved in seismic hazard estimation. A computational scheme involves the following steps: delineation of seismic source zones and their characterization, selection of an appropriate ground motion attenuation relation and a predictive model of seismic hazard. Although these steps are region specific, certain standardization of the approaches is highly essential so that reasonably comparable estimates of seismic hazard can be made worldwide, which are consistent across the regional boundaries. As it is well known, earthquake catalogues and data bases make the first essential input for the delineation of seismic source zones and their characterization. Thus, preparation of a homogeneous catalogue for a region under consideration is an important task. The data from historic time to recent can broadly be divided in to three temporal categories: 1) since 1964, for which modern instrumentation based data are available 2) 1900-1963, the era of early instrumental data, and 3) pre 1900, consisting of pre- instrumental data, which is based primarily on historical and macro-seismic information. The next key component of seismic hazard assessment is the creation of seismic source models, which demand translating seismo- tectonic information into a spatial approximation of earthquake localization and temporal recurrence. For this purpose, all the available data on neo-tectonics, geodynamics, morpho structures etc., need to be compiled and viewed, overlain on a seismicity map.These maps then need to be critically studied for defining areal seismic source zones and active faults. An earthquake recurrence model is then fitted to these source zones, for defining the parameters that characterize the seismicity of the source region, which go as inputs to the algorithm for the computation of seismic hazard viz.

Fig. 3.1 shows a flow chart that presents the key steps in the performance-based design process. It is an iterative process that begins with the selection of performance

objectives, followed by the development of a preliminary design, an assessment as to whether or not the design meets the performance objectives, and finally redesign and reassessment, if required, until the desired performance level is achieved. **(ATC, 40)[26]**

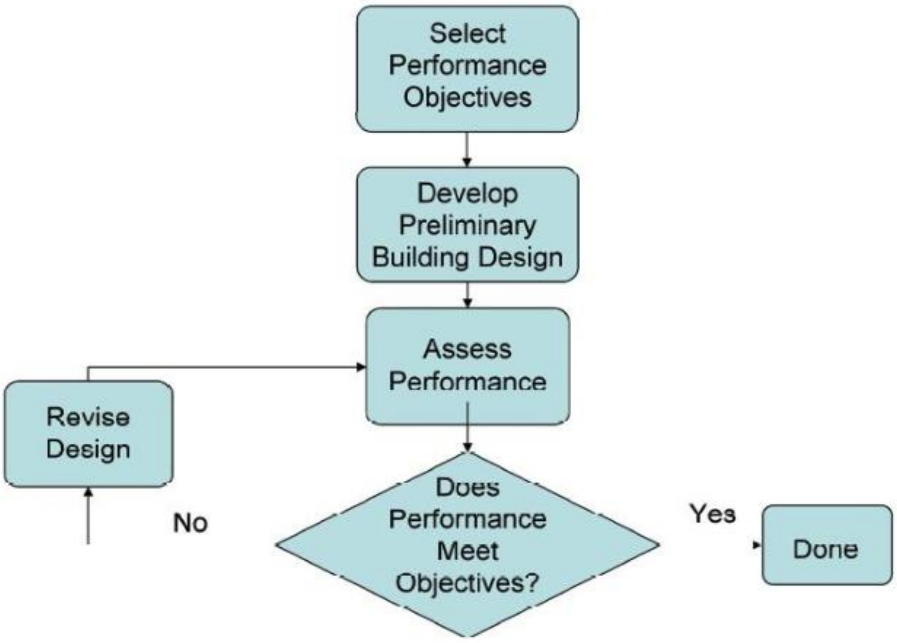

Figure 3.1 Performance-Based Design Flow Diagrams (ATC, 40)

ATC-40[26] and **FEMA 356[25]** documents include modeling procedures, acceptance criteria and analysis procedures for pushover analysis. These documents define force-deformation criteria for potential locations of lumped inelastic behavior, designated as *plastic hinges* used in pushover analysis. As shown in Figure 3.2 below, five points labeled A,B, C, D, and E are used to define the force deformation behavior of the plastic hinge, and three points labeled IO (Immediate Occupancy), LS (Life Safety) and CP (Collapse Prevention) are used to define the acceptance criteria for the hinge. In these documents, if all the members meet the acceptance criteria for a particular performance level, such as Life Safety, then the entire structure is expected to achieve the Life Safety level of performance.

The values assigned to each of these points vary depending on the type of member as well as many other parameters, such as the expected type of failure, the level of stresses with respect to the strength, or code compliance.

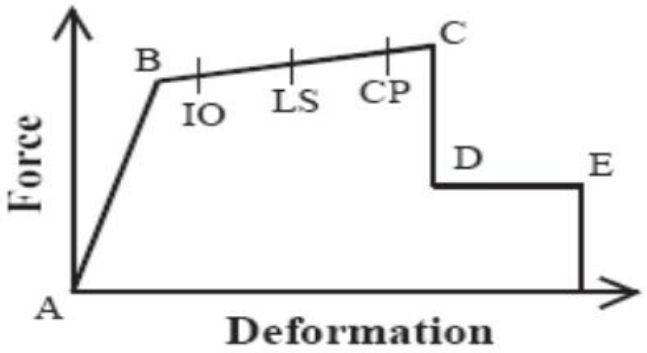

Figure 3.2 Force-Deformation Relation for Plastic Hinge in Pushover Analysis (Habibullah. et al., 1998)

Both the **ATC-40[26]** and **FEMA 356[25]** documents present similar performance-based engineering methods that rely on nonlinear static analysis procedures for prediction of structural demands. While procedures in both documents involve generation of a "pushover" curve to predict the inelastic force-deformation behavior of the structure, they differ in the technique used to calculate the global inelastic displacement demand for a given ground motion. The **FEMA 356[25]** document uses the Coefficient Method, whereby displacement demand is calculated by modifying elastic predictions of displacement demand. The **ATC-40[26]** Report details the Capacity-Spectrum Method, whereby modal displacement demand is determined from the intersection of a capacity curve, derived from the pushover curve, with a demand curve that consists of the smoothed response spectrum representing the design ground motion, modified to account for hysteretic damping effects.

3.2 Structural Performance Levels (ATC, 40)

3.2.1 Immediate Occupancy Performance Level (S-1)

Structural Performance Level S-1, Immediate Occupancy, means the post-earthquake damage state in which only very limited structural damage has occurred. The basic vertical and lateral-force-resisting systems of the building retain nearly all of their pre-earthquake strength and stiffness. The risk of life threatening injury as a result of structural damage is very low, and although some minor structural repairs may be appropriate, these would generally not be required prior to re-occupancy.

3.2.2 Life Safety Performance Level (S-3)

Structural Performance Level S-3, Life Safety, means the post-earthquake damage state in which significant damage to the structure has occurred, but some margin against either partial or total structural collapse remains. Some structural elements and components are severely damaged, but this has not resulted in large falling debris hazards, either within or outside the building. Injuries may occur during the earthquake; however, it is expected that the overall risk of life-threatening injury as a result of structural damage is low. It should be possible to repair the structure; however, for economic reasons this may not be practical.

3.2.3 Collapse Prevention Performance Level (S-5)

Structural Performance Level S-5, Collapse Prevention, means the building is on the verge of experiencing partial or total collapse. Substantial damage to the structure has occurred, potentially including significant degradation in the stiffness and strength of the lateral force resisting system, large permanent lateral deformation of the structure and to more limited extent degradation in vertical-load-carrying capacity. However, all significant components of the gravity load resisting system must continue to carry their gravity load demands. Significant risk of injury due to falling hazards from structural debris may exist. The structure may not be technically practical to repair and is not safe for re-occupancy, as aftershock activity could induce collapse.

3.3 Pushover Analysis Using ETABS

Pushover analysis is an approximate analysis method in which the structure is subjected to monotonically increasing lateral forces with an invariant height-wise distribution until a target displacement is reached. Pushover analysis consists of a series of sequential elastic analysis, superimposed to approximate a force-displacement curve of the overall structure. A two or three dimensional model which includes bilinear or tri-linear load-deformation diagrams of all lateral force resisting elements is first created and gravity loads are applied initially. A predefined lateral load pattern which is distributed along the building height is then applied. The lateral forces are increased until some members yield. The structural model is modified to account for the reduced stiffness of yielded members and lateral forces are again increased until additional members yield. The process is continued until a control displacement at the top of building reaches a certain level of deformation or structure becomes unstable. The roof displacement is plotted with base shear to get the global capacity curve.

Pushover analysis can be performed as force-controlled or displacement-controlled. In force- controlled pushover procedure, full load combination is applied as specified, i.e, force- controlled procedure should be used when the load is known (such as gravity loading). Also, in force-controlled pushover procedure some numerical problems that affect the accuracy of results occur since target displacement may be associated with a very small positive or even a negative lateral stiffness because of the development of mechanisms and P-delta effects.

Pushover analysis has been the preferred method for seismic performance evaluation of structures by the major rehabilitation guidelines and codes because it is conceptually and computationally simple. Pushover analysis allows tracing the sequence of yielding and failure on member and structural level as well as the progress of overall capacity curve of the structure. (**girgin. et., 2007**)

3.3.1 Purpose of Doing Pushover Analysis

The pushover is expected to provide information on many response characteristics that cannot be obtained from an elastic static or dynamic analysis.The following are the examples of such response characteristics:

- The realistic force demands on potentially brittle elements, such as axial force demands on columns, force demands on brace connections, moment demands on beam to column connections, shear force demands in reinforced concrete beams, etc.

- Estimates of the deformations demands for elements that have to form inelastically in order to dissipate the energy imparted to the structure.

- Consequences of the strength deterioration of individual elements on behaviour of the structural system.

- Identification of the critical regions in which the deformation demands are expected to be high and that have to become the focus through detailing.

- Identification of the strength discontinuous in plan elevation that will lead to changes in the dynamic characteristics in elastic range.

- Estimates of the interstory drifts that account for strength or stiffness discontinuities and that may be used to control the damages and to evaluate P-Delta effects.

- Verification of the completeness and adequacy of load path, considering all the elements of the structural systems, all the connections, and stiff non-structural elements of significant strength, and the foundation system. (www.architectjaved.com)

Pushover analysis is a very powerful feature offered only in the non-linear version of ETABS. In addition to performing pushover analyses for performance-based seismic design, this feature can be used to perform general static nonlinear analysis and the analysis of staged (incremental) construction. ETABS menus and documentation refer to pushover analysis as static nonlinear analysis.

Performing any nonlinear analysis takes time and requires patience. The key points for conducting pushover analysis can be summarized as follows:(**ETABS menus and documentation)**

1. Defining how nonlinearity is considered

2. Determining analysis cases

3. Defining loading

4. Selecting the type of load control

5. Analysis Results

6. Procedure for conducting pushover analysis

7. Important Considerations

3.3.2 Defining how nonlinearity is considered

Properly modelling the nonlinear behaviour that the structure is expected to undergo is very important for obtaining credible analysis results. However, more complicated models are not necessarily more accurate. When developing a model, keep in mind that pushover analysis contains inherent simplifications regarding the dynamic behaviour of the building, and select the level of model complexity accordingly. Several types of nonlinear behaviour can be considered in a pushover analysis:

1. Material nonlinearity at discrete, user-defined hinges in frame/line elements. Plastic hinges can be assigned at any number of locations along the length of any frame element wherever yielding or other inelastic behavior is expected. Uncoupled moment, torsion, axial force and shear hinges are available. There is also a coupled P-M2-M3 hinge that considers the interaction of axial force and bending moments at the hinge location. More than one type of hinge can exist at the same location. Both an M3 (moment) and a V2 (shear) hinge to the same end of a frame element. Default hinge properties are provided based on **ATC-40[26]** and **FEMA-356[25]** criteria. For reinforced concrete frame buildings, use coupled P-M hinges when modelling columns and uncoupled moment hinges for beams. Separate shear hinges are recommended. To reduce the size and complexity of the model, a number of analysts check shear forces in each member against that member's shear capacity rather than using shear hinges.

2. Material nonlinearity in the link elements. The available nonlinear behavior includes gap (compression only), hook (tension only), uniaxial plasticity along any

degree of freedom, and two types of base isolators (biaxial plasticity and biaxial friction/pendulum). The link damper property has no effect in a static nonlinear analysis.

3. Geometric nonlinearity in all elements. You can choose between considering only P-delta effects or considering P-delta effects plus large displacements. Large displacement effects consider equilibrium in the deformed configuration and allow for large translations and rotations. However, the strains within each element are assumed to remain small. The P-Delta effects option (without large deformations) is recommended.

4. **Adding or removing elements**. Members can be added or removed in a sequence of stages during each analysis case.

3.3.3 Determining Analysis Cases

Static nonlinear analysis can consist of any number of cases. Each static nonlinear case can have a different distribution of load on the structure. For example, a typical static nonlinear analysis might consist of three cases. The first would apply gravity load to the structure, the second would apply one distribution of lateral load over the height of the structure, and the third would apply another distribution of lateral load over the height of the structure.

A static nonlinear case may start from zero initial conditions, or it may start from the results at the end of a previous case.

Static nonlinear analysis cases are completely independent of all other analysis types in ETABS. In particular, any initial P-delta analysis performed for linear and dynamic analysis has no effect upon static nonlinear analysis cases. The only interaction is that linear mode shapes can be used for loading in static nonlinear cases.

Static nonlinear analysis cases can be used for design. Generally it does not make sense to combine linear and nonlinear results, so static nonlinear cases that are to be used for design should include all loads, appropriately scaled, that are to be combined for the design check.

3.3.4 Defining Loading

The distribution of load applied on the structure for a given static nonlinear case is defined as a scaled combination of one or more of the following:

- **Any static load case.**

A uniform acceleration acting in any of the three global directions. The force at each joint is proportional to the mass assigned to that joint (i.e., that calculated from the tributary area) and acts in the specified direction

A modal load for any eigen or Ritz mode. The force at each joint is proportional to the product of the modal displacement (eigenvector), and the mass tributary to that joint, and it acts in the direction of the modal displacement.

The load combination for each static nonlinear case is incremental, meaning it acts in addition to the load already on the structure if starting from a previous static nonlinear case.

3.3.5 Selecting the Type of Load Control

ETABS has two distinctly different types of control available for applying the load. Each analysis case can use a different type of load control. The choice generally depends on the physical nature of the load and the behavior expected from the structure:

Force control. The full load combination is applied as specified. Force control should be used when the load is known (such as gravity load), and the structure is expected to be able to support the load in the elastic range.

Displacement control. A single Monitored Displacement component (or the Conjugate Displacement) in the structure is controlled. The magnitude of the load combination is increased or decreased as necessary until the control displacement reaches a value that you specify. Displacement control should be used when specified drifts are sought (such as in seismic loading), where the magnitude of the applied load is not known in advance, or when the structure can be expected to lose strength or become unstable.

3.3.6 Analysis Results

ETABS provides several types of output that can be obtained from the static nonlinear analysis:

- Base Reaction versus Monitored Displacement can be plotted.
- Tabulated values of Base Reaction versus Monitored Displacement at each point along the pushover curve, along with tabulations of the number of hinges beyond certain control points on their hinge property force-displacement curve can be viewed on the screen, printed, or saved to a file.
- Base Reaction versus Monitored Displacement can be plotted in the ADRS format where the vertical axis is spectral acceleration and the horizontal axis is spectral displacement. The demand spectra can be superimposed on this plot.
- Tabulated values of the capacity spectrum (ADRS capacity and demand curves), the effective period and the effective damping can be viewed on the screen, printed, or saved to a file.
- The sequence of hinge formation and the color-coded state of each hinge can be viewed graphically, on a step-by-step basis, for each step of the static nonlinear case.
- The member forces and stresses can be viewed graphically, on a step-by-step basis, for each step of the static nonlinear case.
- Member forces and hinge results for selected members can be written to a file in spreadsheet format for subsequent processing in a spreadsheet program.
- Member forces and hinge results for selected members can be written to a file in Access database format.

3.4 Nonlinear Static Procedures

Current standards such as **ASCE 41[24]** provide two alternate methods of estimating the peak displacement demand for use in nonlinear static procedures: the displacement

coefficient method and the capacity spectrum method. Both methods rely on an equivalent linearization approach. The basic assumption in equivalent linearization techniques is that the maximum inelastic deformation of a nonlinear single degree of freedom (SDOF) system is approximately equal to the maximum deformation of a linear elastic SDOF system, provided that the linear elastic system has a period and a damping ratio that are larger than the initial values of those for the nonlinear system.

The displacement coefficient method is conceptually simpler and easier to use, and is not prone to the graphical misinterpretations that can occur with the capacity spectrum method. The authors recommend using the displacement coefficient method, either alone or to check results obtained by using the automated capacity spectrum method capabilities in ETABS.

3.4.1 Displacement Coefficient Method

The displacement coefficient method (simply called the coefficient method in **FEMA 356**[25] is the primary method of estimating displacement for the nonlinear static procedure in **ASCE 41[24]**, and its pre-standard **FEMA 356[25]**. The displacement coefficient method generates an estimate of the maximum global displacement, called the *target displacement*, by modifying the linear elastic response of an equivalent SDOF system. This is accomplished by multiplying the SDOF spectral displacement by a series of coefficients, *Co* through C_3,. Figure 3.2 shows the process used to calculate the target displacement.

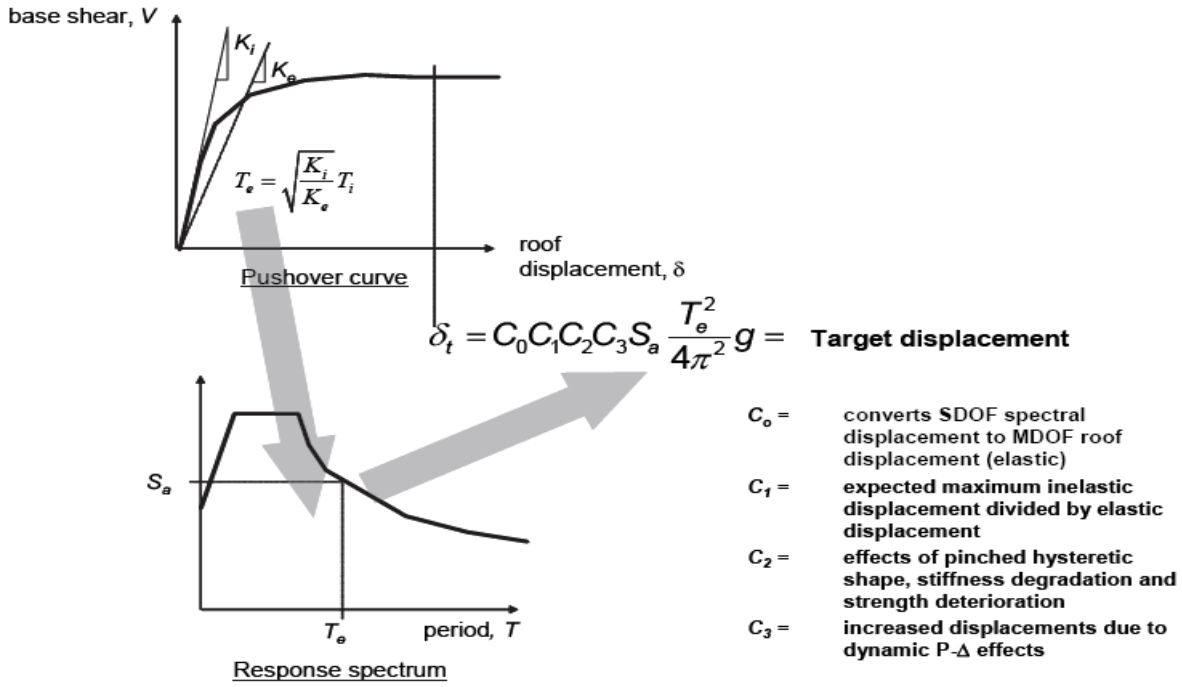

Figure 3.3 Schematic illustration of the process of estimating target displacement using the Displacement coefficient method, for a given response spectrum and effective period, T (reproduced from FEMA 440, a public domain document).

First an effective period, T_e, is generated from the initial period, T_i, by a graphical procedure using an idealized force-deformation curve (i.e., pushover curve) relating base shear to roof displacement, which accounts for some stiffness loss as the system begins to behave in elastically. The effective period represents the linear stiffness of the equivalent SDOF system. The effective period is used to determine the equivalent SDOF system's spectral acceleration, *Sa*, using an elastic response spectrum. The procedure assumes that the damping (usually 5%) is appropriate for a structure in the elastic range.

Then, the peak elastic spectral displacement is determined from the spectral acceleration using the following equation:

$$S_d = \frac{T_{eff}^2}{4\pi^2} S_a \quad \text{----------(3.1)}$$

The Displacement Coefficient Method then uses four coefficients to convert the peak elastic spectral displacement first to elastic displacement at the roof and then to inelastic

displacement at the roof. FEMA 440, Improvement of Nonlinear Static Seismic Analysis Procedures, explains each of the coefficients C_0 through C_3 as follows:

The coefficient C_0 is a shape factor (often taken as the first mode participation factor) that simply converts the spectral displacement to the displacement at the roof. The other coefficients each account for a separate inelastic effect. The coefficient C_1 is the ratio of expected displacement for a bilinear inelastic oscillator to the displacement for a linear oscillator. C_1 depends on the ratio of elastic force, calculated as the spectral acceleration multiplied by the mass, to the yield strength, the period of the SDOF system, T_e and the characteristic period of the spectrum. The coefficient C_2 accounts for the effect of pinching in load-deformation relationships due to degradation in stiffness and strength. Finally, the coefficient C_3 adjusts for second-order geometric nonlinearity (P-Δ) effects. The coefficients are empirical and derived primarily from statistical studies of the nonlinear response-history analyses of SDOF oscillators and adjusted using engineering judgment.

CHAPTER 4 STRUCTURAL MODELING

4.1 Overview

It is very important to develop a mathematical model on which performance based analysis is performed. The first part of this chapter presents a summary of various parameters defining the computational models, the basic assumptions and the geometry of the selected building considered for this study. Infill walls are modeled as eccentric equivalent diagonal strut elements. The last part of the chapter deals with the computational model of the equivalent strut.

4.2 Building Description

Multi-storey rigid jointed frame mixed use building G+9 (Figure 4.1), was selected in the seismic zone (Zone IV) of Ethiopia and designed based on the Ethiopian Building Code Standard ESEN:2015 and European Code-2005 almost similar to new Ethiopian building code (as used by the software).ETABS 2015 was used for the analysis and design of the building by modeling as a 3-D space frame system.

Seismic performance is predicted by using performance based analysis of simulation models of bare and infilled non ductile RC frame buildings with different arrangement of masonry wall. The structure will be assumed to be new, with no existing infill damage. The dimensional and physical properties of the frame, infill panel, and openings are listed in appendix table B.0.1

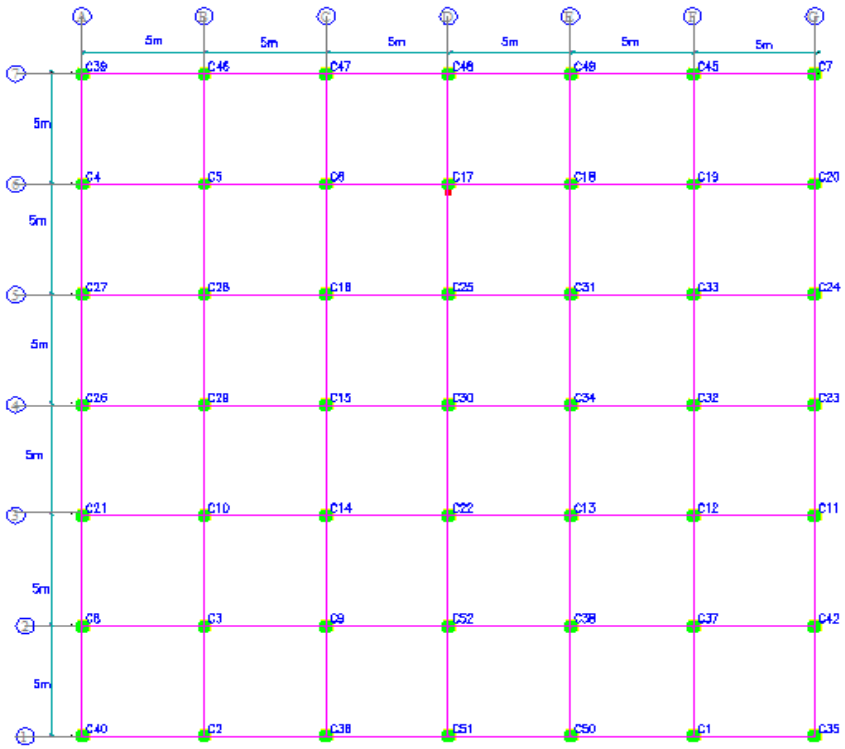

Figure 4.1 Typical building plan

Building Data

- Type of structure = Multi-storey rigid jointed frame
- Layout = as shown in fig. 4.1
- Zone = Iv
- Importance Factor = 1
- Soil Condition = hard
- Number of stories = Ten (G+9)
- Height of Building =30 m
- Floor to floor height = 3 m
- External wall thickness =20cm
- Internal wall thickness=15cm
- Depth of the floor slab =15cm

- depth of roof slab=12cm
- Size of all columns = 70x70cm
- Size of all beams = 70 × 40cm
- Door opening size=100x200cm
- Window opening size =200x120cm

4.3 Structural configuration

The architectural layout of the base structure shown in Figure 4.1 is configured with uniform column spacing of 5meter both along x and y- axis. The building has uniform story height of 3 meter from the base to top roof. The total height of the building is 30 meter. The building is regular both in plan and in elevation. It is because, in order to show the effect of infill panels in seismic performance of reinforced concrete building.

Initial dimensioning of the beams and columns were made on the basis of bare frame. The same sections were used for the cases of fully and partially infilled frame analysis with earthquake load as per **Eurocode-2005;** such that the structure meet the strength and ductility requirements of the new Ethiopian building code of standard**.** Five different models with different configuration of masonry wall were developed to analyze and to understand the effect of infill on seismic response of theRC frame structures.

4.3.1 Different arrangement of the Building Models

To understand the effect of masonry wall in reinforced concrete frame, with a total of five models are developed and pushover analysis has been made in standard computer program ETABS2015.In this particular study pushover loading case along negative X-axis is considered to study seismic performance of all models. Since the out of plane effect is not studied in this paper, only the equivalent strut along X-axis are considered as shown in figure 4.2a to study the in plane effect and masonry walls along Y-axis are not considered in all models. From this different condition, all models are identified by their names which are given below.

Model 1:- Bare reinforced concrete frame.

This is a basic or traditional structure in which no masonry infill are included or considered in structure for improving the seismic performance of the building. As shown in figure 4.2 masonry infill walls are removed from the building along all stories, so the results of the bare reinforced concrete frame can be compared with the results of the other models.

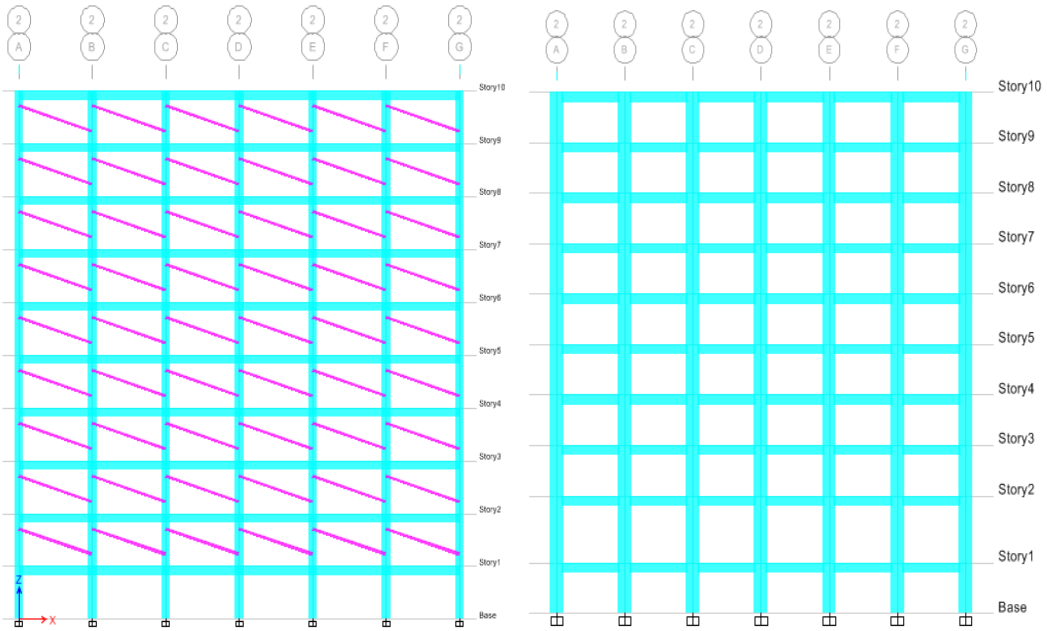

Figure 4.2 Elevation view. a) For Fully infilled frame b) For bare frame

Model 2:-Reinforced concrete frame with 75% of masonry wall removed from fully infilled frame

As shown in fig 4.3 and fig 4.4 some section of the outer periphery of the reinforced concrete building at axis 1 & 7 along X-axis are infilled throughout all stories. In order to indicate the impact of infill on structural integrity in this case 75% of the masonry infill were reduced from the fully infilled reinforced concrete frame model shown in fig 4.6.In order to maintain comparison with other frames; the infill arrangement were kept

symmetrical. There are windows with the dimension of 2m*1.2m on outer periphery of infill panels. Infills with opening are modeled as discussed in chapter 2.

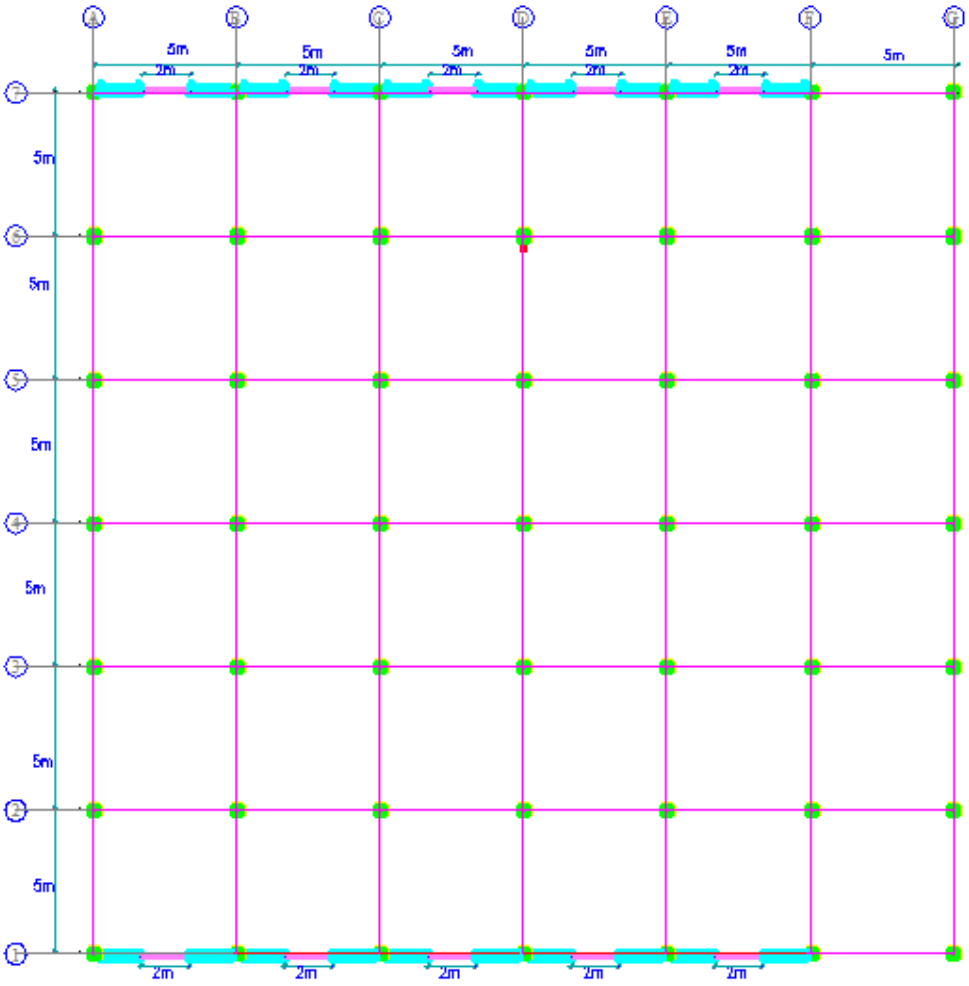

Figure 4.3 Plan View Model 2.

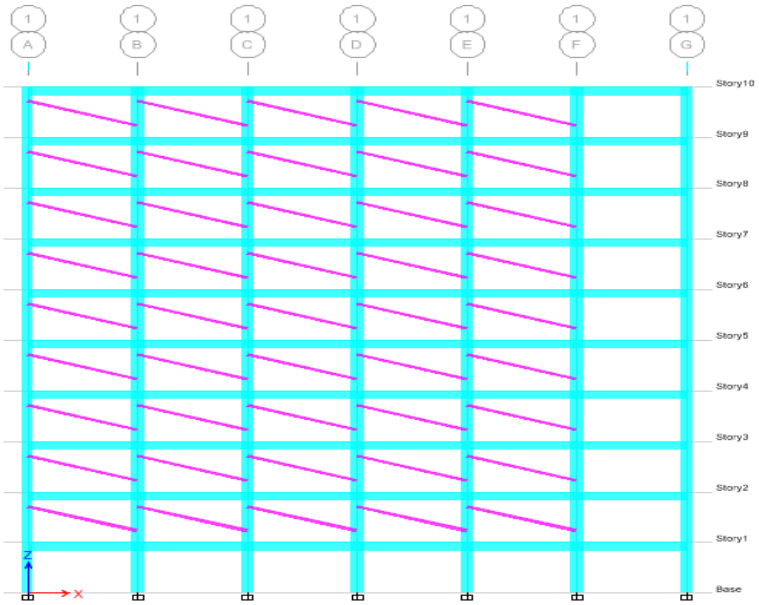

Figure 4.4 Elevation view of Model 2 along axis 1and 7

Model 3:- Reinforced concrete frame with half of of masonry wall removed from fully infilled frame

Comparing with the fully infilled reinforced concrete frame structure, this one is where half of the masonry infill panels were removed. As shown in fig 4.5 the outer periphery of the reinforced concrete building along axis 1 and 7 along X-axis are fully infilled with window openings and also there is masonry infill with door openings along axis 2 and 6 in between C & D throughout all stories except the first. In order to maintain comparison with other frames; the infill arrangement were kept symmetrical. Besides that the opening size and infill location are similar to the other models.

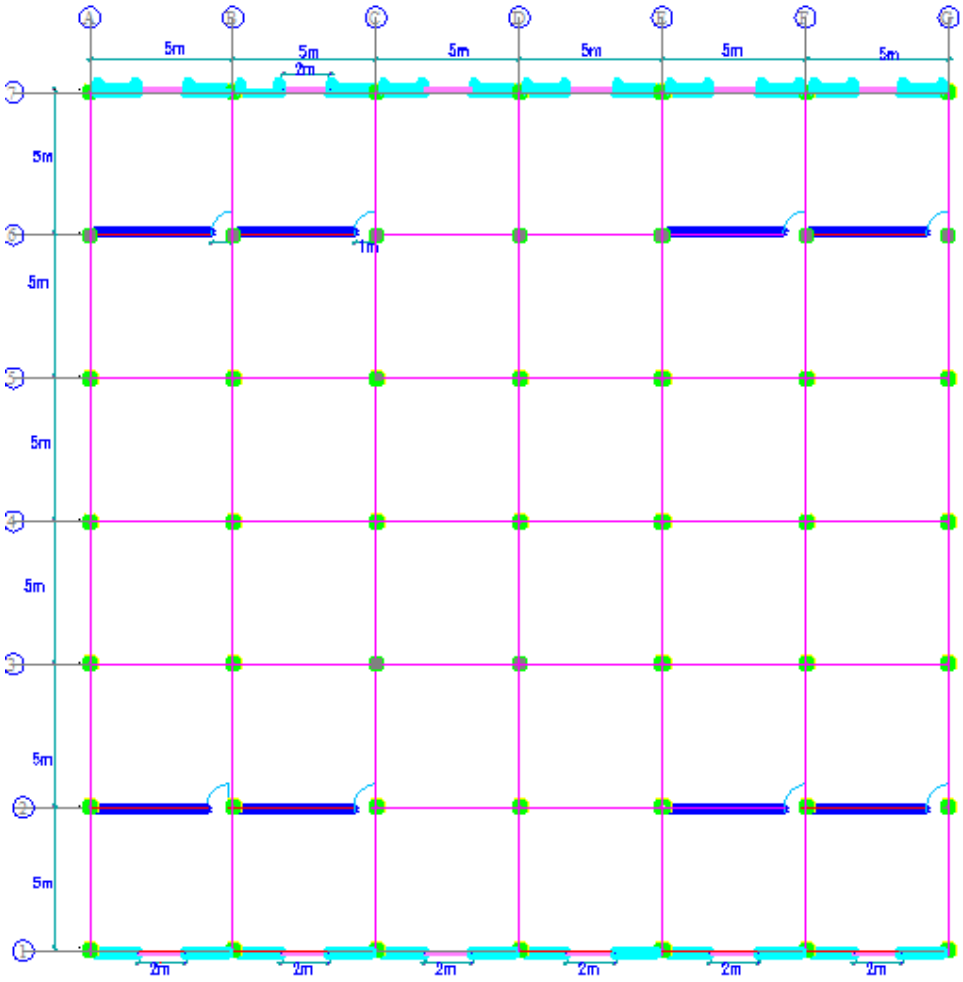

Figure 4.5 plan View of Model 3

Model 4:- Reinforced concrete frame with 25% of masonry wall removed from fully infilled frame

As shown in fig 4.6 and fig 4.7 the outer periphery and some of the interior part of the reinforced concrete building were infilled throughout all stories. In order to indicate the impact of infill on structural integrity in this case 25% of the infill was removed from the fully infilled reinforced concrete frame model along axis 4 and some part along axis 3 and 5.The window and door opening size and infill location are similar to the other models. Infills with opening are modeled as discussed in chapter 2.

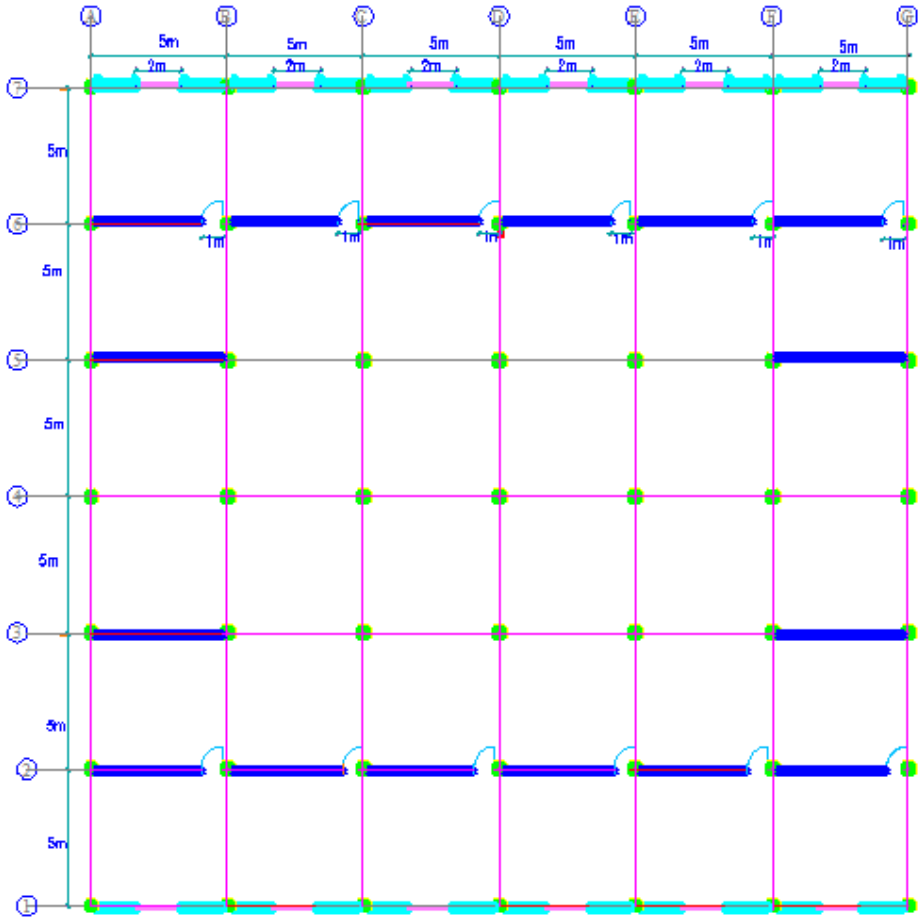

Figure 4.6 Plan view of Model 4

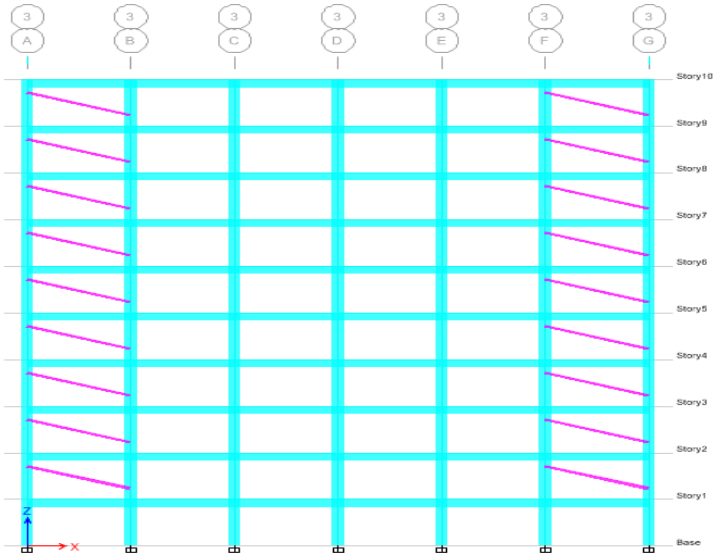

Figure 4.7 Elevation view mode4 along axis 3 and 5

Model 5:- Fully infilled reinforced concrete frame (Base frame)

As shown in fig.4.8 infill panels are arranged symmetrically throughout the building with and without openings. There are windows with the dimension of 2m*1.2m on outer periphery of infill panels. Whereas infills on axis 2,4 and 6 have doors with dimension of 1m*2m.On the other hand infills on axis 3 and 5 have no openings. Comparing with the bare reinforced concrete frame structure, this one is where all of the reinforced concrete frames were fully infilled in all stories except the first.

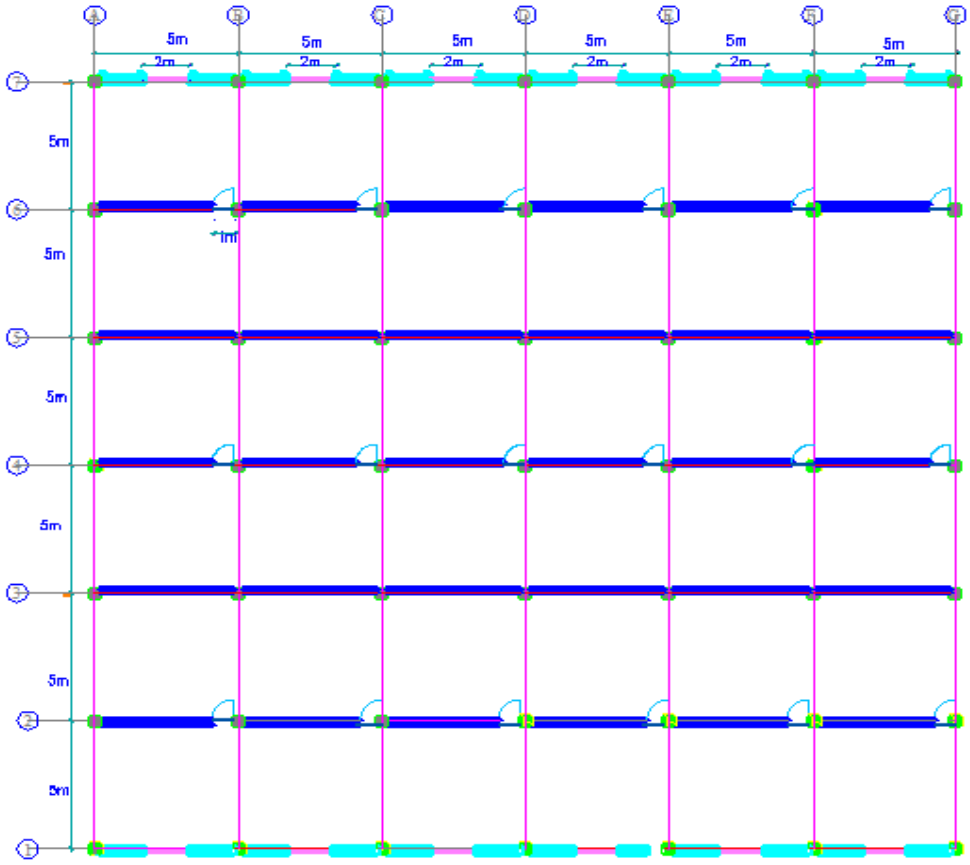

Figure 4.8 Plan view of Model 5.

4.4 Structural Modeling and Analysis

The building is modeled and analyzed for performance based seismic design by pushover analysis using the finite element package ETABS 2015.The analytical models of the buildings include all components that influence the mass, strength and

stiffness. The non-structural elements and components that do not significantly influence the building behavior were not modeled. The floor slabs are assumed to act as diaphragms, which ensure integral action of all the vertical lateral load-resisting elements. Beams and columns were modeled as frame elements with the centerlines joined at nodes. Rigid offsets were provided from the nodes to the faces of the columns or beams. The stiffness for columns and beams were taken as $0.7E_cI_g$,$0.35E_cIg$ respectively accounting for the cracking in the members and the contribution of flanges in the beams.

The weight of the slab was distributed to the surrounding beams as per **ESEN1992:2015[39]**. The mass of the slab was lumped at the centre of mass location at each floor level. This was located at the design eccentricity from the calculated centre of stiffness. Design lateral forces at each storey level were applied at the centre of mass locations independently in two horizontal directions (*X*- and *Y*- directions).

Staircases and water tanks were not modeled for their stiffness but their masses were considered in the static and dynamic analyses. The design spectrum for hard soil as specified in **ESEN1998:2015** [**35**] was used for the analysis. The effect of soil-structure interaction was ignored in the analyses. The columns were assumed to be fixed at the level of the bottom of the base slabs of respective isolated footings.

4.4.1 Material Properties to be used

For this study, the material property for concrete, reinforcing bar and hollow concrete block (HCB) masonry panels are based on **ESEN,2015** and as follows:

For reinforcing bar:

- Yield strength of reinforcing bar $f_y = 500MPa(Fe500)$

For concrete:

- Unit weight $(weight\ per\ unit\ volume) = 25\text{KN/m}^3$
- Grade of Concrete=C30
- Characteristic Compressive strength, $f_c = 24MPa$

- Young's modulus of elasticity, $E_C - 32000MPa$
- Poison's ratio, $v_c = 0$ for concrete crack n_c =0
- Shear Modulus, $G_C = \frac{E_C}{2(1+v_c)}$ =16000MPa

For HCB Masonry Panel:

- Size of HCB = 15 cm x 20cm x 40cm and 20 cm x 20cm x 40cm
- Horizontal mortar thickness = 2cm
- Mortar ratio = 1:3
- Unit weight (Weight per unit volume)=$14\ KN/m^3$
- Characteristic Compressive strength, $f_m = 3MPa$

Young's Elastic modulus of masonry, is calculated by the relation given by (FEMA 273) .The values for the modulus of elasticity of masonry in compression shall be taken as 550 times the expected masonry compressive strength, f_m

- E_m=500$f_m = 500 * 3MPa = 1925MPa$
- Poison's ratio, $v_m = 0$
- Shear Modulus, $G_m = \frac{E_m}{2(1+v_m)} = 963Mpa$

4.4.2 Load cases Used

Dead load: The Unit Weights of Materials used in this study is based on ESEN1991:2015

Imposed Load: the imposed load used in this study is based on ESEN1991:2015

Earthquake Load: ESEN1998:2015 Criteria for Earthquake Resistant design of Structure was used.

Seismic design

A code based equivalent static lateral force analysis and response spectrum analysis was used to size and determine reinforcement amount for all structural members. Following this initial stage of design, the nonlinear pushover analysis was used to understand the global behavior of structural system for its compliance with the design criteria. **ESEN1998,2015** response spectrum has been used. On response spectrum case data scaling factor was used for zone IV. The software generated seismic design in which the software will calculate the period and all the modes after inserting scaling factor on response spectrum case data. Lateral load calculation and its distribution along the height is done. The seismic weight is calculated using full dead load plus 25% of live load (**FEMA 273**)[44]. The load cases defined for the software are:

- DL-(Self Weight)
- DL-(Member Weight i.e. Wall Load)-Super dead
- DL-(Floor Weight i.e. Slab Load)-super dead
- Live load for roof
- Live load for floor
- Response spectrum-X
- Response Spectrum-Y
- Equivalent static lateral force-X
- Equivalent static lateral force-Y

4.4.3 Modeling of masonry infill

In the case of an infill wall located in a lateral load resisting frame the stiffness and strength contribution of the infill are considered by modeling the infill as an equivalent compression strut. Because of its simplicity, several investigators have recommended the equivalent strut concept. In the present analysis, a trussed frame model is considered. This type of model does not neglect the bending moment in beams and columns. Rigid joints connect the beams and columns, but pin joints connect the eccentric equivalent struts to columns as shown in figure 4.10.

Infill parameters (effective width and strength) are calculated using the method recommended by **(Stafford-Smith and Carter 1969)[2]:** described in chapter two

sections 2.7 and 2.8.The length of the strut is given by the diagonal distance *d* of the panel and its thickness is given by the thickness of the infill wall. The initial elastic modulus of the strut E_i is equated to E_m the elastic modulus of masonry. As per FEMA 273, E_m is given as $500f_m$, where f_m is the compressive stress of masonry in MPa.

4.4.4 Modeling of Equivalent Strut

For an infill wall located in a lateral load-resisting frame, the stiffness and strength contribution of the infill has to be considered. Non-integral infill walls subjected to lateral load behave like compression diagonal struts. Thus an infill wall can be modelled as an equivalent diagonal compression strut in the building model.

The equivalent struts modeling parameters (effective width, elastic modulus and strength) were estimated using equations derived by **(Stafford-Smith and Carter 1969)[2].**The length of the strut is given by the diagonal distance (d) of the panel and its thickness is equal to the thickness of the infill wall. The elastic modulus of the strut is equated to the elastic modulus of masonry (Em). For the estimation of width (w) of the strut, a simple expression as given in Eq. 2.5 (Chapter 2) is adopted.

After modeling the bare frame, the equivalent eccentric diagonal struts are added to represent the masonry infill as shown in figure 4.8.Since most of the panels are fully infilled, the struts should, at first, be designed to represent full infill panels, then multi-plied by a proper reduction factor to account for any openings in the infill panel as stated in (chapter 2) section 2.7.

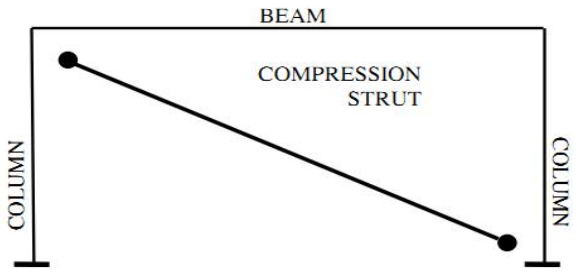

Figure 4.9 Eccentric Compression Strut Connections.

4.5 Plastic Hinge Placement

In order to model nonlinear behavior in any structural element, a corresponding nonlinear hinge must be assigned in the building model. Nonlinear hinges were assigned to the following structural elements expected to undergo inelastic deformation:

To ensure gravity load carrying capability at performance point, PMM hinges are assigned at the ends and shear hinges are assigned at the mid-height level of gravity columns.

Plastic hinges in columns should capture the interaction between axial load and moment capacity. These hinges should be located at a minimum distance l_{column} from the face of the beam as shown in figure 4.10.Hinges in beams need only characterize the flexural behavior of the member. These hinges should be placed at a minimum distance l_{beam} from the face of the column. This distance is calculated from Equations 4.1 and 4.2 where $\theta_{beam}$is the angle at which the infill forces would act if the eccentricity of the equivalent strut was assumed to act on the beam as depicted in Figure 4.11.

$$l_{beam} = \frac{a}{sin\theta_{beam}} \quad ----------(4.1)$$

$$tan\theta_{beam} = \frac{h}{l - \frac{a}{sin\theta_{beam}}} \quad ----------(4.2)$$

Where:

l_{beam} =Distance from the face of the beam to the first beam plastic hinge,cm

l = length of the infill,cm

h = height of the infill panel,cm

a = Equivalent width of infill strut in the elastic range , cm

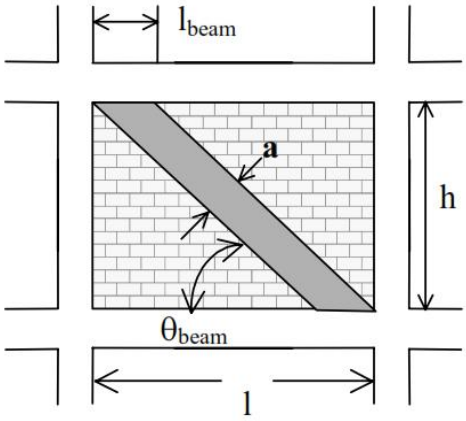

Figure 4.10 Distance to beam hinge(Ghassan Al-Chaar).

Although the infill forces are assumed to act directly on the columns, hinging in the beams will still occur and l_{beam} is a reasonable estimate of the distance from the face of the column to the plastic hinge.

Shear hinges must also be incorporated in both columns and beams. The equivalent strut, however, only needs hinges that represent the axial load. This hinge should be placed at the mid-span of the member. In general, the minimum number and type of plastic hinges needed to capture the inelastic actions of an infilled frame are depicted in Figure 4.11

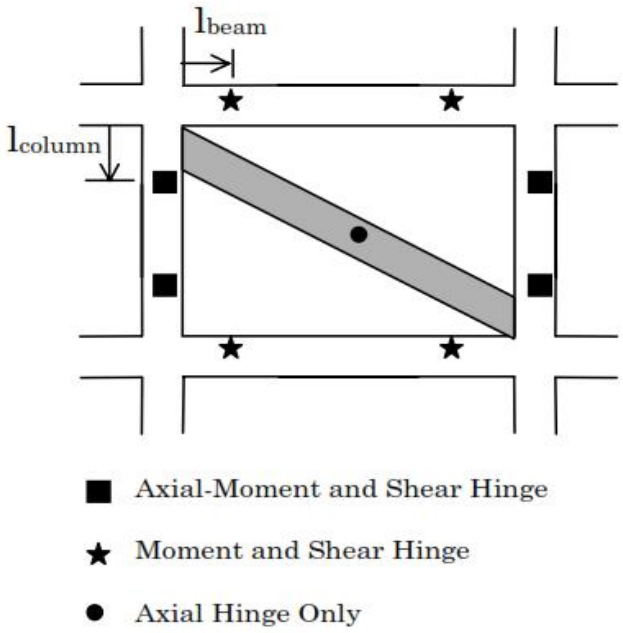

Figure 4.11 Plastic hinge placement(Ghassan Al-Chaar).

4.6 Rigid End Offsets

The frame elements surrounding a panel containing an equivalent strut in the mathematical model will be too flexible. This is because of the lack of confinement produced by the strut that would have been provided had the infill been modeled with finite elements. To counteract this effect, it is recommended that REOs be placed on the frame members surrounding an infilled panel. For beams surrounding infilled panels, REOs should be used from the beam/column joint to a distance of l_{beam} from the face of the column. For columns surrounding infilled panels, REOs should be placed from the beam/column joint to a distance of l_{column} from the face of the beam. These distances also correspond to the locations of the beam and column plastic hinges. The beam or column is therefore assumed to be rigid up to the point of the plastic hinge. Figure 4.12 shows the placement of REOs (shown in black) for an infilled frame.

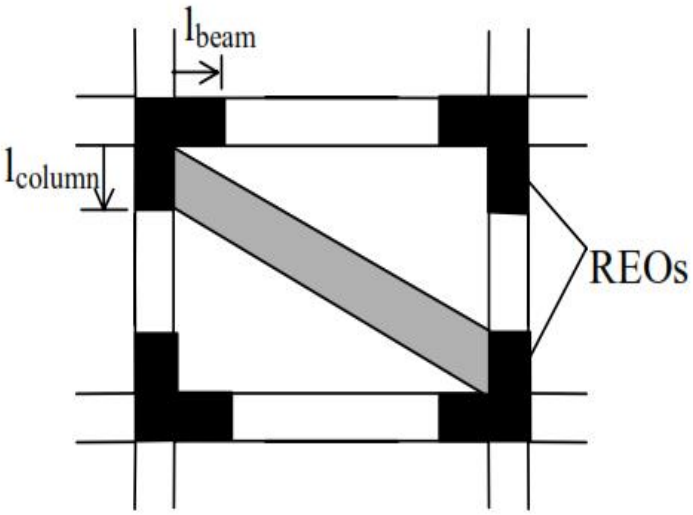

Figure 4.12 Rigid end offset placement(Ghassan Al-Chaar)**.**

4.7 Nonlinear Pushover Analysis Method

The mathematical model should be subjected to monotonically increasing lateral loads until the maximum displacement of the design earthquake is reached or a failure mechanism forms. The target displacement should be calculated following the procedure in **FEMA 273**[44].Gravity loads should be applied as initial conditions prior to the earthquake loadings. The load combinations that should be used are given in **FEMA 273[44]**.

Lateral loads should be applied in a manner that approximates the inertia forces in the design earthquake. It is recommended that a minimum of two different inertia force distributions be used in order to capture the worst-case design forces. The recommended inertia force distributions are given in **FEMA 273**.[44].

Finally, the load and pushover cases are defined. The pushover is defined using the local redistribution member unloading method, with gravity loads as an initial condition.

For present study of pushover analyses, use the total dead load and 25% of the live load (1.0 DL + 0.25 LL). All dead loads in the building (structural components, partitions, architectural finishes and more) should be included in defining the total dead load. Masonry infill walls should be considered as dead loads, because the infill walls are structural elements.

CHAPTER 5 RESULTS AND DISCUSSIONS

5.1 GENERAL

This chapter presents the results of pushover analysis of Reinforced concrete frame with different configuration of masonry wall. Analysis of the models under the static and dynamic loads has been performed using Etabs2015 software. All required data are provided in software and analyzed for total five models to get the result in terms of **Base shear vs monitored roof displacement**, **Storey shear**, **story displacement**, **element force** and **seismic performance assessment**. Subsequently these results are compared for reinforced concrete frame with different configuration of masonry wall.

5.2 Analysis Results for Push(Load Pattern Acceleration X-Dir)

In the present study, non-linear response of reinforced concrete frames with different configuration of masonry wall is modeled as per details discussed in Chapter 4 using nonlinear modeling under the loading has been carried out. Based on the results obtained from the Push (load pattern acceleration X-Dir) numerical analysis, the behavior of different structural systems are compared and described briefly in further section. Thus, five different models; a **bare reinforced concrete frame**, **reinforced concrete frame with 75% of infill reduced from fully infilled frame**, **reinforced concrete frame with 50% of infill reduced from fully infilled frame**, **reinforced concrete frame with 25% of infill reduced from the fully infilled frame** and **fully infilled reinforced concrete frame(base frame) are considered**.

1. Base Shear vs Monitored Roof Displacement Curve

Current standards such as ASCE 41 provide two alternate methods of estimating the peak displacement demand for use in nonlinear static procedures: the displacement coefficient method and the capacity spectrum method. Both methods rely on an equivalent linearization approach. The basic assumption in equivalent linearization techniques is that the maximum inelastic deformation of a nonlinear single degree of freedom (SDOF) system is approximately equal to the maximum deformation of a linear elastic SDOF

system, provided that the linear elastic system has a period and a damping ratio that are larger than the initial values of those for the nonlinear system.

The displacement coefficient method is conceptually simpler and easier to use, and is not prone to the graphical misinterpretations that can occur with the capacity spectrum method. The authors recommend using the displacement coefficient method, either alone or to check results obtained by using the automated capacity spectrum method capabilities in ETABS.

- **Displacement Coefficient Method**

The displacement coefficient method (simply called the coefficient method in **FEMA 356[25]** is the primary method of estimating displacement for the nonlinear static procedure in **ASCE 41[24]**, and its pre-standard **FEMA 356[25]**.The displacement coefficient method generates an estimate of the maximum global displacement, called the *target displacement*, by modifying the linear elastic response of an equivalent SDOF system. This is accomplished by multiplying the SDOF spectral displacement by a series of coefficients, *Co* through C_3,. Figure 5.1 shows the process used to calculate the target displacement.

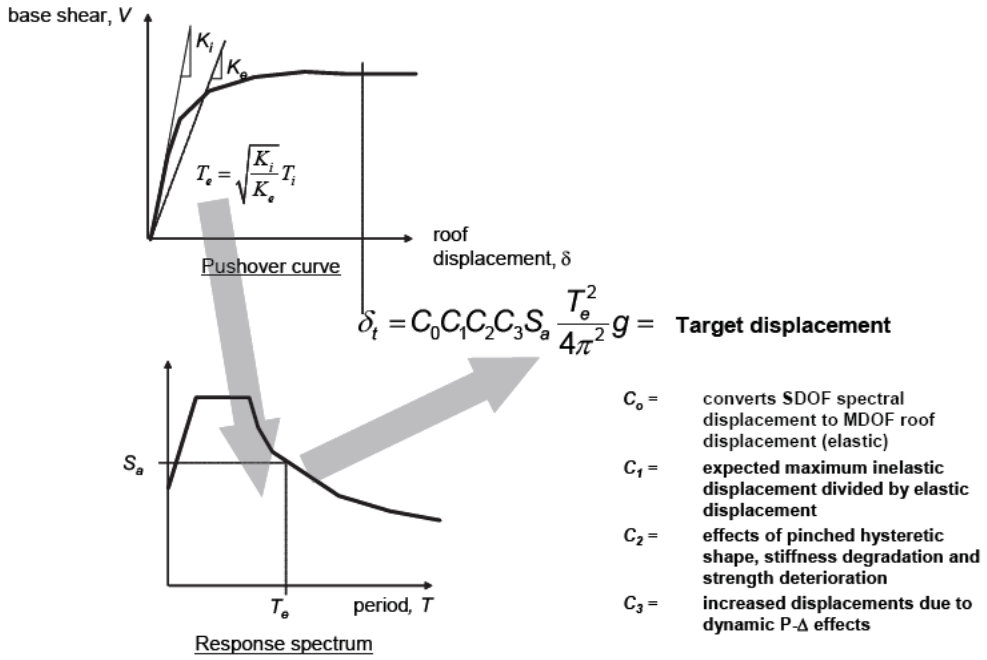

Figure 5.1 Schematic illustration of the process of estimating target displacement using the Displacement coefficient method, for a given response spectrum and effective period, T (Reproduced from FEMA 440, Figure 2-12, a public domain document).

First an effective period, T_e, is generated from the initial period, T_i, by a graphical procedure using an idealized force-deformation curve (i.e., pushover curve) relating base shear to roof displacement, which accounts for some stiffness loss as the system begins to behave in elastically. The effective period represents the linear stiffness of the equivalent SDOF system. The effective period is used to determine the equivalent SDOF system's spectral acceleration, *Sa*, using an elastic response spectrum. The procedure assumes that the damping (usually 5%) is appropriate for a structure in the elastic range.

Then, the peak elastic spectral displacement is determined from the spectral acceleration using the following equation:

$$S_d = \frac{T_{eff}^2}{4\pi^2} S_a \quad \text{----------5.1}$$

The Displacement Coefficient Method then uses four coefficients to convert the peak elastic spectral displacement first to elastic displacement at the roof and then to inelastic

displacement at the roof. FEMA 440, Improvement of Nonlinear Static Seismic Analysis Procedures, explains each of the coefficients C_0 through C_3 as follows:

The coefficient C_0 is a shape factor (often taken as the first mode participation factor) that simply converts the spectral displacement to the displacement at the roof. The other coefficients each account for a separate inelastic effect. The coefficient C_1 is the ratio of expected displacement for a bilinear inelastic oscillator to the displacement for a linear oscillator. C_1 depends on the ratio of elastic force, calculated as the spectral acceleration multiplied by the mass, to the yield strength, the period of the SDOF system, T_e and the characteristic period of the spectrum. The coefficient C_2 accounts for the effect of pinching in load-deformation relationships due to degradation in stiffness and strength. Finally, the coefficient C_3 adjusts for second-order geometric nonlinearity (P-Δ) effects. The coefficients are empirical and derived primarily from statistical studies of the nonlinear response-history analyses of SDOF oscillators and adjusted using engineering judgment.

Based up on the Displacement coefficient method of **ASCE 41-13[24]** described above all the five building models as described in chapter 4 are analyzed in ETABS 2015 standard structural software and the static pushover curve is generated as shown in figure 5.2.

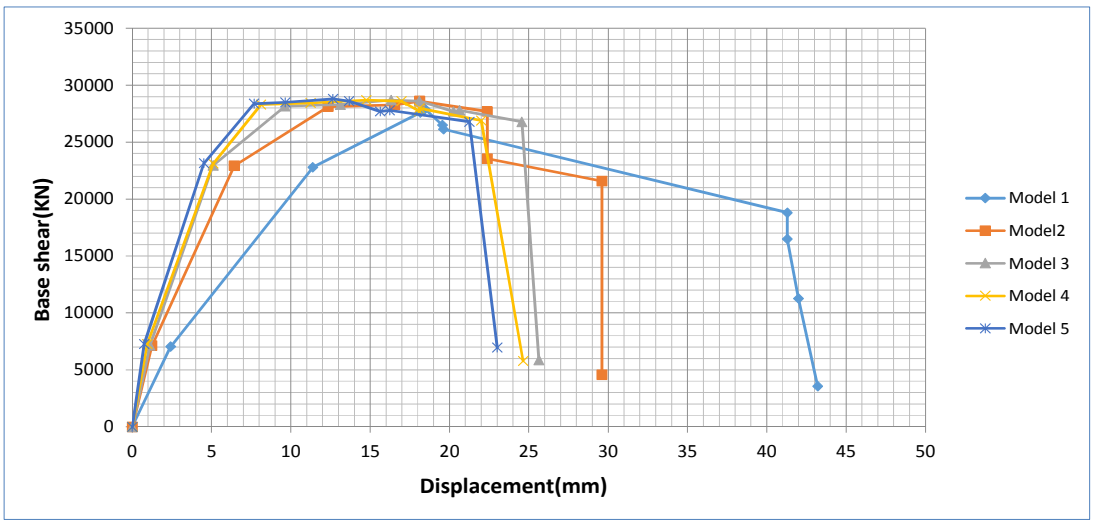

Figure 5.2 pushover analysis result for 10-story RC building

Results from static pushover analysis for the case study buildings are shown in Fig. 5.2 and summarized in appendix Table C.1.Lateral loads were applied according to the equivalent lateral force distribution specified in **ASCE 7-05[24].**

The presence of the infill wall both strengthens and stiffens the system, as illustrated in Fig. 5.2. For the case study building, the fully-infilled frame has approximately 3 times larger intial stiffness and 1.5 times greater peak strength than the bare frame. In Fig.5.2, the first drop in strength for the fully and partially-infilled frame is due to the brittle failure of masonry materials initiating in the first-story infill walls. This behavior after first-story wall failure is due to wall-frame interaction and depends on the relative strength of the infill and framing.

So, based on these results, infill walls can be beneficial as long as they are properly taken into consideration in the design process and the failure mechanism is controlled.

2. Story displacement for different models

After analyzed all models in ETABS 2015 , the storey response results obtained in terms of storey displacement of the models. First of all consider model 1 “BARE FRAME (G+9)” because, it is a basic or traditional structure in which no other element are included or considered in structure for improving the performance of the building, so the results of the Bare frame (G+9) can be compared with the results of the other models. Results from static pushover analysis for the case study buildings are shown in Fig. 5.3 and summarized in appendix Table C.2

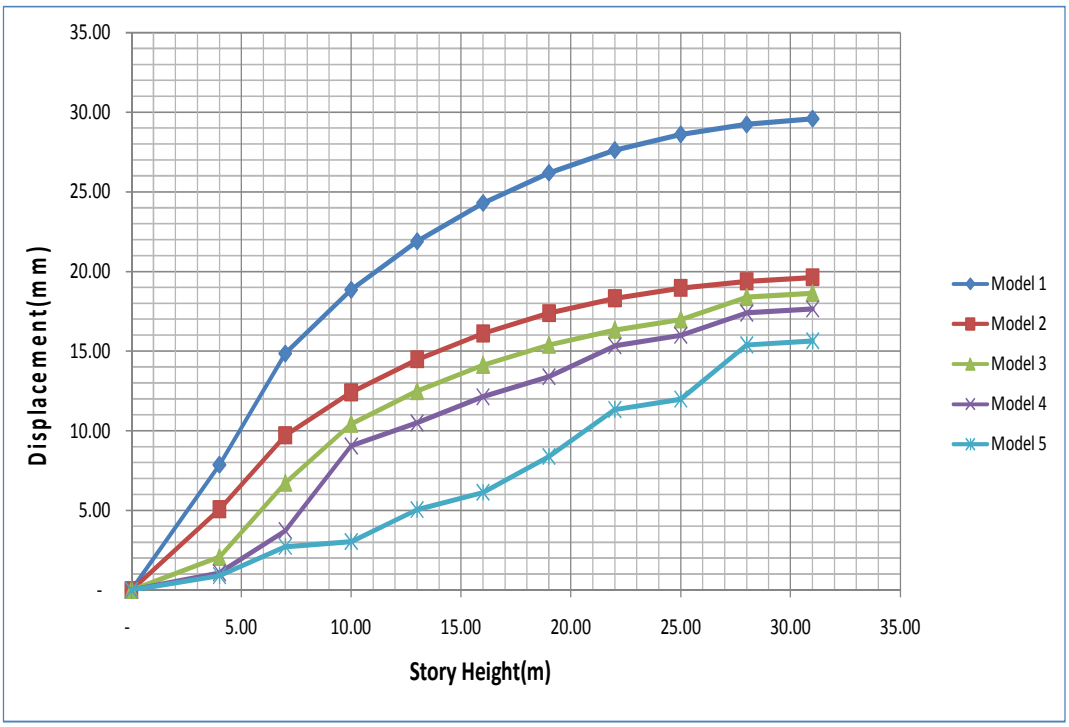

Figure 5.3 Comparison of Story displacements for different models

Figure 5.3 show the comparative study of seismic demand in terms of lateral story displacement amongst all the five types of reinforced concrete frame with different configuration of infill .The lateral displacement obtained from the bare frame model is the maximum which is about 60% greater than that of fully infilled frame, nearly 50% greater than that of frame with 25% of the masonry wall reduced, about 40% greater than that of frame with 50% of the masonry wall reduced and 30% greater than that of frame with 75% of the masonry wall reduced.

Thus, the infill panel reduces the seismic demand of reinforced concrete buildings. The lateral story displacement is dramatically reduced due to introduction of infill. This probably is the cause of building designed in conventional way behaving near elastically even during strong earthquake.

3. Member Forces

Next, the effect of infill on the member forces in beams and columns were studied. In general compared to bare frame model, the infilled models predicted higher axial and shear forces in columns but lower bending moments in both beams and columns. Thus,

the effect of infill panel is to change the predominantly a frame action of a moment resisting frame system towards truss action.

In this project to understand the effect of different configuration of infill in reinforced concrete frame; study of the behavior of the column in all models for axial loads was conducted. Total of five nonlinear models are analyzed in ETABS 2015 and all models have same plan of building, therefore the position and label of columns are same in all plans of models which is shown in chapter 4 figure 4.1. After analysis consider the column no. 1(C_1) shown in fig.4.1 from all models for pushover load case and get the axial forces of column at performance point at every story from software, which is given in table no 5.1 and the values for each model is compared with the bare frame model .

Table5.1 comparison of axial force for different models

Column Axial Force(KN)-C1						
Story	**Elevation(m)**	Model 1	Model 2	Model 3	Model 4	Model 5
Story 10	31	161	168	170	180	192
Story 9	28	444	454	459	470	488
Story 8	25	728	740	748	763	780
Story 7	22	1011	1025	1035	1052	1070
Story 6	19	1290	1309	1320	1340	1358
Story 5	16	1569	1589	1605	1628	1646
Story 4	13	1842	1865	1882	1907	1927
Story 3	10	2120	2145	2168	2192	2212
Story 2	7	2384	2412	2435	2467	2485
Story 1	4	2577	2608	2635	2662	2682

From this observation, it is evident that when an infilled frame is loaded laterally, the columns take the majority of the force and shear force exerted on the frame by the infill which is modeled as the eccentric equivalent struts. Generally, the relative increase of axial force is observed when the percentage of infill in reinforced concrete frame increases. It is observed that fully infilled reinforced concrete frame showed around 10% increase in axial force relative to bare frame model. The other infill models showed a lesser increase. The effect of infill on columns is to increase the shear force and to reduce bending moments.

Similarly in the case of beam, the effect of infill is to reduce the shear force as well as bending moment when subjected to seismic loading. The shear force and bending

moment of fully infilled frame predicted about 20 % decrease of the bare frame model whereas; the other infill models showed a lesser decrease.

4. Story shear

Story shear is the total horizontal seismic shear force at the base of structure. Results from static pushover analysis at performance point for the case study buildings are shown in Fig. 5.5 and summarized in appendix Table C.3

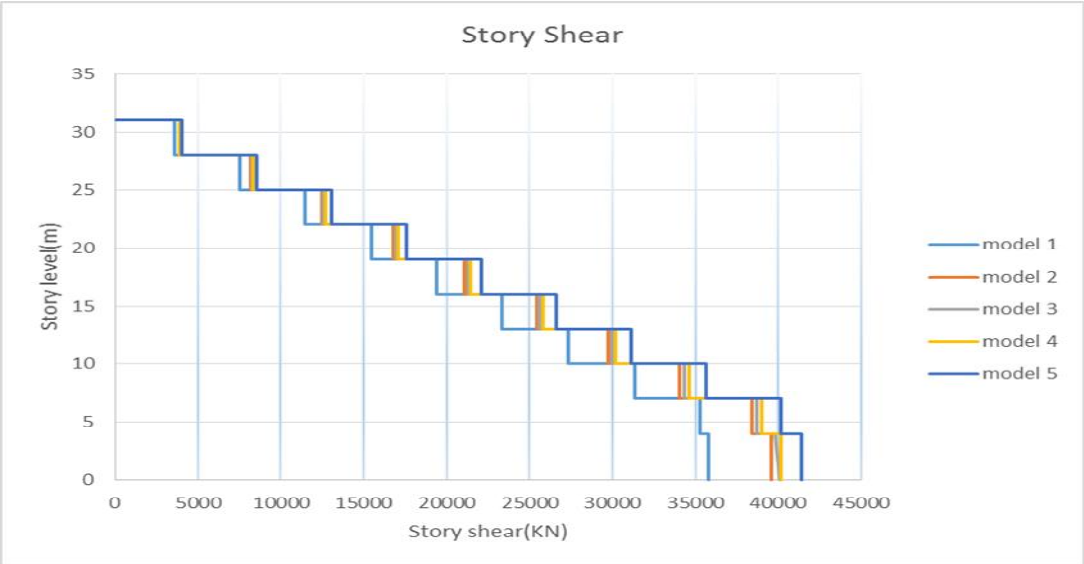

Figure 5.4 comparison of story shear for different model

As observed from the figure 5.5 the story shear calculated on the basis of bare frame model gave a lesser value than the other infilled frames; It was observed that the story shear in fully infilled frame is nearly 15% greater compared to bare frame model and frame with 25% of the masonry wall reduced was nearly 10% greater compared to the bare frame, frame with 50% of the masonry wall reduced is nearly 8% greater compared to the bare frame and frame with 75% of the masonry wall reduced is about 5 % greater compared to the bare frame.

Since the bare frame models do not take in to account the stiffness rendered by the infill panel, it gives significantly longer time period. And hence smaller lateral forces. And when the infill is modeled, the structure becomes much stiffer than the bare frame model. Therefore, it has been found that calculation of earthquake forces by treating RC frames

as ordinary frames without regards to infill leads to underestimation of base shear. This is because of bare frame is having larger value of fundamental natural time period as compared to other models due to absence of masonry infill walls. Fundamental natural period get increased and therefore base shear get reduced.

5. Assessing Seismic Performance

The procedure for assessing seismic performance applies the methodology for performance-based earthquake engineering based on **FEMA 356** document which present performance-based engineering methods that rely on nonlinear static analysis procedures for prediction of performance level. Lateral loads were applied according to the equivalent lateral force distribution specified in ASCE 7-05.

The presence of masonry walls has a significant effect on the collapse mechanism. To illustrate, Fig. 5.6 & Fig. 5.7 present the dominant failure modes of bare frame and fully-infilled frames for the 10-story building respectively. Deflected shapes display the pushover deformed shape on step-by-step basis to view the pushover displacement shape and sequence of hinge formation (hinges appear when they yield and color coded based on their state).The color of the hinges indicates the state of the hinge, i.e, where it is along its force displacement curve described in figure 3.2

The pushover deformed shape representing the state of hinge is taken at final step(step 10) shown in table 5.2 and table 5.3.

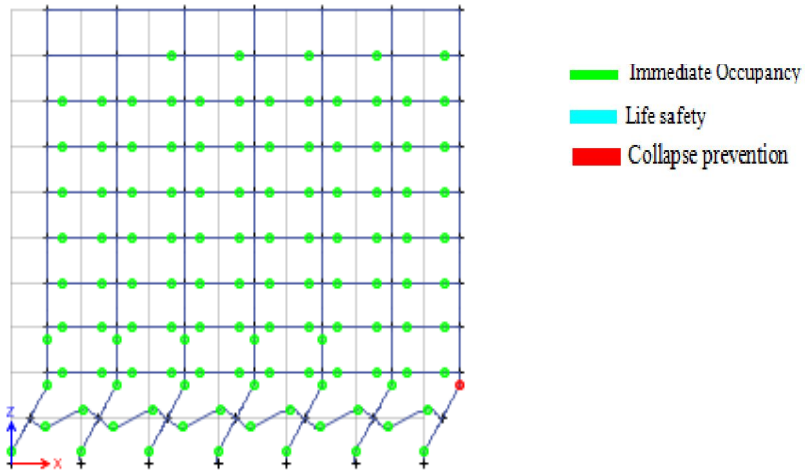

Figure 5.3 Typical failure mode observed for bare frame at step 10

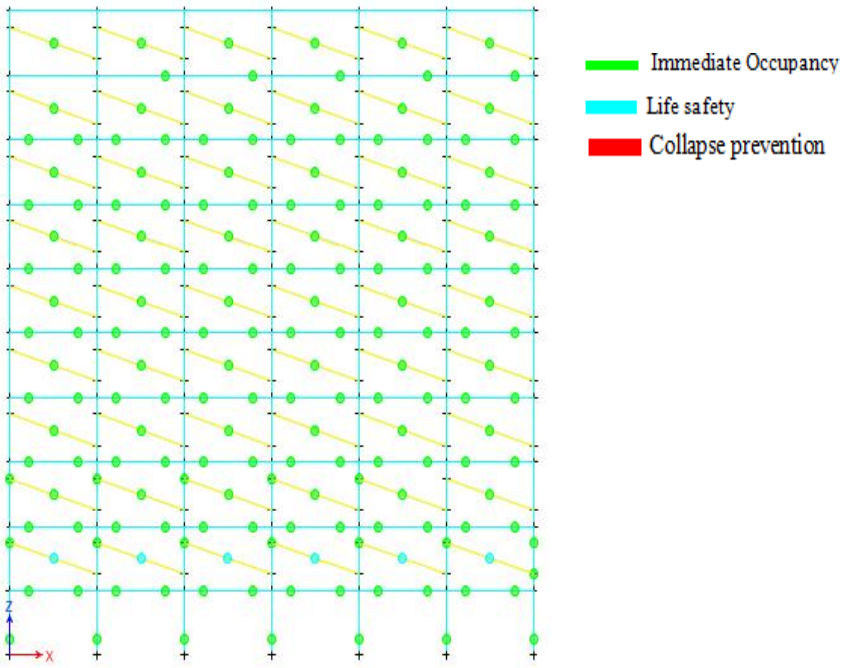

Figure 5.4 Typical failure mode observed for fully infilled frame at step 10

A table also obtained which gives the coordinates of each step of the pushover curve and summarizes the number of hinges in each state (for example, between IO, LS, CP or between D and E). This data is shown in Table. 5.2 and Table5.3.

Table 5.2 Tabular data for the number of hinges in each state of fully infilled frame

Step	Displacement	Base Force	A-B	B-C	C-D	D-E	>E	A-IO	IO-LS	LS-CP	>CP	Total
	mm	kN										
0	0	0	2986	98	0	0	0	3084	0	0	0	3084
1	0.75	7250.26	2981	103	0	0	0	3084	0	0	0	3084
2	4.52	23140.23	2383	701	0	0	0	3084	0	0	0	3084
3	7.68	28370.23	2287	797	0	0	0	3084	0	0	0	3084
4	9.645	28500.23	2279	805	0	0	0	3084	0	0	0	3084
5	12.65	28798.23	2266	818	0	0	0	3084	0	0	0	3084
6	13.68	28597.23	2261	823	0	0	0	3084	0	0	0	3084
7	15.63	27697.23	2191	891	2	0	0	2926	156	2	0	3084
8	16.23	27789.36	1890	1192	0	0	2	2926	158	0	0	3084
9	16.23	44868.09	1813	1185	84	0	2	2816	184	84	0	3084
10	16.24	45256.23	1813	1185	84	0	2	2816	268	86	0	3084

Table 5.3 Tabular data for the number of hinges in each state of bare frame model

Step	isplacemen	Base Force	A-B	B-C	C-D	D-E	>E	A-IO	IO-LS	LS-CP	>CP	Total
	mm	kN										
0	-	0	2660	0	0	0	0	2660	0	0	0	2660
1	2.43	7046.501	2655	5	0	0	0	2660	0	0	0	2660
2	11.39	22772.54	2058	602	0	0	0	2660	0	0	0	2660
3	18.16	28007.24	1961	699	0	0	0	2660	0	0	0	2660
4	18.46	28129.99	1953	707	0	0	0	2660	0	0	0	2660
5	19.55	28450.99	1946	714	0	0	0	2660	0	0	0	2660
6	19.63	28458.9	1944	716	0	0	0	2660	0	0	0	2660
7	41.30	24562.35	1877	780	3	0	0	2478	182	12	0	2660
8	41.30	16487.26	1831	826	0	0	3	2478	181	21	1	2660
9	41.29	37280.1	1831	821	5	0	3	2478	181	14	1	2660
10	43.15	3618.509	1826	826	5	0	3	2478	179	56	3	2660

The presence of masonry walls has a significant effect on the collapse mechanism observed. The bare frame (Fig. 5.6) pushover results shows some of the hinges of the columns at second story level are beyond collapse prevention performance level whereas all the beams and columns at other story level are yielded to some extent but still they are elastic at immediate occupancy level. The fully-infilled frame (Fig. 5.7) shows some of the hinges of the masonry wall at second story level get beyond life safety performance level due to the brittle failure nature of masonry walls, though columns and beams are still elastic at immediate occupancy level. This shows that the frames are at immediate occupancy level where as the masonry walls are already failed due to its brittle nature.

Seismic performance assessment generally shows that the fully-infilled frames have the highest collapse safety of the all infill configurations considered. The fully-infilled frames exhibit better seismic performance due to the added strength of the masonry walls in the system.

This study agrees with the results of **Madan** and **Hashmi (2008)[14],** who observed that the infilled frames experienced less damage than either the bare frame or partially-infilled buildings, due to higher stiffness and strength. The superior performance of infilled buildings is also consistent with past experimental results (e.g. **Klingner** and **Bertero** 1978)**[5].**

CHAPTER 6 CONCLUSIONS AND RECOMMENDATIONS

6.1 Conclusions

This study focuses on the Seismic Performance of reinforced concrete building with different configuration of masonry infill. Infill panels are modeled by nonlinear strut element, which only have compressive strength.

Eccentric equivalent struts for masonry wall modeling were chosen for this study because, when an infilled frame is loaded laterally, the columns take the majority of the forces exerted on the frame by the infill. Furthermore, the loss of a column is much more detrimental to a structure than the loss of a beam. Therefore, for ultimate capacity purposes, failure was assumed to occur when the columns failed from the infill forces. These forces act as a result of separation of the frame from the infill due to lateral loading. The equivalent struts were estimated using equations derived by **Stafford-Smith** and **Carter** (1969)**[2]** for their consistently accurate predictions of infilled frame in-plane behavior when compared with experimental results **(Ghassan Al-Chaar)[29].**

Nonlinear models of the frame-wall system are subjected to a series of incremental static analysis in order to assess seismic performance. The main observations and conclusions drawn are summarized below:

1. Results of pushover curve show an increase in initial stiffness, strength, and energy dissipation of the infilled frame, compared to the bare frame, despite the wall's brittle failure modes.

2. Due to the introduction of infill the displacement capacity decreases as depicted from the displacement profile (Figure 5.3). The lateral displacement obtained from the bare frame model is the maximum which is about 60% greater than that of infilled frame.

3. The presence of masonry walls is to change a frame action of a moment resisting frame structure towards a truss action. When infills are present, shear and axial force demands are considerably higher leaving the beam or column vulnerable to shear failure. The axial force and shear force of the bare frame is less than that of the infilled frame. Columns take the majority of the forces exerted on the frame by the infill because

the eccentrically modeled equivalent struts transfers the axial load and shear force transferred from the action of lateral loads directly to the columns. On the other hand, the effect of infill on infilled frame is to reduce the bending moments. Similarly in the case of beam, the effect of infill is to reduce the shear force as well as bending moment when subjected to seismic loading.

4. Likewise, pushover analysis results indicate that fully-infilled frame has the lowest collapse risk and the bare frames are found to be the most vulnerable to earthquake-induced collapse. The better collapse performance of fully-infilled frames is associated with the larger strength and energy dissipation of the system, associated with the added walls. Similar trends are observed for both the models with shear walls and without shear walls of 10-story RC frames.

5. The story shear calculated on the basis of bare frame model gave a lesser value than the other infilled frames. It was observed that fully infilled frame is nearly 15% greater compared to bare frame model and frame with 25% of the masonry wall reduced was nearly 10% greater compared to the bare frame, frame with 50% of the masonry wall reduced is nearly 8% greater compared to the bare frame and frame with 75% of the masonry wall reduced is about 5 % greater compared to the bare frame.

This is because the bare frame models do not takes in to account the stiffness rendered by the infill panel, it gives significantly longer time period.

6.2 Future Recommendations

1. The study can be extended to a building frame with greater number of story to see the effect of infill panels on tall structure during seismic excitation.

2. The macro modeling approach used here takes into account only the equivalent global behavior of the infill in the analysis. As a result, the approach does not permit study of local effects such as frame-infill interaction within the individual infilled frame subassemblies. More detailed micro-modeling approaches need to be used to capture the local conditions within the infill.

3. The present study was done based on the strut width derived by **Stafford-Smith** and **Carter** (1969). Many researchers had recommended different strut width to replace infill panel. The study could be extended to more strut width and compared with experimental result to find out the most suitable one.

4. The present study was carried out using nonlinear static analysis method for the seismic analysis. This could be extended to nonlinear dynamic analysis to cater for the structure with horizontal as well as vertical irregularity.

5. The frames were subjected only to the in-plane action of seismic forces. The out-of-plane action and its interaction with the in-plane action is a subject for further study in 3-D analysis

6. Due to the limitation of the experimental data the material of infill was hollow concrete block. It can be replaced by other materials such as reinforced brick, solid concrete block and stone masonry in order to reveal the influence in the variation of materials.

References

.[1] Polyakov, S. V., 1960. On the interaction between masonry filler walls and enclosing frame when loaded in the plane of the wall, *Τρανσλατιονσ ιν Εαρτηθυακε Ενγινεερινγ*. EERI, San Francisco, 36–42.

[2] Stafford-Smith, B., and Carter, C., 1969. A method for the analysis of infilled frames, *Προχ. Ινστν. Χιϖ. Ενγρσ.,* 44, 31–48.

[3] Stafford-Smith, B., 1962. Lateral stiffness of infilled frames, *Θ. Στρυχτ.Διϖ.*, 88 (6), 183–199.

[4] Mainstone, R. J., 1971. On the stiffness and strength of infilled frames, *Προχ. Ινστν. Χιϖ. Ενγρσ.*,Supplement IV, 57–90 (paper 7360S). `

[5] Klingner, R. E., and Bertero, V. V. Earthquake resistance of infilled frames,

Journal of structural Devision,ASCE,vol 104,NO.ST6,1978,pp.973-989

[6] Mehrabi, A. B., Shing, P. B., Schuller, M., Noland, J., 1996. Experimental evaluation of masonry-infilled RC frames. Journal of structural Devision,ASCE,vol 122 ,NO.ST 3,1996,pp.228-237

[7] Holmes M. Steel frames with brickwork and concrete infilling. Proceedings of the Institution of Civil Engineers 19,1961

[8] Flanagan, R. D., Bennett, R. M.. In-plane behavior of structural clay tile infilled frames, Journal of structural Devision,ASCE,vol 125,NO.ST 6,1999,pp.590-599

[9] Dhanasekar, M., Page, A.W., 1986. The influence of brick masonry infill properties on the behavior of infilled frames, *Προχ. Ινστ. Χιϖ. Ενγρσ.*, London, 81, 593 – 605.

[10] Mehrabi, A. B., Shing, P. B. Finite element modeling of masonry-infilled RC frames, Journal of structural Devision,ASCE,vol 123 ,NO.ST 3,1997,pp.604-613

[11] Stavridis A., Shing P. B., 2009. Finite element modeling of nonlinear behavior of masonry-infilled RC frames, Journal of structural Devision,ASCE,vol 136 ,NO.ST 3,2009,pp.285-296

[12] Dolsek M., Fajfar P., 2008. The effect of masonry infills on the seismic response of a four storey reinforced concrete frame—a probabilistic assessment, Engineering Structures 30, 1991–2001.

[13] Dymiotis C, Kappos AJ, Chryssanthopoulus MK., 2001. Seismic Reliability of Masonry-Infilled RC Frames, Journal of structural Devision,ASCE,vol 127 ,NO.ST 3,2001,pp.296-305

[14] Madan A, Hashmi AK., 2008. Analytical prediction of the seismic performance of masonry infilled reinforced concrete frames subjected to near-field earthquakes, Journal of structural Devision,ASCE,vol 134 ,NO.ST 9,2008,pp.1569-1581

[15] D. B. Karwar and Dr. R. S. Londhe(2014), Performance of RC Framed Structure by Using Pushover Analysis, International Journal of Emerging Technology and Advanced Engineering.

[16] A. K. Chopra, Dynamics of Structures, Prentice Hall, Englewood Cliffs, NJ, USA, 1995.

[17] C. S. BARBOSA , Strength and deformability of hollow concrete blocks

[18] Catherin Jeselia M., Modeling of Masonry infills, American Journal of Engineering ,2013

[19] Korkmaz, K.A., F.Demir, and M.Sivri, Earthquake Assessment of R/C Structures with Masonry Infill Walls. International Journal of Science and Technology, 2007.2: p. 155-164.

[20] Murty,C.V.R.,etal.,ATRISK:The Seismic Performance of Reinforced Concrete Frame Buildings with Masonry Infill Walls .2006,Earthquake Engineering Research Institute and the International Association for Earthquake Engineering:Oakland.p.83.

[22] D.V.Mallick and R.T Severn,The Behavior of Infilled Frames under Static Loading,Proc.ofICE,39(113),1967,pp.639-656.

[23] ETABS, User Interface Reference Manual.2002,Computers & Structures(CSi): California.

[24] American Society of Civil Engineers, ASCE-41: Seismic Rehabilitation of Existing Buildings. 2006: Virginia.

[25] Federal Emergency Management Agency, FEMA-356: Prestandard and Commentary for the Seismic Rehabilitation of Buildings. 2000: Washington DC.

[26] Applied Technology Council,ATC-40:Seismic Evaluation and Retrofit of Concrete buildings. 1996: California.

[27] Patnala VSNeelima,Ramancharla Pradeep Kumar, Seismic Behavior of RC Frame with URM Infill: Case Study, International Journal of Education and Applied Research (IJEAR),Vol.4,Issue Spl-2,Jan-June 2014.

[28] Dasd and murty cvr, Brick Masonry Infills in Seismic Design of RC Frame Buildings: Part 2- Behaviour, The Indian Concrete Journal, 2004.

[29] Ghassan Al-Chaar, Evaluating Strength and Stiffness of Unreinforced Masonry Infill Structures. 2002:US army corps of Engineers

[30] M.Selim Gunay ,A practical Guide to Nonlinear static analysis of reinforced concrete buildings with masonry infill walls, *University of California,Berkeley*

[31] Mohammad H. Jinya V. R. Patel, Analysis Of Rc Frame With And Without Masonry Infill Wall With Different Stiffness With Outer Central Opening: International Journal of Research in Engineering and Technology,2014

[32] Siamak Sattar and Abbie B. Liel,Seismic performance of Reinforced concrete Frame Structures with and without Masonry infill walls: University of Colorado.

[33] Humar,J.M.,D.Lau,and J.-R.Pierre,Performance of buildings during the 2001 Bhuj earthquake. Canadian Journal of Civil Engineering, 2001.28(6): p. 979-991.

[34] W.AxleyandV.V.Bertero,Infill Panels: Their Influence on Seismic Response of Buildings, EERC, University of California,Berkeley,CA, Rep.UCB/EERC-79/28.1969

[35] ESEN1998:2015., Design of Structures for Earthquake Resistance. Ethiopian Building Code Standard prepared by Ministry of Works and Urban Development. Addis Ababa, Ethiopia.

[36] Asteris et al,P.G. and Tzamtzis,A.D.,2003."On the Use of a Regular Yield Surface for the Analysis of Unreinforced Masonry Walls". Electronic Journal of Structural Engineering.

[37] V.K.R.Kodur, M.A.Erki and J.H.P.Quenneville "Seismic analysis of infilled frames" Journal of Structural EngineeringVol.25, No.2, July 1998 PP 95 -102.

[38] A. AMATO G, CAVALERI L, FOSSETTI M, AND PAPIA M, Infilled Frames: Influence of Vertical Load on The Equivalent Diagonal Strut Model, The 14th World Conference on Earthquake Engineering, Beijing, China, 2008.

[39] ESEN1992:2015., Design of Concrete Structures. Ethiopian Building Code Standard prepared by Ministry of Works and Urban Development. Addis Ababa, Ethiopia.

[40] ESEN1996:2015., Design of Masonry Structures. Ethiopian Building Code Standard prepared by Ministry of Works and Urban Development. Addis Ababa, Ethiopia.

[41] EN 1998-1-1:2005, — Eurocode 8: Design of structures for earthquake

[42] T. Paulay and M. Priestley, Seismic Design of Reinforced Concrete and Masonry Buildings. New York: Jhon Wiley & Sons, 1992

[43] ESEN1991:2015,--Basis of design and actions on structure Ethiopian Building Code Standard prepared by Ministry of Works and Urban Development. Addis Ababa, Ethiopia.

[44] FEMA 273, NEHRP Commentary on the Guidelines for the Seismic Rehabilitation of Buildings,FEMA, October 1997.

[45] T. C. Liauw and K. H. Kwan, "Nonlinear Behavior Of Non-Integral Infilled Frames," *Computers & Structures*, vol. 18, pp. 551-560, 1984

[46] A. W. Hendry, *Structural Masonry*, 2nd ed. Macmillan Press, London, 1998

[47] FEMA 306, "Evaluation of Earthquake Damaged Concrete and Masonry Wall Buildings: Basic Procedures Manual," *Federal Emergency Management Agency.*,1998.

[48] Macgregor, J.G.(1997). Reinforced concrete mechanics and design.(3rd edition):Prentice Hall,Inc.

[49] Konuralp Girgin and Kutlu Darılmaz. Seismic Response of Infilled Framed Buildings Using Pushover Analysis. Department of Civil Engineering, Istanbul Technical University, 34469, Maslak, Istanbul, Turkey. VOLUME 54, NUMBER 5. 5 December 2007.

[50] FEMA 310, Handbook for the Seismic Evaluation of Buildings – A Prestandard, FEMA, January 1998.

- www.wikipedia.com
- www.architectjaved.com

Appendix- A: Verification of pushover analysis

In pushover analysis model, Equivalent strut width estimates calculated from both Mainstone (1971) and Stafford-Smith and Carter (1969) (as calculated by Eq B.1 and Eq B.2 were implemented in the pushover analyses to determine displacement at ultimate load.

Experimental and pushover displacement data were available for six different half-scale models **(Ghassan Al-Chaar).**It is summarized as follows.

Table A.0.1 Displacement summary in mm.

Model Description	Exp. Results	Pushover Results	% Difference
3x3 fully infilled	32.22	33.63	4.4
1 Bay Brick	19.83	17.94	-10.5
1 Bay CMU	18.87	16.85	-12
Bay CMU	70.13	65.2	-7.56
Bay Brick	82.63	75.8	-8.9
1 Bay Bare	7.7	12.15	-21.5

Appendix- B: Modeling the Frame

This illustration details the procedure for estimating the equivalent width of masonry wall, hinge placement position for frames and strut capacity for modeling in a structural analysis program (ETABS) push-over analysis.

Table B. 0.1 Physical properties of the frame and infill panel

Frame	Infill	openings
$E_c = 32000MPa$	E_m=$1925MPa$	h_{door}=200cm
$f_c = 24MPa$	$f_m = 3MPa$	b_{door}=100cm
$f_y = 500MPa$	H=300cm	h_{window}=120cm
$h_c = 70cm$	h=240cm	b_{window}=200cm
$b_c = 70cm$	l=430cm	A_{panel}=103200cm^2
$I_c = 1080000cm^4$	t_{ext}=20cm	$A_{openings}$=44000cm^2
$h_b = 70cm$	t_{int}=15cm	
$b_b = 40cm$	D=492cm	
$I_b = 364583.33cm^4$	$\theta - 0.5rad$	

The first step is to model the bare frame according to its proper dimensions and physical properties as listed in Table B.1.The frame should be modeled according to standard modeling procedures for R/C frames.

After modeling the bare frame, the equivalent eccentric diagonal struts are added to represent the masonry infill. Since most of the panels are fully infilled,the struts should,

at first, be designed to represent full infill panels, then multiplied by a proper reduction factor to account for any openings in the infill panel.

The equivalent strut width is evaluated by first using Equation 2.4 to calculate the parameter λ_1, as shown in Equation B.1. λ_1 is then inserted into Equation 2.5 to determine the equivalent strut width, *a*, as illustrated in Equation. B.2. Since the infill panels are assumed to be undamaged, R_2 is taken to be 1.0.

$$\lambda_1 = \sqrt[4]{\frac{E_m t \sin 2\theta}{4 E_c I_{col} h}} \quad \text{(Eq B.1)}$$

$$\lambda_1 = \sqrt[4]{\frac{1925 * 20 * \sin(2 * 0.5)}{4 * 32000 * 1080000 * 240}}$$

$$\lambda_1 = 0.0056$$

$$a = 0.175 D (\lambda_1 H)^{-0.4} \quad \text{(Eq B.2)}$$

$$a = 0.175 * 492 (0.0056 * 300)^{-0.4}$$

$$a = 70\text{cm}$$

Next, the eccentric placement for the strut must be determined by calculating the distance (l_{column}). The distance (l_{column}) is found by simultaneously solving Equations 2.7 and 2.8 for l_{column} and θ_{column}, as shown in Equations B.3 and B.4.

$$l_{column} = \frac{a}{Cos\theta} \quad (EqB.3)$$

$$l_{column} = \frac{70}{cos\theta_{colun}}$$

$$tan\theta_{column} = \frac{h - \frac{a}{cos\theta_{colun}}}{l} \quad ---------- (Eq\ B.4)$$

$$tan\theta_{column} = \frac{240 - \frac{70}{cos\theta_{colun}}}{430}$$

$$l_{column} = 77cm$$

$$\theta_{column} = 0.42rad$$

The equivalent diagonal struts should therefore be placed at a distance of 77cm along the column from the beam-column joints with moment releases at each end.

The strut should be defined as a concrete material with the same material properties as the masonry panel.

Next, a strut reduction factor, $(R_1)_i$ is applied to represent the panel with door and window openings. This factor is computed using Equation 2.9 then the reduced strut width is calculated from Equation 2.6, as shown in Equations B.5 and B.6.

$$(R_1)_i = 0.6\left(\frac{A_{open}}{A_{Panel}}\right)^2 - 1.6\left(\frac{A_{open}}{A_{Panel}}\right) + 1 \quad ---------- (Eq\ B.5)$$

$$(R_1)_i = 0.6\left(\frac{32000}{103200}\right)^2 - 1.6\left(\frac{32000}{103200}\right) + 1$$

$$(R_1)_i - 0.562$$

$$a_{red} = a(R_1)_i(R_2)_i \quad ---------- (Eq\ B.6)$$

$$a_{red} = 70 * (0.562) * (1.0)$$

$$a_{red} = 39.34\text{cm}$$

Next, plastic hinges are defined to represent possible failure points for the frame. Hinges controlled by the combination of axial, moment, and shear forces are placed at a distance (l_{column}) from the joints along the columns. Conversely, hinges along the beam account for only moment and shear forces, and are placed at a distance (l_{beam}) from the joints. This distance (l_{beam}) is found by simultaneously solving Equations 4.1 and 4.2 for l_{beam} and θ_{column}, as shown in Equations B.7 and B.8.

$$l_{beam} = \frac{a}{sin\theta_{beam}} - (Eq\ B.7)$$

$$l_{beam} = \frac{70}{sin\theta_{beam}}$$

$$tan\theta_{beam} = \frac{h}{l - \frac{a}{sin\theta_{beam}}} - (Eq\ B.8)$$

$$tan\theta_{beam} - \frac{240}{430 - \frac{70}{sin\theta_{beam}}}$$

$$l_{beam} = 108.7cm$$

$$\theta_{beam} = 0.7rad$$

Single hinges controlled only by axial forces are placed at the midpoints of the struts. Figure B.1 shows the hinge types and placement around a sample panel.

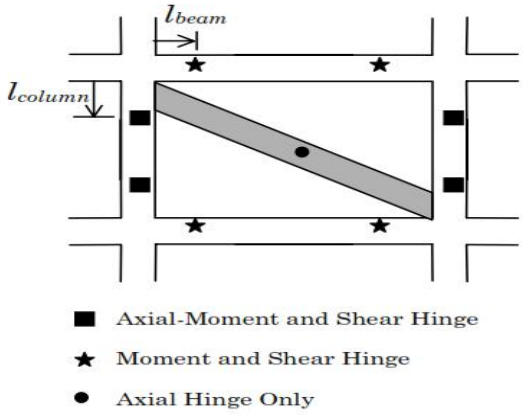

Figure B.1 Plastic hinge placement(Ghassan Al-Chaar)

Upon placement of the hinges, the capacity of the strut hinges (R_{strut}) should be computed. The compressive strength (R_{strut}) should be calculated using Equations 2.12 as illustrated in Equations B.9-B.12.

$$R_{cr} = a_{red} t_{eff} f'_m \quad \text{(Eq B.9)}$$

$$R_{cr} = 393.4 * 48 * 3.5*10^{-3}$$

$$R_{cr} = 66.1\text{KN}$$

$$R_{shear} = A_n f'_v (R_1)_i (R_2)_i \quad \text{(EqB.10)}$$

$$R_{shear} = 176500 * 1.83*0.565$$

$$R_{shear} = 182.5\text{KN}$$

$$tan\theta_{strut} = \frac{h - 2l_{column}}{l} \quad \text{(Eq.B.11)}$$

$$tan\theta_{Strut} = \frac{240 - 2 * 70}{430}$$

$\theta_{Strut} = 14^0$

$$R_{strut} = min\begin{cases} R_{cr} \\ R_{shear}/_{cos\theta_{strut}} \end{cases} \text{ – (Eq B.12)}$$

$$R_{strut} = min\begin{cases} 66.1\text{KN} \\ 182.5\text{KN}/_{\cos 14^0} \end{cases}$$

$R_{strut} = 66.1KN$

Next, rigid end offsets (REOs) are placed to increase the rigidity of the joints, as well as ensure that the maximum stresses computed are located at the defined plastic hinges. The REOs should have a rigid zone factor of one and span from the beam column joints outward to a distance (l_{beam}) along the beams and a distance (l_{column}) along the column.

Appendix- C: Tabulated Results

Results from static pushover analysis for the case study buildings for all models are summarized in Tables below.

Table C. 6.1 Comparison of Monitored Displacement vs Base shear for different models

	Model1		Model 2		Model 3		Model 4		Model 5	
Step	Displ	Base Force	Displ	Base Force	Displ	Base Force	Displ	Base Force	Displ	Base Force
	mm	kN	mm	kN	mm	kN	mm	kN	mm	kN
0	0	0	0	0	0	0	0	0	0	0
1	2.43	7046.501	1.25	7112	1.11	7149	0.95	7249.56	0.75	7250.26
2	11.39	22772.54	6.43	22918.23	5.1	22954.23	5.1	23126.35	4.52	23140.23
3	18.16	27589.24	12.356	28115.2	9.632	28156.23	8.12	28298.23	7.68	28370.23
4	18.46	27896.33	16.54	28276.25	13.125	28288.23	11.25	28437.25	9.645	28500.23
5	19.55	26478.26	18.125	28589.23	16.32	28700	14.76	28700.52	12.65	28798.23
6	19.63	26135.46	18.1	28597.23	18.1	28597.23	16.98	28597.23	13.68	28597.23
7	41.3	18798.35	22.4	27697.23	20.25	27697.23	18.12	27697.23	15.63	27697.23
8	41.3	16487.26	22.4	23546.23	20.65	27789.36	18.12	27973.25	16.23	27789.36
9	42	11256.35	29.6	21568.32	24.56	26785.23	22	26895.23	21.26	26785.23
10	43.21	3546.12	29.6	4562.35	25.645	5874.23	24.63	5800.35	23	6956.56

Table C. 6.2 Comparison of story displacement for different models

TABLE: Story Displacement(mm)						
Story	Elevation(m)	Model1	Model2	Model3	Model4	Model 5
ROOF	31.00	29.59	19.63	18.64	17.64	15.64
8F	28.00	29.23	19.38	18.39	17.39	15.39
7F	25.00	28.61	18.96	16.98	15.98	11.98
6F	22.00	27.62	18.32	16.33	15.33	11.33
5F	19.00	26.19	17.38	15.39	13.39	8.39
4F	16.00	24.30	16.11	14.13	12.13	6.13
3F	13.00	21.89	14.48	12.49	10.49	5.05
2F	10.00	18.85	12.41	10.43	9.04	3.04
1F	7.00	14.85	9.71	6.73	3.73	2.73
GF	4.00	7.86	5.07	2.08	1.08	0.91
Base	0	0	0	0	0	0

Table C. 6.3 comparison of story shear for different model

TABLE: Story Shear(KN)							
Story	**Elevation(m)**	**Location**	Model 1	Model 2	Model 3	Model 4	Model 5
ROOF	31	Top	3562.1067	3863.494	3899.504	3915.799	4022.809
	31	Bottom	3562.0646	3863.492	3899.509	3915.797	4022.807
8F	28	Top	7519.84	8177.815	8244.833	8299.214	8536.174
	28	Bottom	7519.8945	8177.817	8244.839	8299.217	8536.182
7F	25	Top	11479.1893	12489.33	12587.28	12679.77	13046.59
	25	Bottom	11479.2034	12489.32	12587.28	12679.76	13046.59
6F	22	Top	15440.5134	16801.89	16930.81	17061.35	17558.02
	22	Bottom	15440.4353	16801.9	16930.79	17061.41	17558.1
5F	19	Top	19404.2185	21115.81	21275.67	21444.3	22070.85
	19	Bottom	19404.629	21115.97	21275.83	21444.53	22071.1
4F	16	Top	23372.2935	25431.88	25622.79	25829.32	26585.76
	16	Bottom	23371.3476	25431.69	25622.38	25829.4	26585.89
3F	13	Top	27343.3064	29754.26	29971.76	30216.63	31103
	13	Bottom	27343.3064	29755.44	29973.12	30217.89	31104.24
2F	10	Top	31327.7262	34087.3	34328.12	34609.72	35625.91
	10	Bottom	31327.7262	34084.93	34324.5	34608.52	35624.82
1F	7	Top	35309.9533	38424.2	38684.22	39009.37	40155.57
	7	Bottom	35309.9533	37862.43	38127.38	38444.45	39588.5
GF	4	Top	35798.3529	39581.19	39830.6	40201	41414.3
	4	Bottom	35798.3529	39620.39	40100	40250.6	41455.2
Base	0	Top	0	0	0	0	0
	0	Bottom	0	0	0	0	0